DANMARKS OG GRØNLANDS GEOLOGISKE UNDERSØGELSE RAPPORT 2005/33

Cenozoic maps of the Danish North Sea area

Rasmussen, E. S., Piasecki, S., Andsbjerg, J., Dybkjær, K.,
Vejbæk, O. V., Jacobsen, C., Britze, P. & Bryde-Auken, M.

CONFIDENTIAL
FORTROLIG

GEOLOGICAL SURVEY OF DENMARK AND GREENLAND
MINISTRY OF THE ENVIRONMENT

GEUS

DANMARKS OG GRØNLANDS GEOLOGISKE UNDERSØGELSE RAPPORT 2005/33

Cenozoic maps of the Danish North Sea area

Rasmussen, E. S., Piasecki, S., Andsbjerg, J., Dybkjær, K.,
Vejbæk, O. V., Jacobsen, C., Britze, P. & Bryde-Auken, M.

GEOLOGICAL SURVEY OF DENMARK AND GREENLAND
MINISTRY OF THE ENVIRONMENT

G E U S

DANMARKS OG GRØNLANDS GEOLOGISKE UNDERSØGELSE RAPPORT 2005/33

Cenozoic maps of the Danish North Sea area

Rasmussen, E. S., Piasecki, S., Andsbjerg, J., Dybkjær, K.,
Vejbæk, O. V., Jacobsen, C., Britze, P. & Bryde-Auken, M.

G E U S

TGS NOPEC GEOPHYSICAL COMPANY

GEOLOGICAL SURVEY OF DENMARK AND GREENLAND
MINISTRY OF THE ENVIRONMENT

G E U S

Contents

Introduction

Exploration for hydrocarbons in the Danish area of the North Sea started in 1963. Since then, large amounts of seismic data have been acquired and more than 125 exploration wells have been drilled. The seismic data were originally interpreted on paper sections but since digital formats became available in the 1980s, interpretation has been carried out on workstations. This Atlas of Cenozoic Maps is a compilation of interpretations of the Cenozoic succession of the Danish sector of the North Sea carried out at GEUS. In order to improve understanding of the petroleum systems in the area the study has concentrated on the succession deposited in the Neogene, which was the time of major hydrocarbon generation and trapping. The subdivision of the Palaeogene succession is based on Schiøler *et al.* (2005) and the dating of the Neogene succession is based on very detailed biostratigraphy (dinoflagellates) that has been developed at GEUS since 2000. The subdivision of the Neogene succession into sequences is developed from onshore studies of Neogene deposits (Dybkjær 2004; Piasecki 1980; Rasmussen 2004) and new datings of key wells in the North Sea area by Dybkjær (2003) and Piasecki & Rasmussen (2004).

The Atlas contains a brief review of the geological setting followed by a stratigraphy section where a number of well-log panels illustrate the subdivision of the Cenozoic succession into units (Paleocene) and sequences (Neogene). The main part of the Atlas contains a series of maps of the units and sequences in two-way time, depth and as isochore maps. Each map is accompained by a seismic section showing the unit/sequence in question and a palaeogeographic map.

Geological setting

The North Sea Basin was formed during thermal subsidence after the formation of the Central Graben in the Jurassic (Ziegler 1982; Vejbæk 1992). The basin was open towards the north via a narrow strait between the Shetland Islands and Norway that occasionally acted as a barrier so that the North Sea became brackish at times. The basin extended from Norway, along Scania to the Baltic region and north Germany. The southern margin passed through northern France and Belgium and, towards the west, the basin margin followed eastern England and Scotland to the Shetland Islands.

Maximum flooding by the sea in this basin was in the Late Cretaceous with deposition of chalk. Alpine folding and impact of the Iceland plume in the Late Cretaceous–Paleocene affected the basin by inversion tectonics and probably uplift of the Fennoscandian Shield (Danielsen *et al.* 1995). The coastline prograded significantly from Scandinavia in the north in the Eocene but density flow deposits of Paleocene age at the Ringkøbing-Fyn High (Danielsen *et al.* 1995) may indicate that progradation had already started at that time.

Palaeo-water depths were about 500–700 metres in the central part of the basin but significantly lower towards the east in present-day Denmark, especially during the Paleocene (Heilmann-Clausen *et al*. 1985; Clausen & Huuse 2002).

Outbuilding of the slope–shelf system continued during the Oligocene (Michelsen *et al.* 1998) possibly as a result of late Eocene tectonic events that resulted in uplift of the Fennoscandian Shield. The Oligocene deposits in the Danish area were laid down partly as pro-delta sediments and partly as contourites (Hansen *et al.* 2004). Turbidite deposition took place locally at the toe of the slope and on the basin floor. A distinct tectonic event occurred in the mid-Oligocene (Rasmussen 2004) that resulted in reactivation of older faults and movement of salt structures. In the Miocene, coastal plain deposits reached the Danish area of the North Sea and three major delta progradations of Aquitanian–Burdigalian age have been recorded (Rasmussen 2004). The deltas were predominantly wave-dominated (Rasmussen *et al.* 2004). During deposition of the third delta, renewed tectonic movements took place (Rasmussen 2004) associated with accelerated subsidence in the North Sea area (Koch 1989; Clausen *et al*. 1999; Rasmussen 2004).

Marine transgression in the Langhian, middle Miocene, and faulting recorded from the Odderup Formation (Koch 1989) marked a significant phase of basin development when the source of sediments changed from north-east to east. At this middle Miocene time, the global climate was warm and eustatic sea level was high, so most of the Danish region was probably flooded. The sea-level fall that followed during the late Miocene was a response to global cooling, but this was compensated by increased regional subsidence of the Danish region. Regression resumed during the latest Miocene resulting in progradation of the coastal plain and, at the end of the Miocene, the shoreline reached the Central Graben area (Rasmussen 2005). Up to 400 metres of upper Miocene sediments were deposited in mid-Jylland during this progradation (Japsen *et al.* 2002).

In the early Pliocene, marine sediments were deposited in most of the Danish area of the North Sea and tectonic movements occurred, indicated by halokinesis (Rasmussen *et al*. 2005). After the early Pliocene tectonics, renewed progradation took place in the late Pliocene and deltas were located in the extreme western part of the Danish area of the North Sea at the end of the Pliocene. Strong late Neogene up-lift and Holocene glacial erosion have removed the younger sediments but they are preserved in parts in the present off-shore region such as where the well Tove-1 was drilled.

Stratigraphy of the Danish area of the North Sea

The stratigraphy used in the Atlas (Fig. 1) is based on a number of older publications (Rasmussen 1961; Heilmann-Clausen *et al*. 1985) and recent studies carried out at GEUS (Schiøler *et al.* 2005; Dybkjær & Rasmussen 2003; Dybkjær 2003; Piasecki & Rasmussen 2004). Dating using dinoflagellates has proved particularly efficient in making correlations between outcrop and borehole data.

Methodology

Biostratigraphy

Dinoflagellate stratigraphy

Neogene dinoflagellate stratigraphy has improved significantly in recent decades due to extensive studies especially in the North Atlantic region. Studies on DSDP/ODP wells rangefrom Baffin Bay and the Labrador Sea in the north to the Norwegian shelf (Manum 1976; de Vernal & Mudie 1989a, b; Head *et al.* 1989a, b, c; Manum *et al.* 1989; Poulsen *et al.* 1996; Smelror 1999; Williams & Manum 1999; Williams *et al.* 2004). Further studies along the western margin of Europe provide data from the mid-latitudes of the northern North Atlantic (Harland 1979; Edwards 1984). De Verteuil and Norris's (1996) studies onshore eastern USA were a break-through and studies of type sections in Italy have also been important for Neogene dinoflagellate stratigraphy (Powell 1986; Zevenboom *et al.* 1994; Zevenboom 1995).

Several of the excellent studies mentioned above do not, however, include the uppermost Neogene. Consequently, most relevant for the present study are studies of the uppermost Miocene and Pliocene successions in the United Kingdom and Belgium areas of the North Sea by de Schepper *et al.* (2004), Head (1996, 1997, 1998); Head & Norris (1999); Louwye (1999); Louwye & Laga (1998) and Louwye *et al.* (1999, 2004). The stratigraphic records and the description of many new species restricted to the uppermost Neogene have certainly provided the basis of an improved Messinian–Pliocene stratigraphy and of our understanding of the influence of palaeoclimate on stratigraphy.

Mapping procedure (Log stratigraphy and seismic stratigraphy)

Mapping of the Cenozoic succession is based on different criteria as specified below. Log-panels (gamma-logs from selected wells), structural maps, isochore maps, seismic sections and palaeogeographical reconstructions are used to illustrate the development of the succession.

The units of the Palaeogene succession that are mapped are formations that were all defined in offshore wells in the Norwegian and U.K. sectors of the North Sea. The formations are all easily recognisable in wells in the Danish sector and they can be correlated to the Danish onshore (Fig. 1).The lowermost horizon mapped is the top of the Chalk Group. The second unit mapped is equivalent to the Rogaland Group of the Norwegian North Sea and consists of the Vaale, Lista, Sele and Balder Formations. The horizon at the top of this unit is the top of the Balder Formation, which is easily identified on the seismic data and in wells. The third unit mapped is the Horda Formation. In the Central Graben area, the top of the Horda Formation is also the top of the Eocene. However, in the eastern parts of the the Danish North Sea the top Horda horizon is older because of non-deposition and the top Eocene has been traced along one of the lowermost toes of the Lark Formation.

The lower part of the Neogene succession is sub-divided into sequences defined onshore (Rasmussen 2004). The correlation to the North Sea is based on dating of the S-1, R-1 and Frida-1 wells (Laursen 1995; Dybkjær & Rasmussen 2003). The sequences defined were afterwards tied to seismic data and seismic interpretation of regional reflectors was used to map them over the whole of the Danish area of the North Sea. Where a condensed succession occurs, the seismic picks have been consistently held within individual peaks and troughs to avoid horizon-crossings. Consequently there may be some discrepancy between the seismic pick and the sequence boundaries recognised in the wells due to lack of resolution (Fig. 2). The upper part of the Neogene succession (Pliocene) is subdivided into seismic sequences based on regional seismic unconformities (Vail *et al*. 1976) and their dating is from a recent study of the Tove-1 well (Piasecki & Rasmussen 2004).

The seismic interpretation of the Neogene succession forms the basis for the correlation shown in the log panels (Figs 3 –7). Thus division into sequences and units is not based solely on interpretation of log patterns but are mainly ties from seismic data to the well logs.

Seismic Mapping

The twelve horizons interpreted were imported into ZMAP-PLUS® software and converted into a grid by utilizing the contour gridding algorithm (Figs 8 –19). The contour increment used is 500m, except in Sequence I where the increment used is 1000m due to the poor data coverage of that sequence.

The resulting grids were tied to nine wells (Mona-1, E-1X, Tove-1, Alma-1, Inez-1, C-1X, R-1X, S-1X, Frida-1 and L-1X) and regridded. The deviations between grid and well information were calculated and the contours were carefully adjusted to the correct level. The maps are diplayed on a UTM (Zone 32) projection on a Hayford 1909 spheroid with asemi-major axis of 6 378 388.0 metres and semi-minor axis of 6 356 911.946 metres.

Depth conversion

Depth conversion of Post Chalk group surfaces was done by application of a multilayer velocity model consisting of 11 layers each with an individual interval velocity function as described by Japsen (1993, 1994). Each layer is assigned a surface velocity V_0 and a depth gradient K according to the equation:

$$V(z) = V_0 + Kz$$

where V(z) is the instantaneous velocity for the layer at depth z. To fit the equations to the wells, lateral deviations from the average interval velocity functions were applied by calculating a parameter dV that is added to the V_0 parameter. The equation thus becomes:

$$V(z) = (V_0 + dV) + Kz$$

where dV varies laterally. Units for all parameters are given in Table 1. Detailed description of this relationship may be obtained from Japsen (1993, 1994) and only the main points are given here.

The V_0's and K's necessary for the depth conversion can be approximated by applying a simple linear regression (e.g. in a spread sheet) to cross-plots of interval velocity versus mean depth for the various sediment packages in the wells that are defined by the interpreted seismic reflectors. This method of fitting is only approximate as scatter in the cross plot is not related to the dV parameter in a simple way. In this project, the velocity parameters were derived from detailed studies of regional velocity variations (e.g. Japsen 1998, 1999, 2000).

Generation of maps of the deviations of velocity (using the average velocity functions and the dV parameter) requires lists of these deviations together with the coordinates for each well, which then can be interpolated nto maps.
The dV values are given from:

$$dV = \frac{\Delta Z \cdot K}{\exp^{K \cdot \Delta T} - 1} - V_0 - Z_t \cdot K$$

Depth conversion using the linearly increasing instantaneous velocity assumption

$$V_i = V_0 + Kz$$

is done layer by layer downwards.

The thickness of a layer is found from:

$$\Delta Z = \frac{1}{K}(V_0 + dV + (K \cdot Z_t))(\exp^{K\Delta t} - 1)$$

where ΔT is one-way time.

Table 1. *The symbols in depth conversion and their units.*

Symbol	Meaning	Unit
ΔZ	Thickness	metres
V_0	Surface velocity	m/sec
dV	Velocity deviation	m/sec
K	Velocity gradient	sec^{-1}
Z_t	Depth to top of layer	metre
Z_b	Depth to base of layer	metre
T_t	Two-way time to top of layer	sec
T_b	Two-way time to base of layer	sec
ΔT	Thickness in one-way reflection time	sec

Post-chalk interval

The Cenozoic velocity model consists of two layers separated at a mid-Miocene reflector (base sequence E) approximately corresponding to the top of the overpressured section (upper and lower post-Chalk Group in Table 2). We have used parameters for these layers determined by Britze *et al.* (1995) and Japsen (1999). The parameters are applicable to most of the North Sea as they are based on a large well data-base from the entire North Sea (see e.g. Japsen 2000).

Table 2. *Parameters used in the depth conversion.*

Velocity Unit	V_0 (ft/s)	K (1/s)
upper post Chalk Group	1725	0.4
lowe post Chalk Group	1517.2	0.6

References

Britze, P., Japsen, P. & Andersen, C., 1995: The Danish Central Graben: Top Chalk and the Post Chalk Group. (Two way travel time, depth, and interval velocity), Danmarks Geologiske Undersøgelse, Map Series **47**, 1:200,000, 5 pp., 3 maps.

Clausen, O.R. & Huuse, M. 2002. A post mid-Cretaceous North Sea model. Geological Society of Denmark Bulletin **49**, 171–186.

Clausen, O.R., Gregersen, U., Michelsen, O. & Sørensen, J.C. 1999: Factors controlling the Cenozoic sequence development in the eastern parts of the North Sea. Journal of the Geological Society (London) **156**, 809–816.

Danielsen, M., Clausen, O.R. & Michelsen, O. 1995: Stratigraphic correlation of late Paleocene sand deposits in the Søgne Basin area of the Danish and Norwegian central North Sea. Terra Nova **7**, 516–527.

de Schepper, S., Head, M.J. & Louwye, S. 2004: New dinoflagellate cysts and Incertae Sedis taxa from the Pliocene of Northern Belgium, southern North sea Basin. Journal of Paleontology **78**(4), 625–644.

de Vernal, A. & Mudie, P.J. 1989a: Late Pliocene to Holocene palynostratigraphy at ODP Site 645, Baffin Bay. In: Srivastava, S.P. *et al.* (eds): Proceedings of the Ocean Drilling Program, Scientic Results **105**, 387–397.

de Vernal, A. & Mudie, P.J. 1989b: Pliocene and Pleistocene palynostratigraphy at the ODP sites 646 and 647, eastern and southern Labrador Sea. In: Srivastava, S.P. *et al.* (eds): Proceedings of the Ocean Drilling Program, Scientific Results **105**, 401–422.

Dybkjær, K. 2003: Palynostratigraphy of the Upper Oligocene – Middle Miocene succession in the Frida-1 well. Geological Survey of Denmark and Greenland Report **28**, 28pp.

Dybkjær, K., 2004: Dinocyst stratigraphy and palynofacies studies used for refining a sequence stratigraphic model - uppermost Oligocene to Lower Miocene Jylland, Denmark. Review of Palaeobotany and Palynology 131, 201–249.

Edwards, L.E. 1984: Miocene dinoflagellate cysts from Deep Sea Drilling Project Leg 81, Rockall Plateau, eastern North Atlantic Ocean. In: Roberts, D.G., et al. (eds): Initial Reports of the Deep Sea Drilling Project 81, 581–594.

Hansen, J.P.V., Clausen, O.R., & Huuse, M. 2004: Origin of ambiguous erosional features at major Cenozoic sequence boundaries in the North Sea revealed by 3D seismic mapping. 3D seismic advances in the understanding of stratigraphic and structural architecture conference, 14–16 Nov. 2001, London, Appendix 2. Poster presentation.

Harland, R. 1979: Dinoflagellate biostratigraphy of Neogene and Quarternary sediments at Holes 400/400A in the Bay of Biscay. In: Montadert, L. & Roberts, D.G. (eds): Initial Reports of the Deep Sea Drilling Project **48**, 531–545.

Head, M.J. 1996: Late Cenozoic dinoflagellates from the Royal Society borehole at Ludham, Norfolk, eastern England. Journal of Paleontology **70**, 543–570.

Head, M.J. 1997: Thermophilic dinoflagellate assemblages from the mid Pliocene of eastern England. Journal of Paleontology **71**, 165–193.

Head, M.J. 1998: Marine environmental change in the Pliocene and early Pleistocene of eastern England: the dinoflagellate evidence reviewed. Mededelingen Nederlands Instituut voor Toegepaste Geowettenschappen TNO **60**, 199–226.

Head, M.J. & Norris, G. 1999: Pliocene and Lower Pleistocene dinoflagellates and acritarchs of the North Atlantic: Taxonomy, magnetobiostratigraphy, and paleoclimatology. Palynology **20**, Abstract, 241 only.

Head, M.J., Norris, G. & Mudie, P.J. 1989b: 25. Palynology and dinocyst stratigraphy of the Upper Miocene and lowermost Pliocene, ODP Leg 105, Site 646, Labrador Sea. In: Srivastava, S.P. *et al.* (eds): Proceedings of the Ocean Drilling Program, Scientific Results **105**, 423–451.

Head, M.J., Norris, G. & Mudie, P.J. 1989c: New species of dinoflagellate cysts and a new species of acritarch from the Upper Miocene and lowermost Pliocene, ODP Leg 105, Site 646, Labrador Sea. In: Srivastava, S.P. *et al.* (eds): Proceedings of the Ocean Drilling Program, Scientific Results **105**, 453–466.

Heilmann-Clausen, C., Nielsen, O.B. & Gersner, F. 1985: Lithostratigraphy and depositional environments in the upper Palaeocene and Eocene of Denmark. Bulletin of the Geological Society of Denmark **33**, 287–323.

Japsen, P. 1993. Influence of lithology and Neogene uplift on seismic velocities in Denmark: Implications for depth conversion of maps. American Association of Petroleum Geologists Bulletin **77**, 194–211.

Japsen, P. 1994. Retarded compaction due to overpressure deduced from a seismic velocity/depth conversion study in the Danish Central Trough, North Sea. Marine and Petroleum Geology **11** 715–733.

Japsen, P. 1998: Regional velocity-depth anomalies, North Sea Chalk; a record of over-pressure and Neogene uplift and erosion. American Association of Petroleum Geologists Bulletin **82**, 2031–2074.

Japsen, P. 1999: Overpressured Cenozoic shale mapped from velocity anomalies relative to a baseline for marine shale, North Sea. Petroleum Geoscience **5**, 321–336.

Japsen, P., 2000: Fra kridthav til Vesterhav, Nordsø bassinets udvikling vurderet ud fra seismiske hastigheder. Dansk Geologisk Foreningen Tidskrift , 36 pp.

Japsen, P., Bidstrup, T. & Rasmussen, E.S. 2002: Cenozoic evolution of the eastern Danish North Sea. Discussion. Marine Geology **177**, 571–575.

Koch, B.E. 1989: Geology of the Søby–Fasterholt area. Danmarks Geologiske Undersøgelse Serie A **22**, 177 pp.

Laursen, G.V. 1995: Foraminiferal biostratigraphy of Cenozoic sections in five wells from the Danish area. AFP-92 project: Basin development of the Tertiary of the Central Trough with emphasis on possible hydrocarbon reservoirs. Aarhus University, 33pp.

Louwye, S. 1999: New species of organic-walled dinoflagellates and acritarchs from the Upper Miocene Diest Formation, northern Belgium (southern North Sea Basin). Review of Palaeobotany and Palynlogy **107**, 109–123.

Louwye, S. 2002: Dinoflagellate cyst biostratigraphy of the Upper Miocene Deurne Sands (Diest Formation) of northen Belgium, southern North Sea. Geological Journal **37**, 55–67.

Louwye, S. & Laga, P. 1998: Dinoflagellate cysts of the shallow marine Neogene succession in the Kalmthout well, northern Belgium. Bulletin of the Geological Society of Denmark **45**, 73–86.

Louwye, S., de Coninck, J. & Verniers, J. 1999: Dinoflagellate cyst stratigraphy and depositional history of Miocene and Lower Pliocene formations in northern Belgium (southern North Sea Basin). Geologie en Mijnbouw **78**, 31–46.

Louwye, S., Head, M.J. & de Schepper, S. 2004: Dinoflagellate cyst stratigraphy and palaeoecology of the Pliocene in northern Belgium, southern North Sea. Geological Magasine **141**, 353–378.

Manum, S. 1976: Dinocysts in Tertiary Norwegian-Greenland Sea sediments (Deep Sea Drilling Project Leg 38), with observations on palynomorphs and palynodebris in relation to environment. In: Talwani, M. *et al*. (eds): Initial Reports of the Deep Sea Drilling Project **38**, 897–919.

Manum, S., Boulter, M.C., Gunnarsdottir, H., Rangnes, K. & Scholze, A. 1989: Eocene to Miocene palynology of the Norwegian Sea (ODP Leg 104). In: Eldolm, O. *et al.* (eds): Proceedings of the Ocean Drilling Program, Scientific Results **104**, 611–662.

Michelsen, O., Thomsen, E., Danielsen, M., Heilmann-Clausen, C., Jordt, H. & Laursen, G.V. 1998: Cenozoic sequence stratigraphy in the eastern North Sea. In: De Graciansky P.C. *et al.* (eds): Mesozoic–Cenozoic sequence stratigraphy of western European basins. Society of Economic Paleontologists and Mineralogists Special Publication **60**, 91–118.

Piasecki, S. 1980: Dinoflagellate cyst stratigraphy of the Miocene Hodde and Gram Formations, Denmark. Bulletin of the Geological Society of Denmark **29**, 53–76.

Piasecki, S. & Rasmussen, E.S. 2004: Neogene dinoflagellate stratigraphy of the S-1 and Tove-1 wells in the Danish North Sea. Geological Survey of Denmark and Greenland Report **2004/94**, 43pp.

Poulsen, N., Manum, S., Williams, G.L. & Ellegaard, M. 1996: Tertiary dinoflagellate biostratigraphy of Sites 907, 908, and 909 in the Norwegian-Greenland Sea. In: Thiede, J. *et al.* (eds): Proceedings of the Ocean Drilling Program, Scientific Results **151**, 255–287.

Powell, A.J. 1986: A dinoflagellate cyst biozonation for the Late Oligocene to Middle Miocene succession of the Langhe region, northwest Italy. American Association of Stratigraphical Palynologists Contribution Series **17**, 105–127.

Rasmussen, E.S. 2004: Stratigraphy and depositional evolution of the uppermost Oligocene – Miocene succession in Denmark. Geological Society of Denmark Bulletin **51**, 89–109.

Rasmussen, E.S. in press: The depositional environment of the upper Middle – Upper Miocene Gram Formation, Denmark. Paleontos.

Rasmussen, E.S., Dybkjær, K. & Piasecki, S. 2004: The Billund delta: a possible new giant aquifer in the central and western Jutland. Geological Survey of Denmark and Greenland Bulletin **4**, 21–24.

Rasmussen, E.S., Vejbæk, O.V., Bidstrup, T., Piasecki, S & Dybkjær, K. 2005: Late Cenozoic depositional history of the Danish North Sea Basin: implications for the petroleum systems in the Kraka, Halfdan, Siri and Nini fields. In: A.G. Dore & B.A. Vining (eds) Petroleum geology of North-West Europe and Global perspectives, Proceedings of the 6th Conference, 1347–1358. London: Geological Society.

Rasmussen, L.B. 1961: De Miocæne Formationer i Danmark. Danmarks Geologisk Undersøgelse IV. Række 4, 35 pp.

Schiøler, P., Andsbjerg, J., Clausen, O.R., Dam, G., Dybkjær, K., Hamberg, L., Heilmann-Clausen, C., Kristensen, L.E., Prince, I. & Rasmussen, J.A., in press: A revised lithostratigraphy for the Palaeogene–lower Neogene of the Danish North Sea. Geological Survey of Denmark and Greenland Bulletin.

Smelror, M. 1999: Pliocene–Pleistocene and redeposited dinoflagellate cysts from the western Svalbard margin (Site 986): Biostratigraphy, paleoenvironments, and sediment provenance. In: Raymo, M.E. *et al.* (eds): Proceedings of the Ocean Drilling Program, Scientific Results **162**, 83–98.

Vail, P.R., Mitchum, R.M. Jr., Todd, R.G., Widmier, J.M., Thompson, S. III, Sangree, J.B., Bubb, J.N. & Hatlelid, W.G., 1977: Seismic stratigraphy and global changes of sea level. In: Payton C.E. (ed.) Seismic stratigraphy: Applications to hydrocarbon exploration. American Association of Petroleum Geologists Memoir, **26**, 49–212.

Vejbæk, O.V. 1992: Geodynamic modelling of the Danish Central Trough. In: Larsen R.M. *et al.* (eds.) Structural and tectonic modelling and its application to petroleum geology. Norwegian Petroleum Society Special Publication **1**, 1–17.

Williams, G.L. & Manum, S.B. 1999: Oliocene–early Miocene dinocyst stratigraphy of hole 985A (Norwegian Sea). In: Raymo, M.-E. *et al.* (eds): Proceedings of the Ocean Drilling Program Scientific Results **162**, 99–109.

Williams, G.L., Brinkhuis, H., Pearce, M.A., Fensome, R.A. & Weegink, J.W. 2004: Southern ocean and global dinoflagellate cyst events for the latest Cretaceous-Neogene. In: Exon, N.F., Kenneth, J.P. & Malone, M.J. (eds): Proceedings of the ocean drilling Program, Scientific results **189**, 98 pp.

Zevenboom, D. 1995: Dinoflagellate cysts from the Mediterraneanand late Oligocene and Miocene, 221 pp. Unpublished thesis, Universiteit Utrecht, Netherlands.

Zevenboom, D., Brinkhuis, H. & Visscher, H. 1994: Dinoflagellate cyst palaeoenvironmental analysis of the Oligocene/Miocene transition in northwest and central Italy. Gionale di Geologica, Revista di geologia sedimentaria e geologia marina serie 3a **56**, 155–169.

Ziegler, P.A., 1982: Geological Atlas of Western and Central Europe. 130 pp. Amsterdam: Elsevier.

Fig. 1: Lithostratigraphy of the Danish North Sea and onshore area.

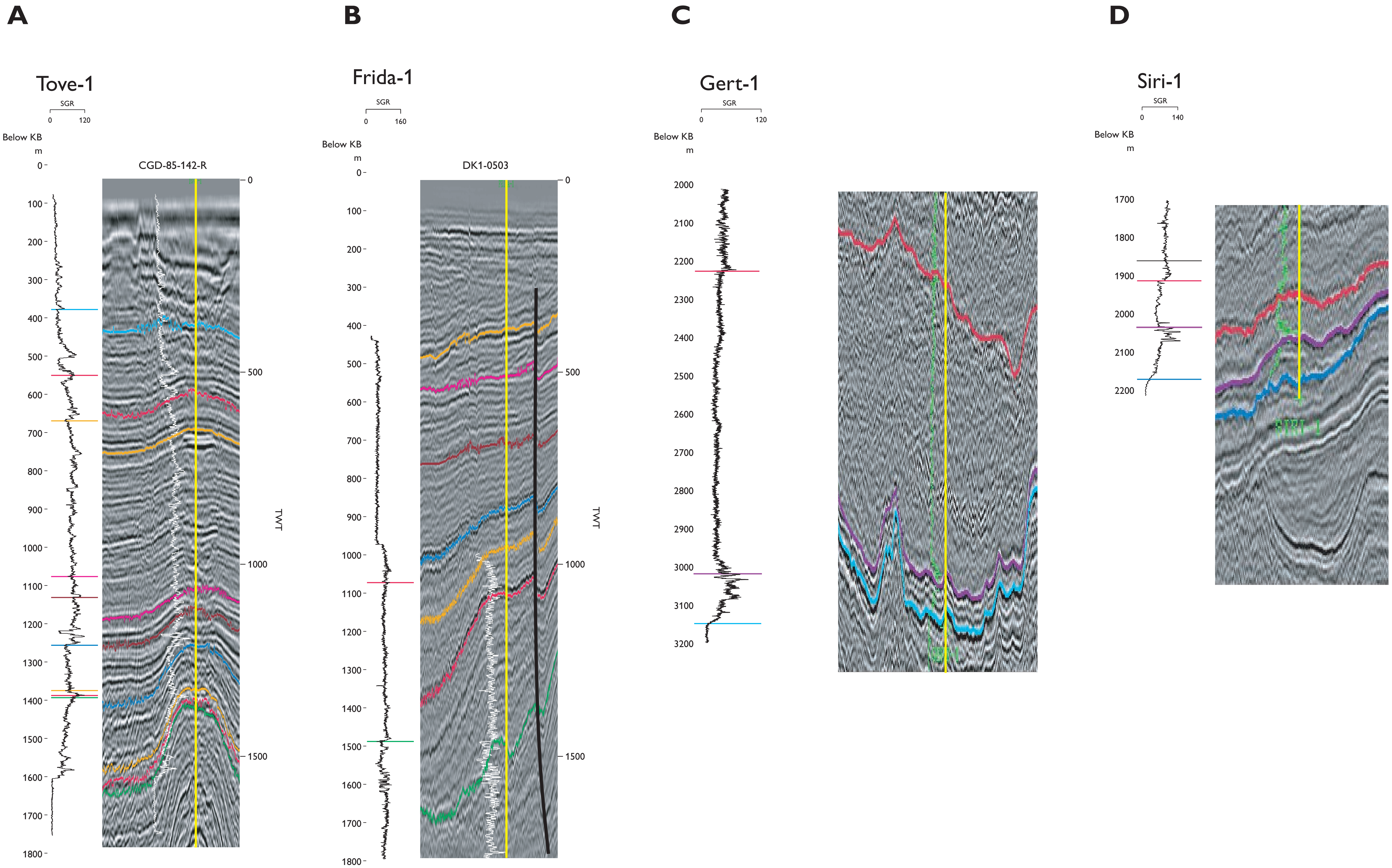

Fig. 2: Seismic to well ties from four selected wells. A and B shows the tie of the Neogene succession. C and D shows the tie of the Palaeogene succession.

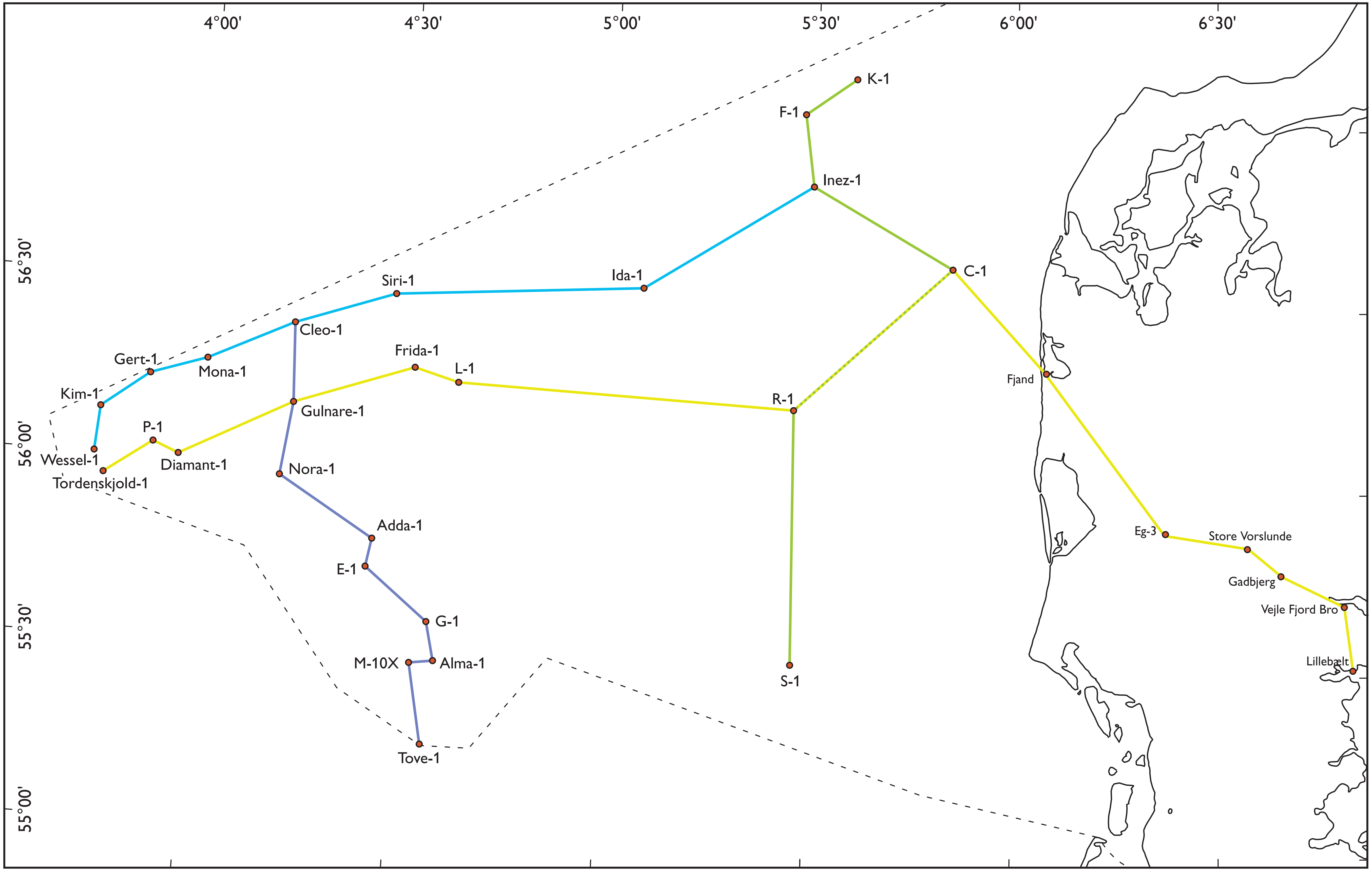

Fig. 3: Wells used for log correlation.

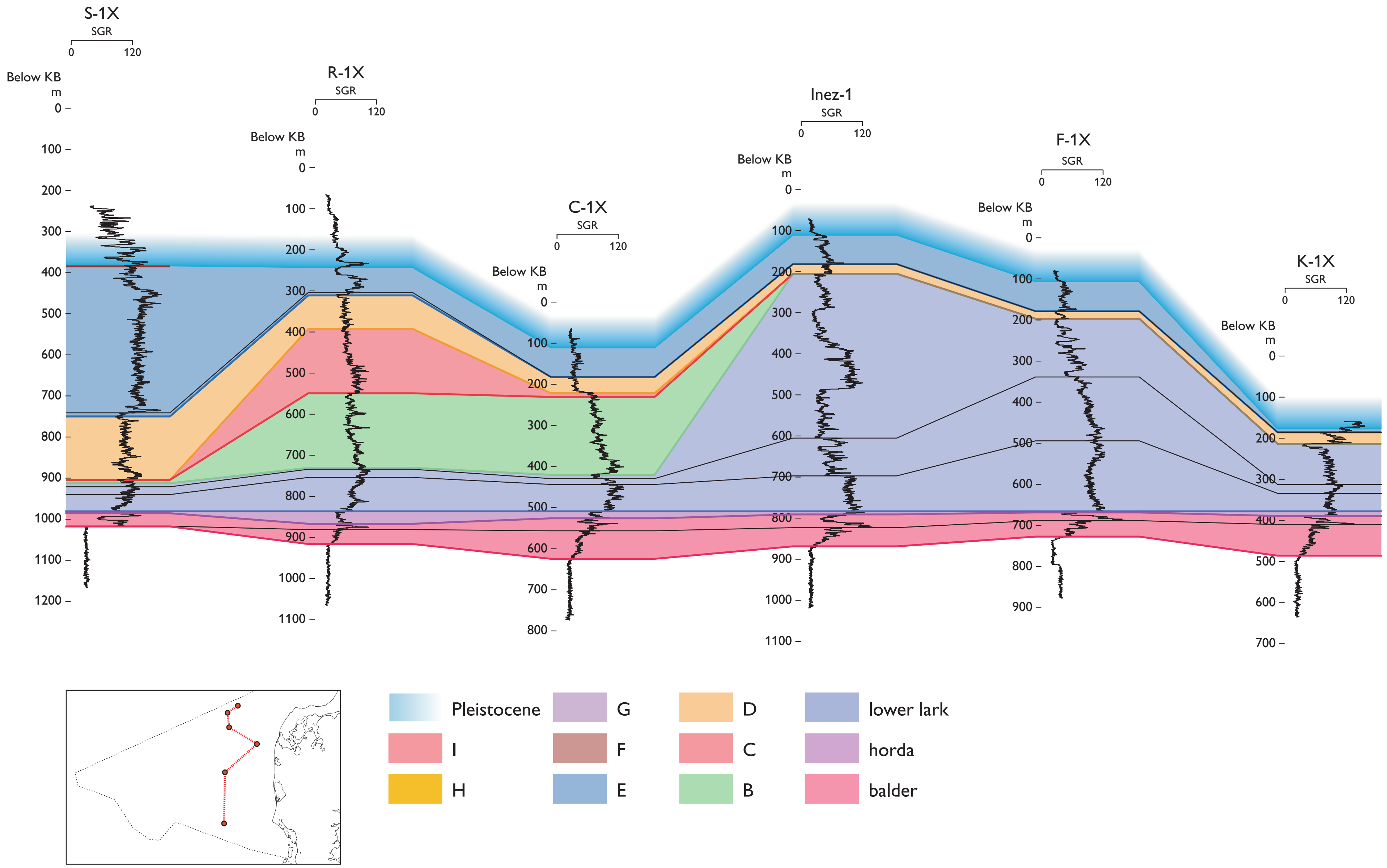

Fig. 4: N-S striking correlation panel of selected wells off Jylland.

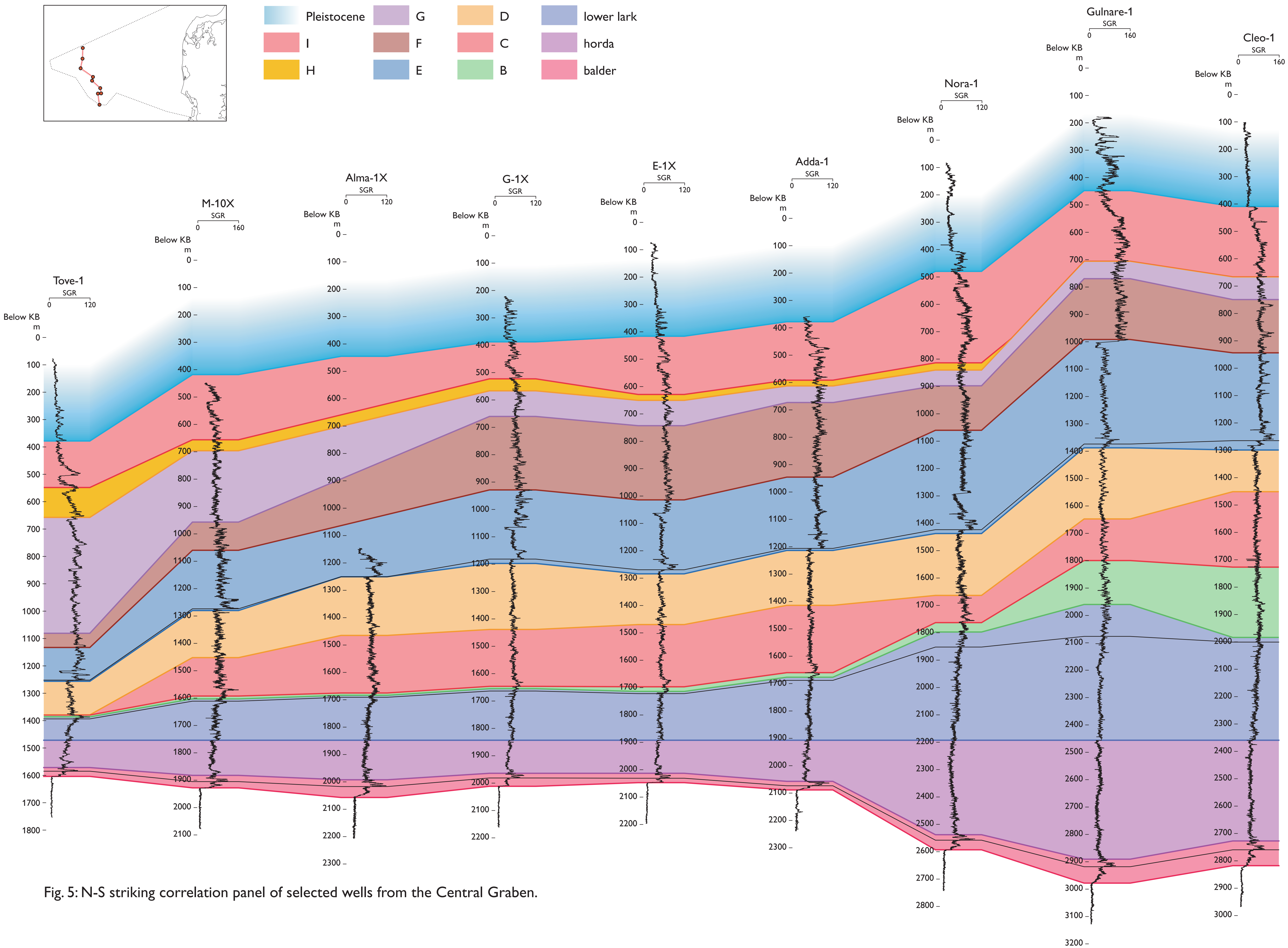

Fig. 5: N-S striking correlation panel of selected wells from the Central Graben.

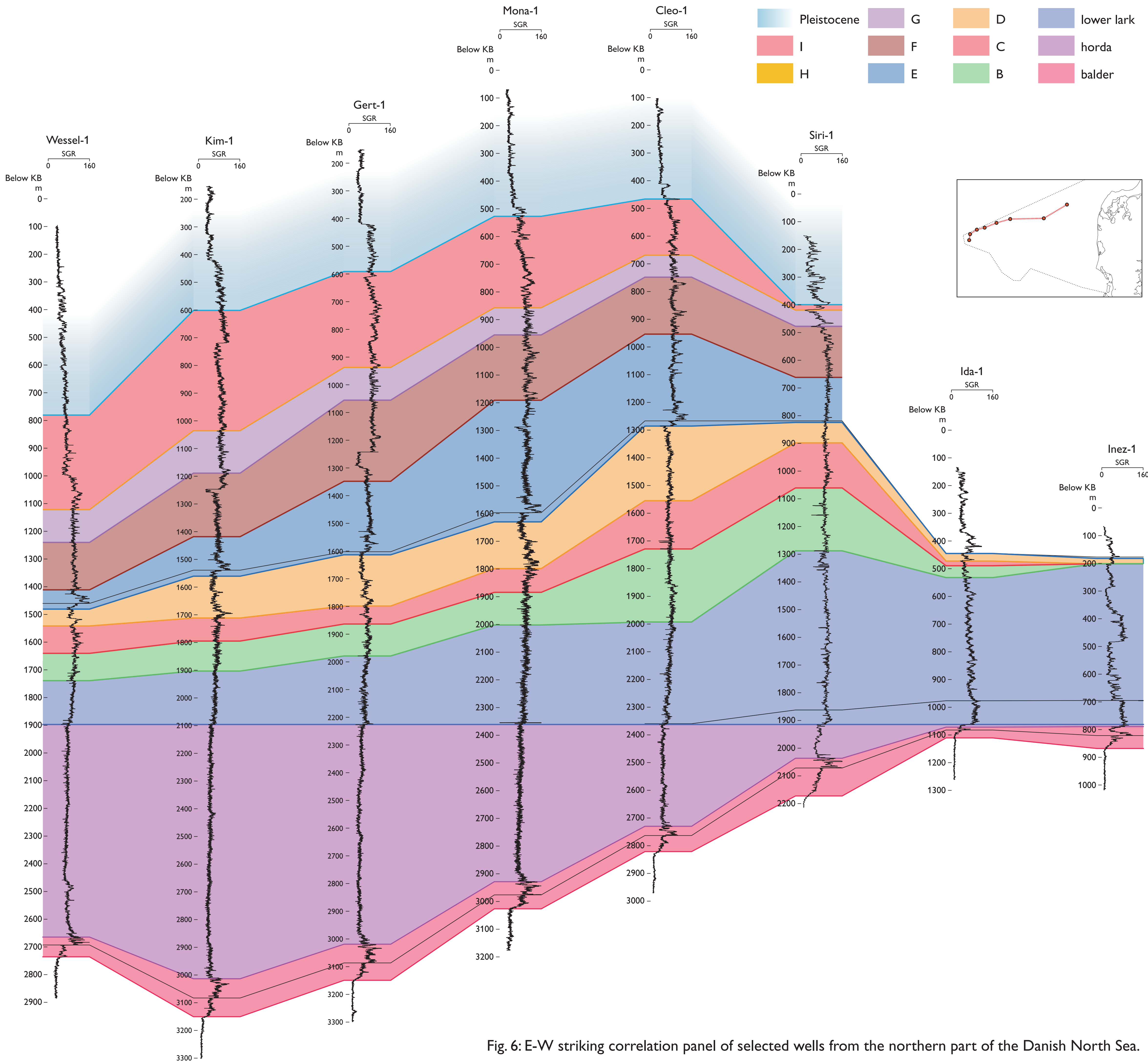

Fig. 6: E-W striking correlation panel of selected wells from the northern part of the Danish North Sea.

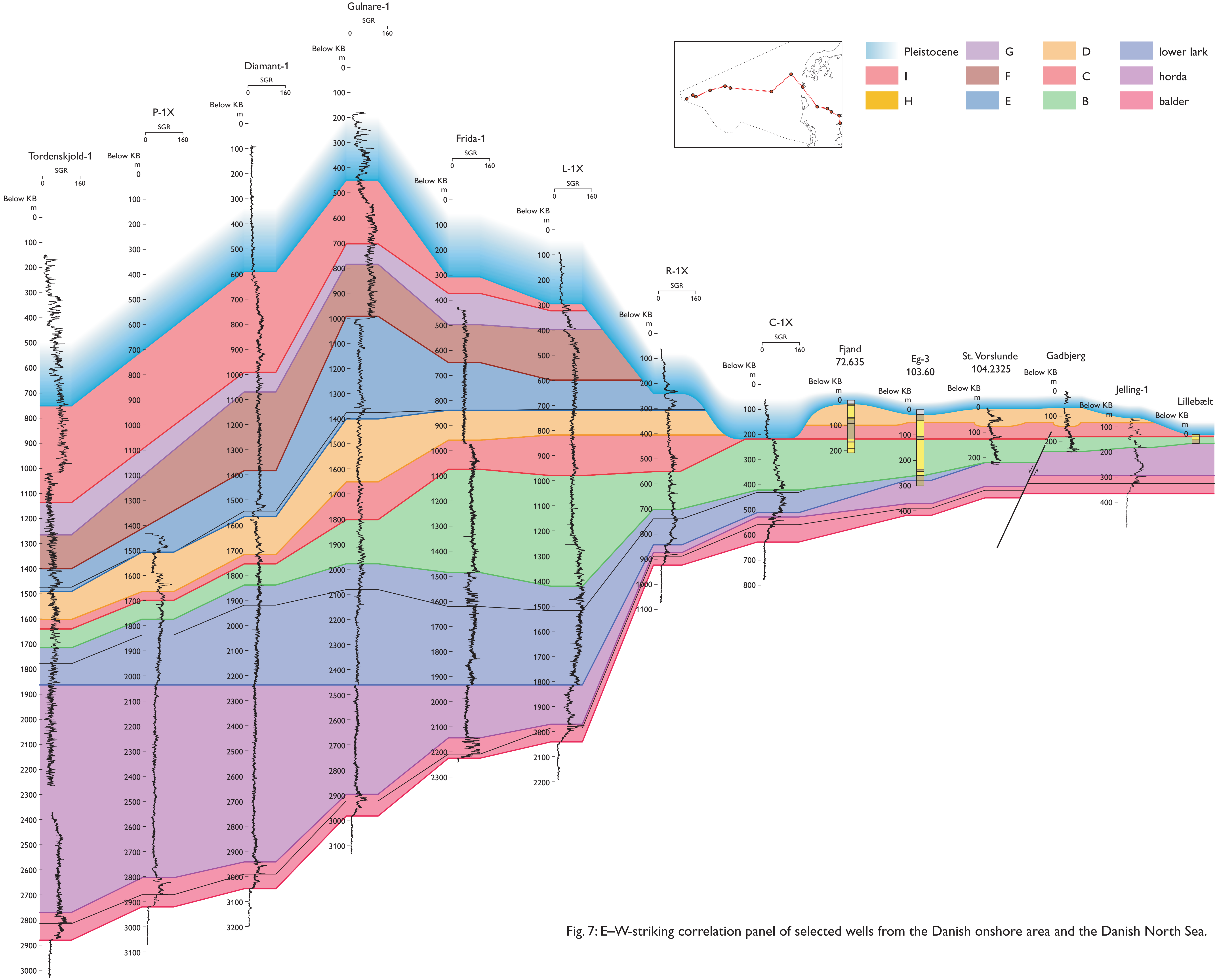

Fig. 7: E–W-striking correlation panel of selected wells from the Danish onshore area and the Danish North Sea.

balder

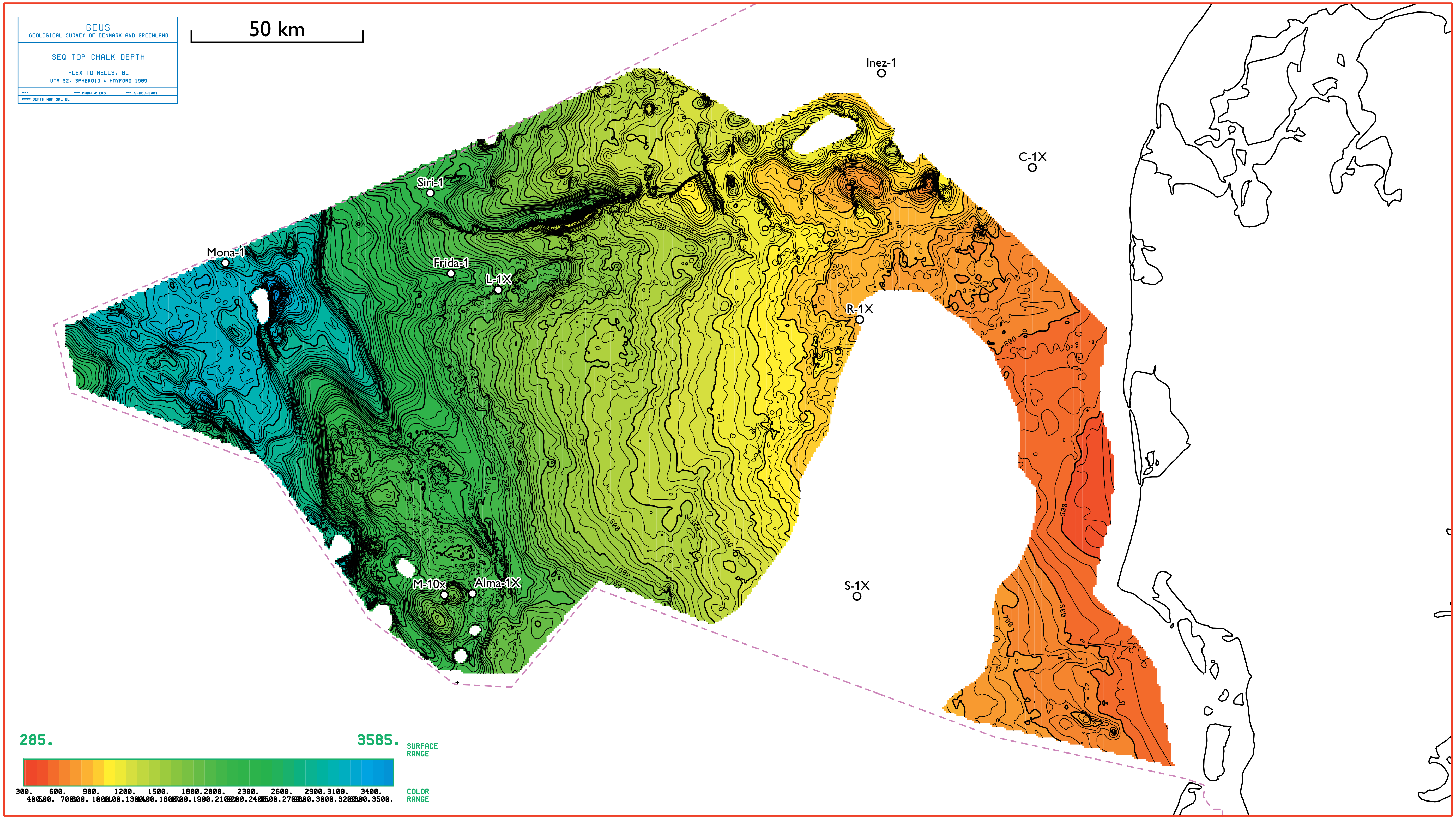

Fig. 8: Rogaland Seismic Sequence

The base surface forms a west-south-westward-dipping monocline whose minimum depth is 285 m and maximum depth is 3585 m. Steepest dip of the surface is found west and south-west of well L-1 and on the western flank of a spur that trends north-north-westwards from well Tove-1.

The thickness of the sequence varies from 5–395 m. The main depocentre was located in the westernmost part of the Danish Central Graben south of the Gert-1 well. Subordinate depocentres are present in a south east–north-west-trending area north-east of Alma-1 and north-east of the Siri-1 well. The depositional environment was characterised by open marine conditions in most of the area. Shallow marine and coastal conditions may have existed in the north-eastern and south-easternmost parts of the map area. The water depth probably did not exceed a few hundred metres. Sands that were laid down as gravity deposits are encountered in a more than-10-km-wide submarine canyon system (the Siri Canyon), oriented north-east–south-west. It originates from a shelf margin in the Norwegian sector, passes through the area around the Siri-1 well and the canyon mouth is located south-west of Cleo-1 and north of Gulnare-1 at the north-eastern boundary of the Central Graben.

balder

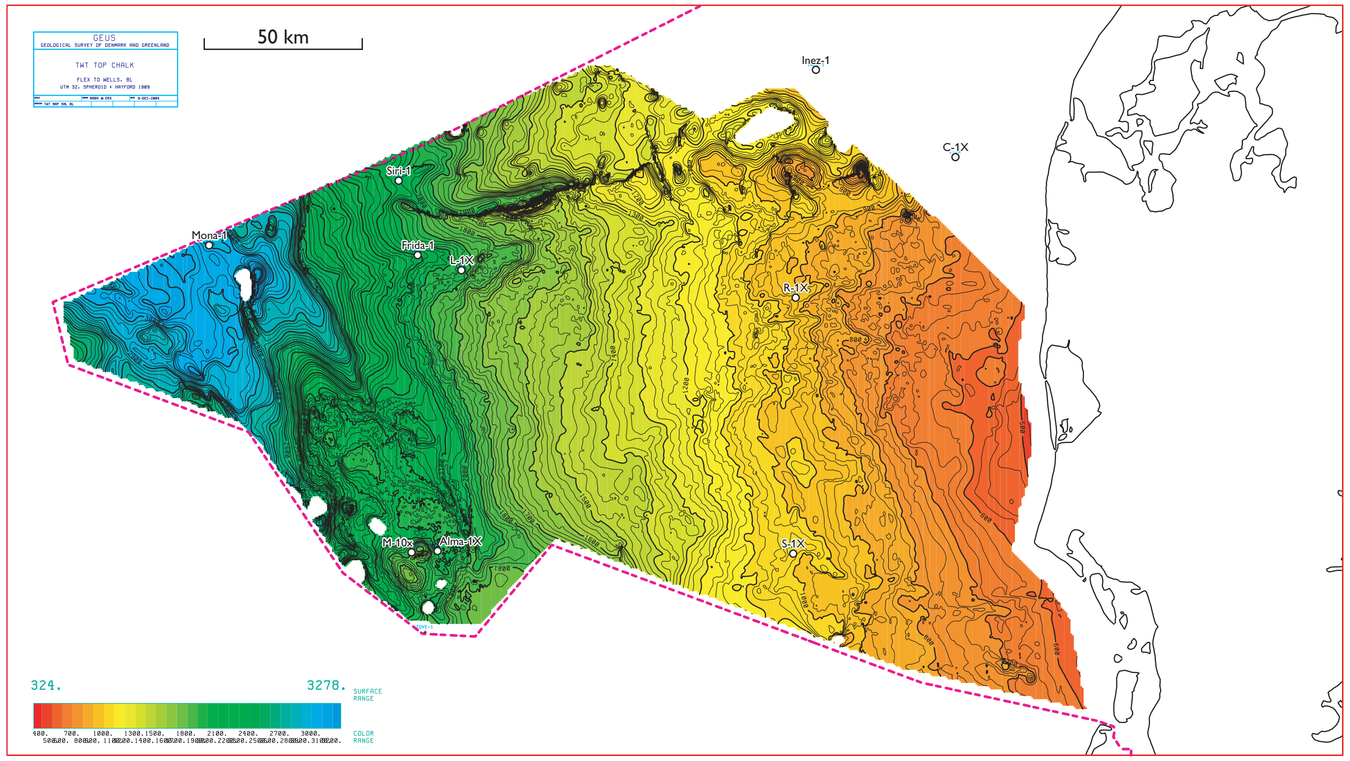

50 km
Inez-1
C-1X
Siri-1
Mona-1
Frida-1
L-1X
R-1X
S-1X
M-10x
Alma-1X
324.
3278.

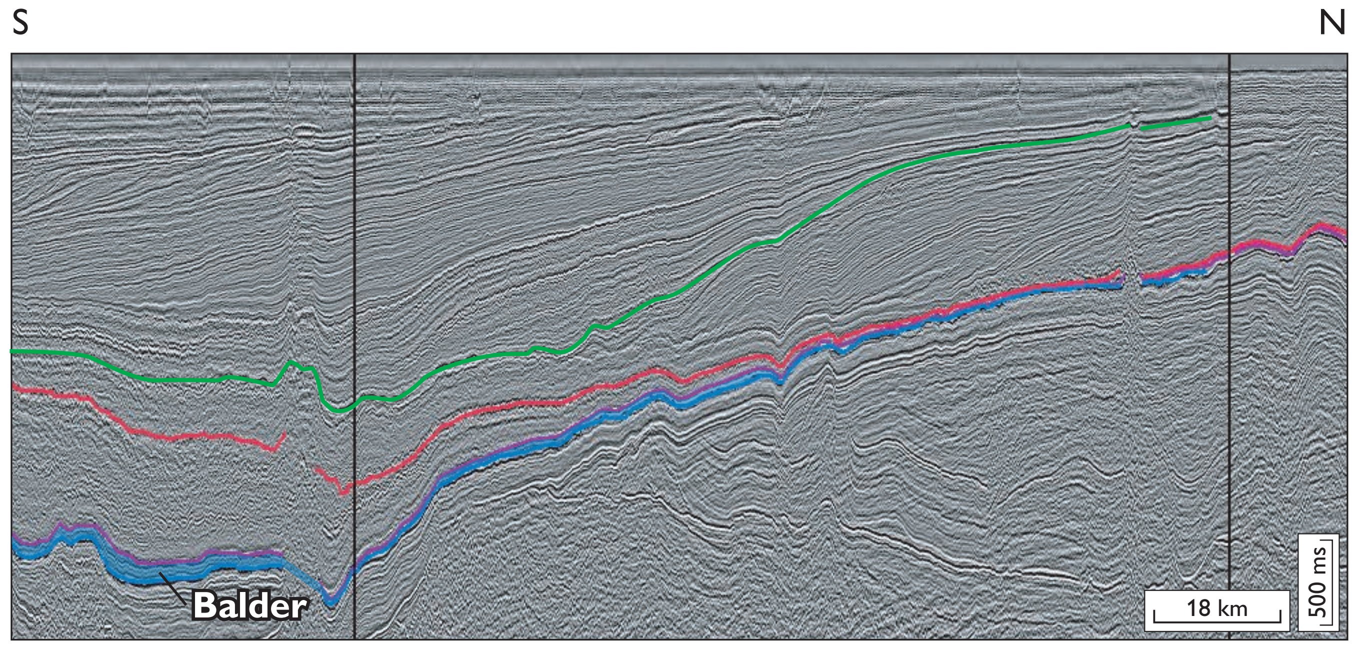

S
N
Balder
18 km
500 ms

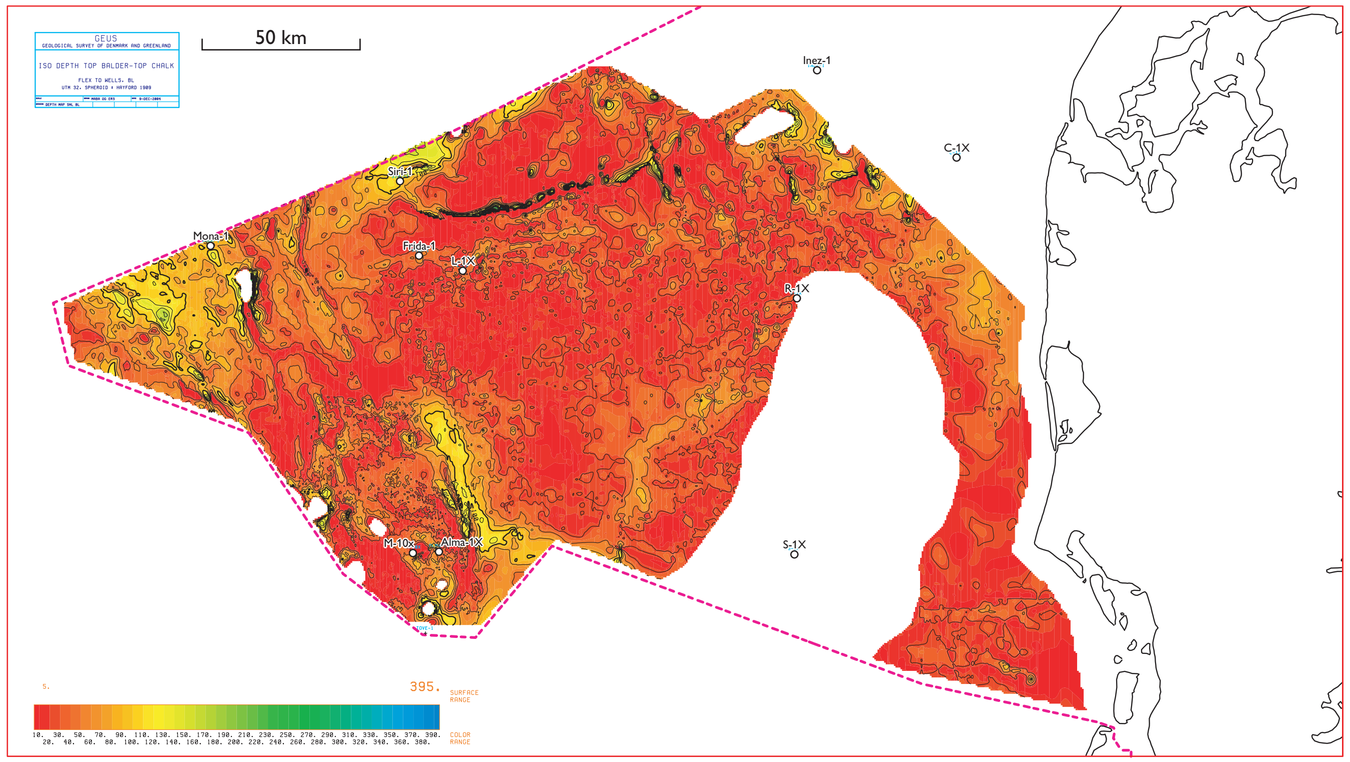

50 km
Inez-1
C-1X
Siri-1
Mona-1
Frida-1
L-1X
R-1X
S-1X
M-10x
Alma-1X
395.

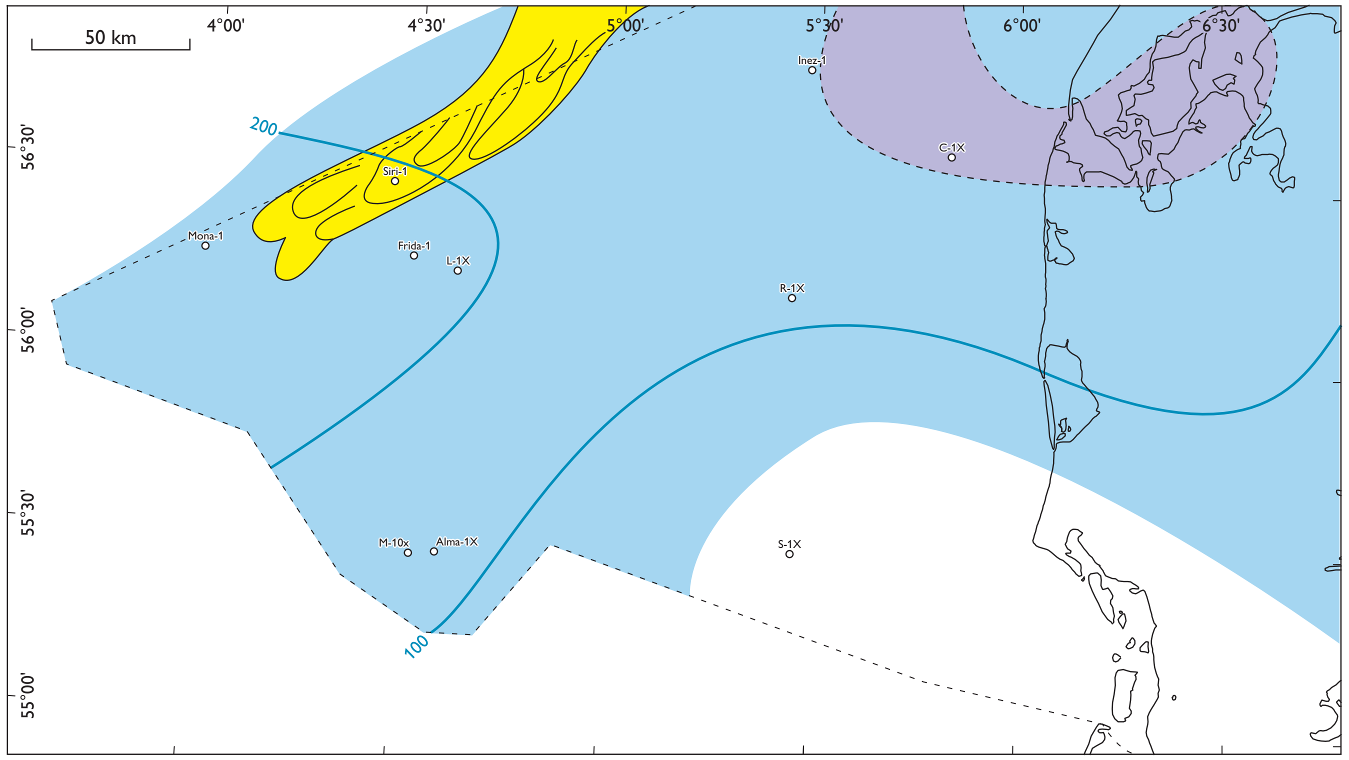

50 km
4°00'
4°30'
5°00'
5°30'
6°00'
6°30'
56°30'
56°00'
55°30'
55°00'
200
100
Inez-1
C-1X
Siri-1
Mona-1
Frida-1
L-1X
R-1X
M-10x
Alma-1X
S-1X

horda

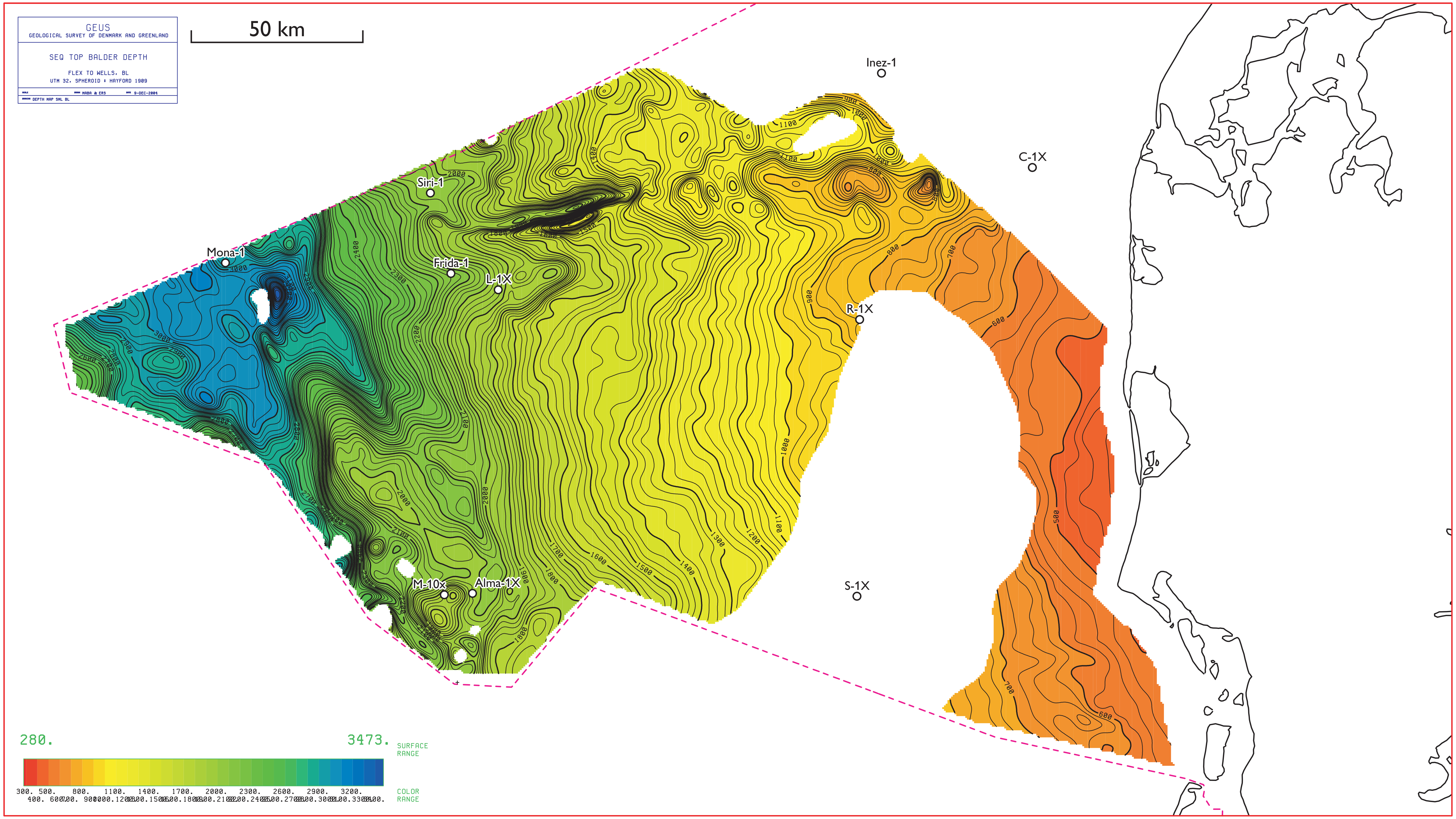

Fig. 9: horda Seismic Sequence

The Base surface forms a west-south-westward-dipping monocline whose minimum depth is 280 m and maximum depth is 3473 m. Steepest dip of the surface is found along a north–south trend immediately west of Siri-1 and on the western flank of a spur that trends north–north-west from well Tove-1.

The sequence varies from 0–904 m thick. The main depocentre was located in the westernmost part of the Danish Central Graben area along a trend to the south and south-east of well Kim-1. The depositional environment was characterised by open marine conditions throughout the area and. The water depths may have exceeded 900 m in the western part of the area. Submarine fan deposits known from the Norwegian “sector north of the wells Siri-1 and Cleo-1 may extend into the study area.

horda

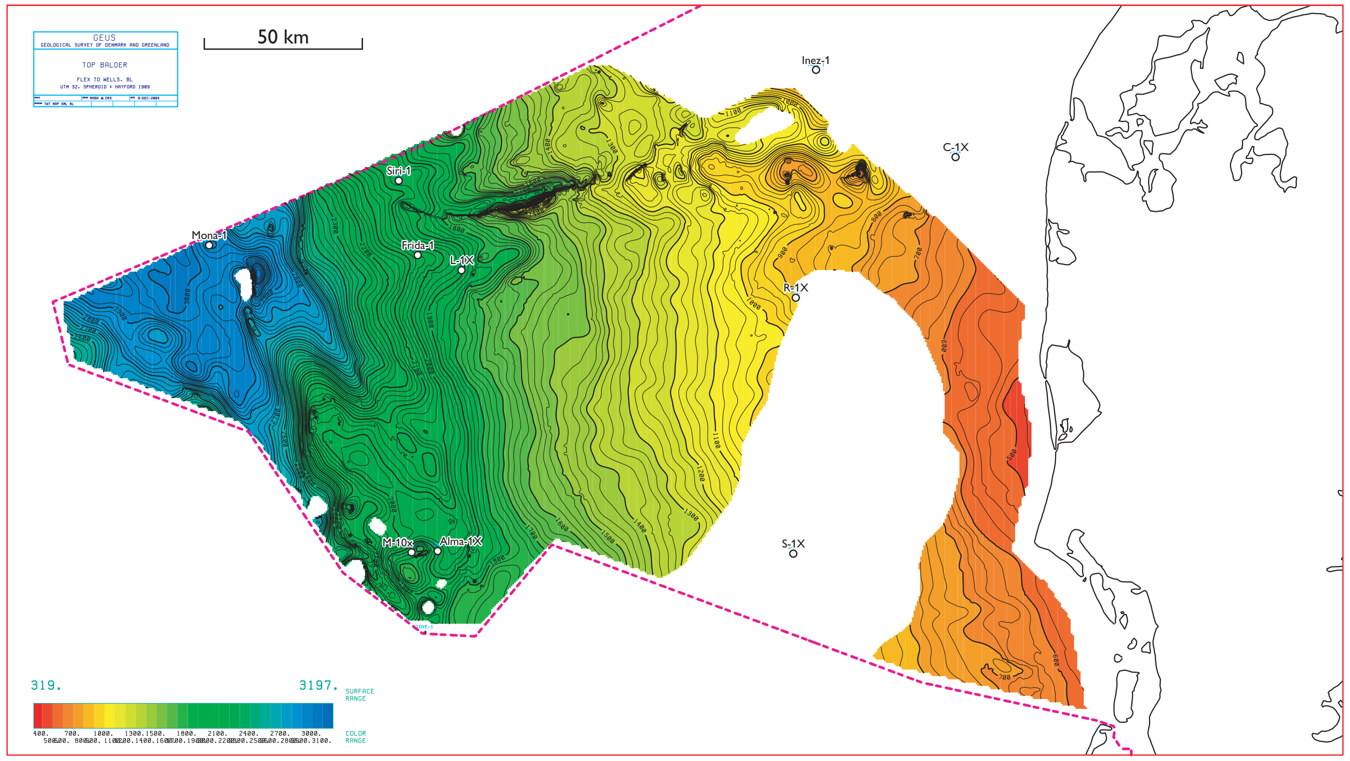
GEUS
TOP BALDER
50 km
Inez-1
C-1X
Siri-1
Mona-1
Frida-1
L-1X
R-1X
S-1X
M-10x
Alma-1X
319.
3197.

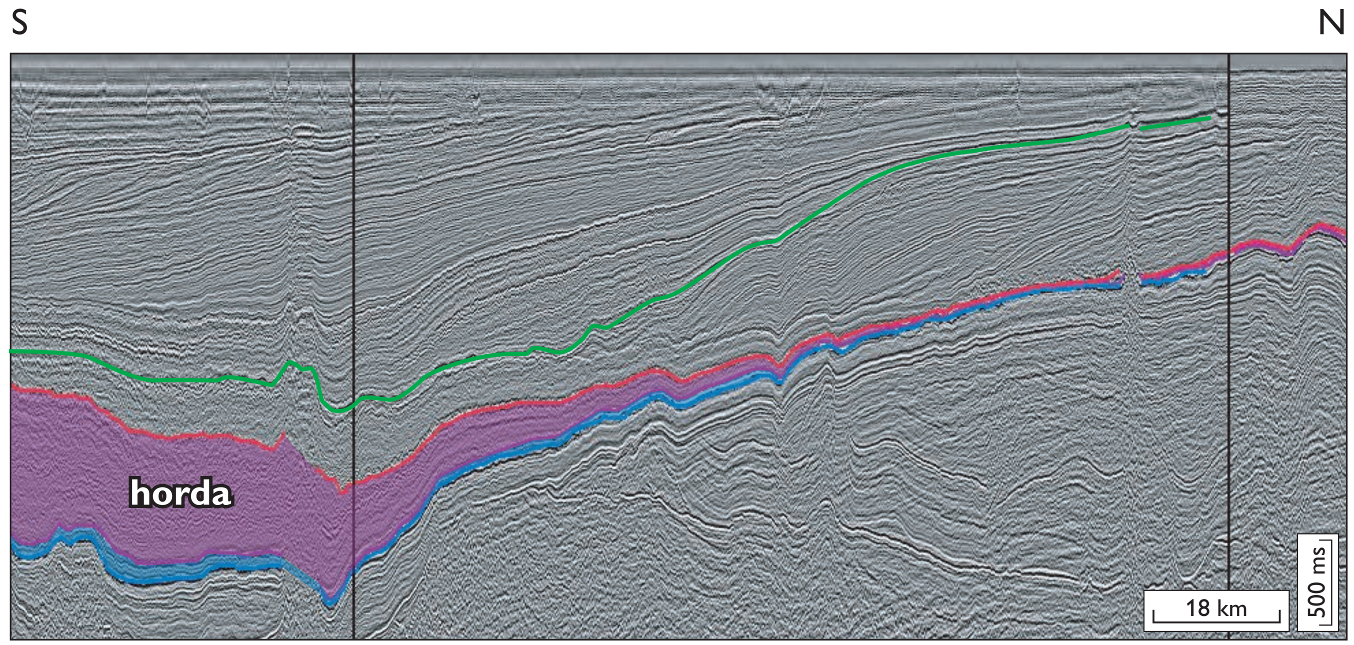
S
N
horda
18 km
500 ms

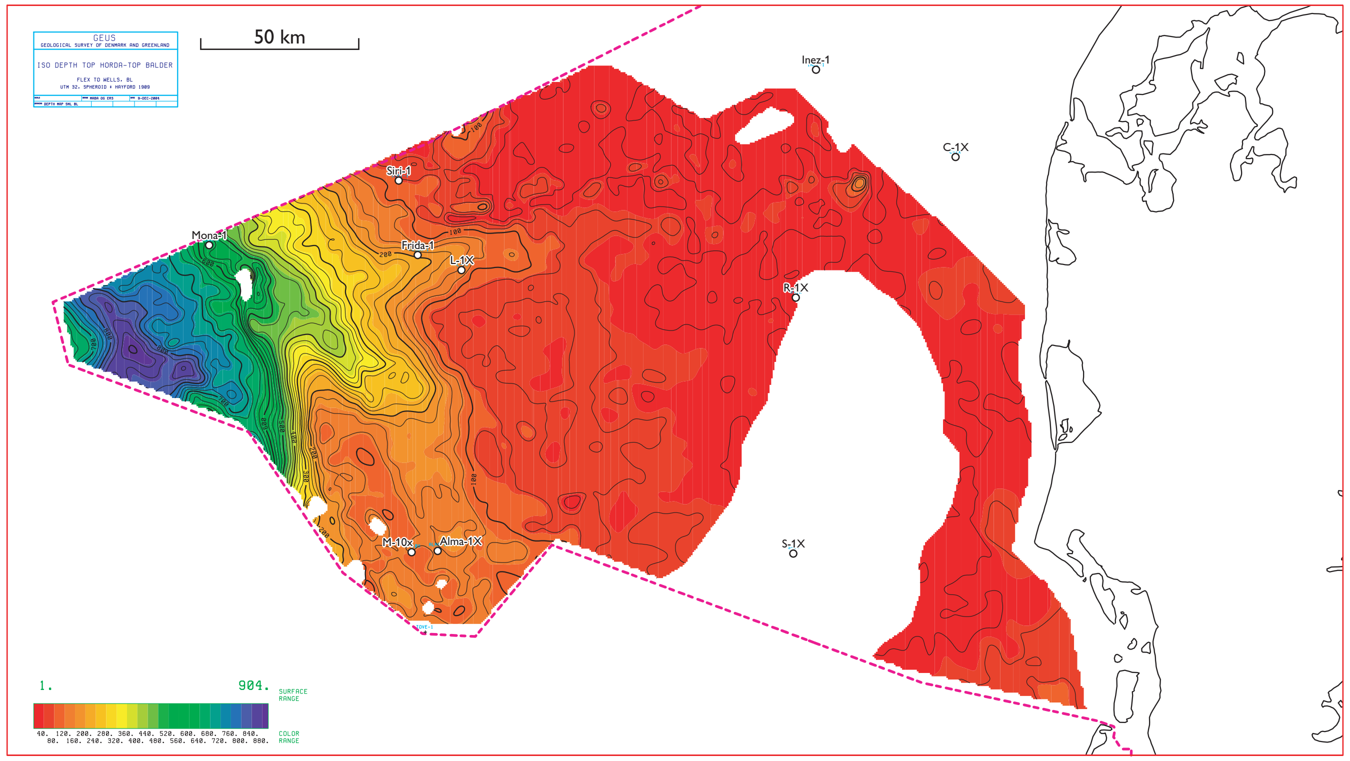
GEUS
50 km
Inez-1
C-1X
Siri-1
Mona-1
Frida-1
L-1X
R-1X
S-1X
M-10x
Alma-1X
1.
904.

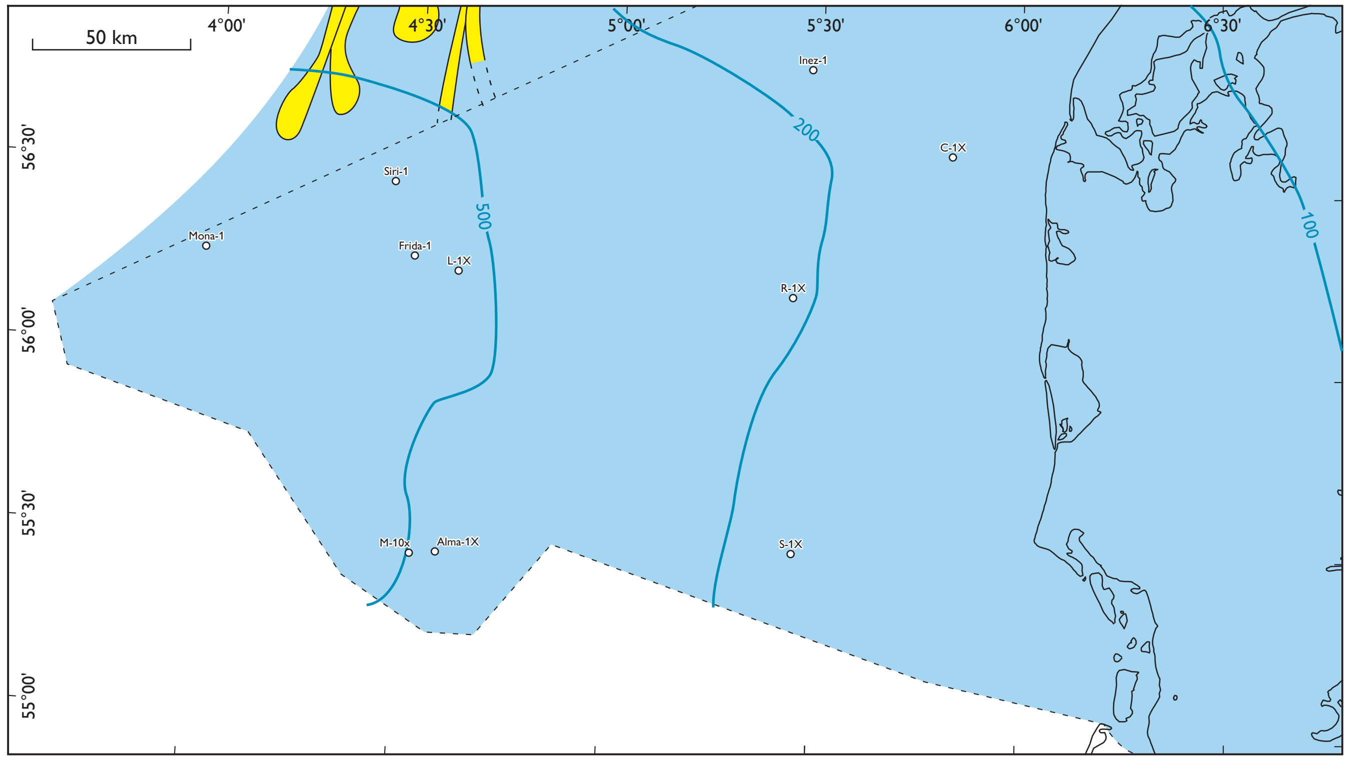
50 km
4°00'
4°30'
5°00'
5°30'
6°00'
6°30'
56°30'
56°00'
55°30'
55°00'
Inez-1
C-1X
Siri-1
Mona-1
Frida-1
L-1X
R-1X
S-1X
M-10x
Alma-1X
500
200
100

lower lark

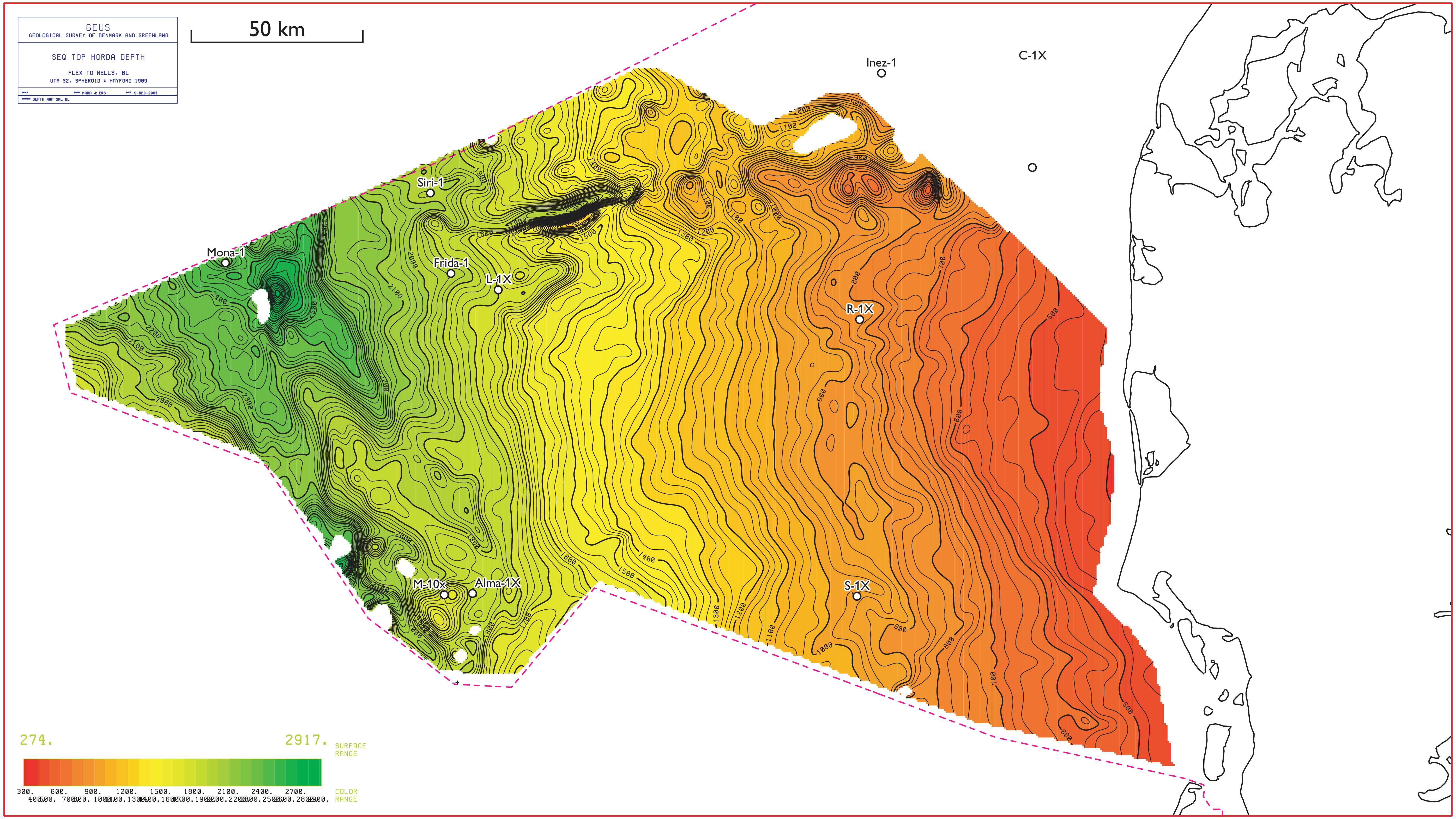

Fig. 10: lower lark Seismic Sequence

The base surface forms a west-south-westward-dipping monocline whose minimum depth is 274 m and maximum depth is 2917 m. Steepest dip of the surface is found along a north–south trend immediately west of Siri-1 and on the western flank of a spur that trends north-north-west from well Tove-1. Increased dips are also found along a north–south trend east of the Siri-1 well. The thickness of the sequence varies from 5 to 1124 m. The main depocentre was located north-east of the Siri-1 well.

The depositional environment was characterised by marginal marine to coastal plain in the north-eastern part of the area and by open marine conditions in the south-western part of the area. The water depth may have exceeded 800 m in the western part of the area. Submarine fans entered the deep-marine basins from entry points on an east–west-trending shelf break. One entry point was near the F-1 well and thick submarine fanswere deposited in the Inez-1 area. Turbidite sand deposits encountered in the area around the Frida-1 well are likely to have had an entry point north of the Siri-1 well in the Norwegian sector. Thinner fan sands may be encountered in the feeder channel systems that emerged from the entry points.

lower lark

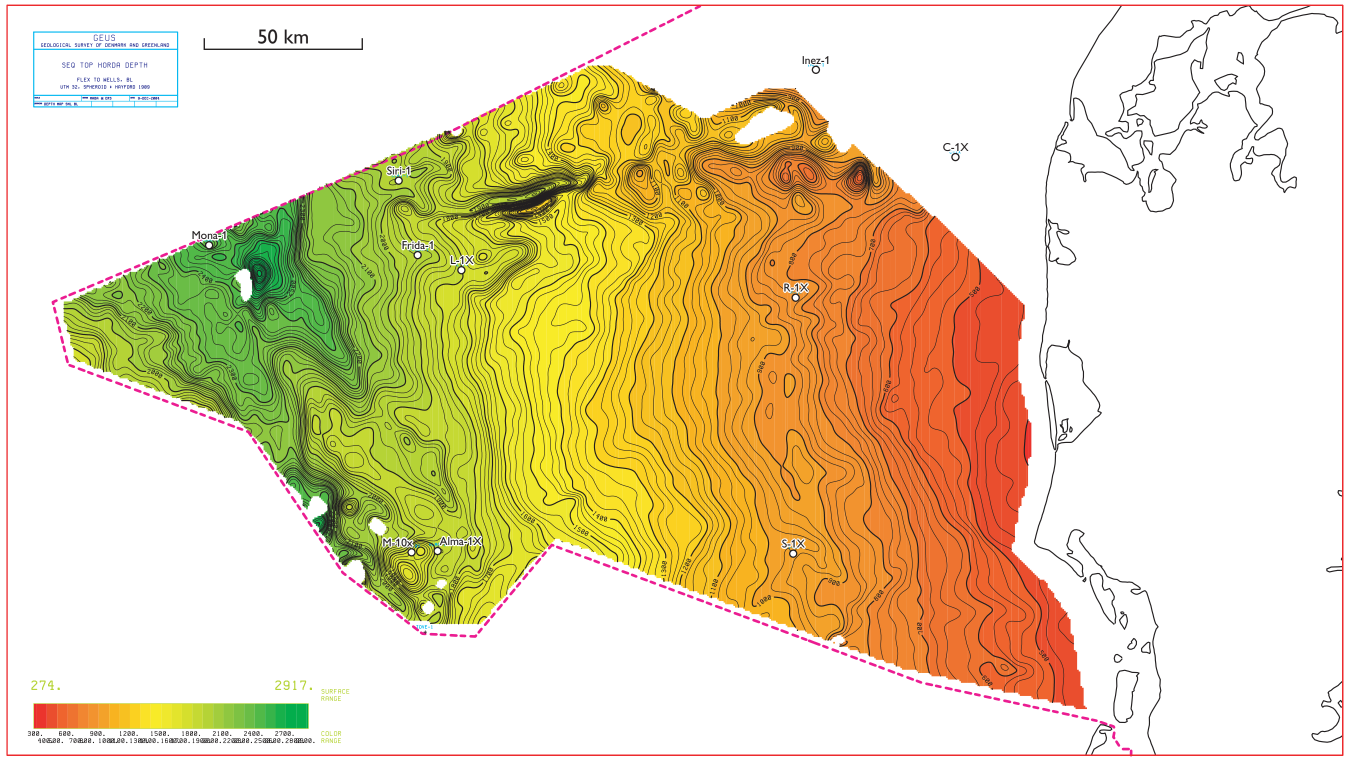

50 km
Inez-1
C-1X
Siri-1
Mona-1
Frida-1
L-1X
R-1X
M-10x
Alma-1X
S-1X
274.
2917.

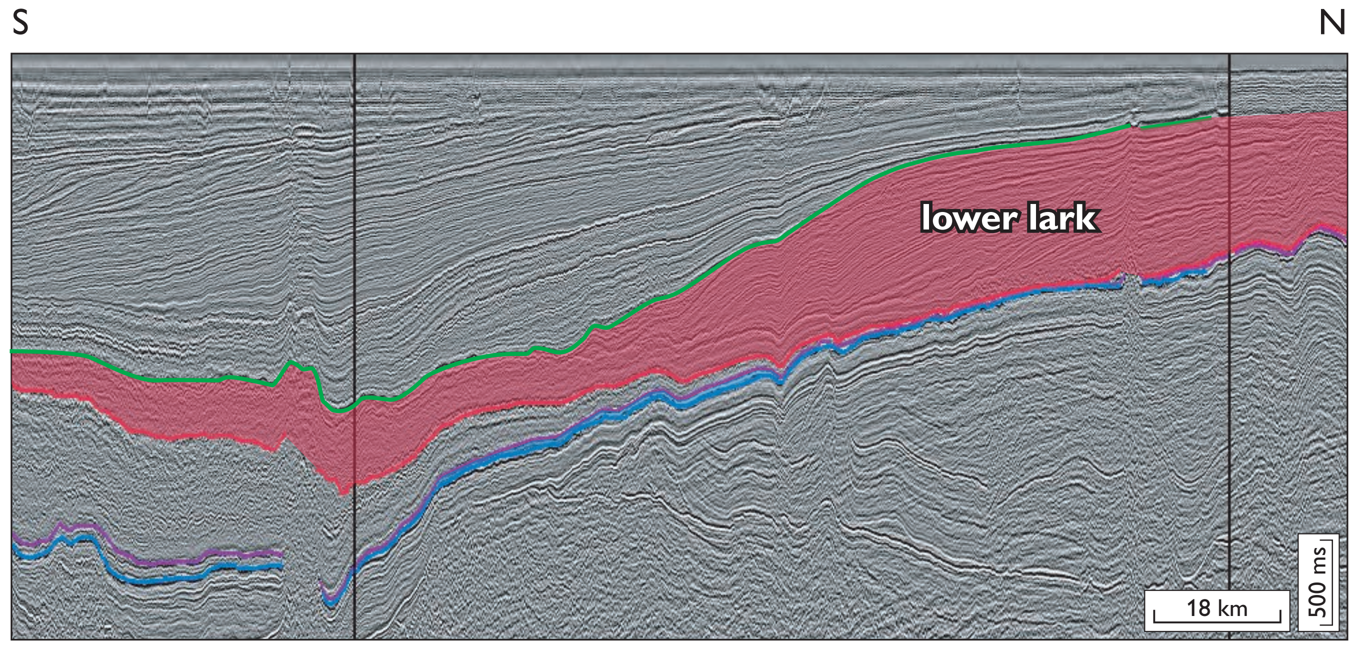

S
N
lower lark
18 km
500 ms

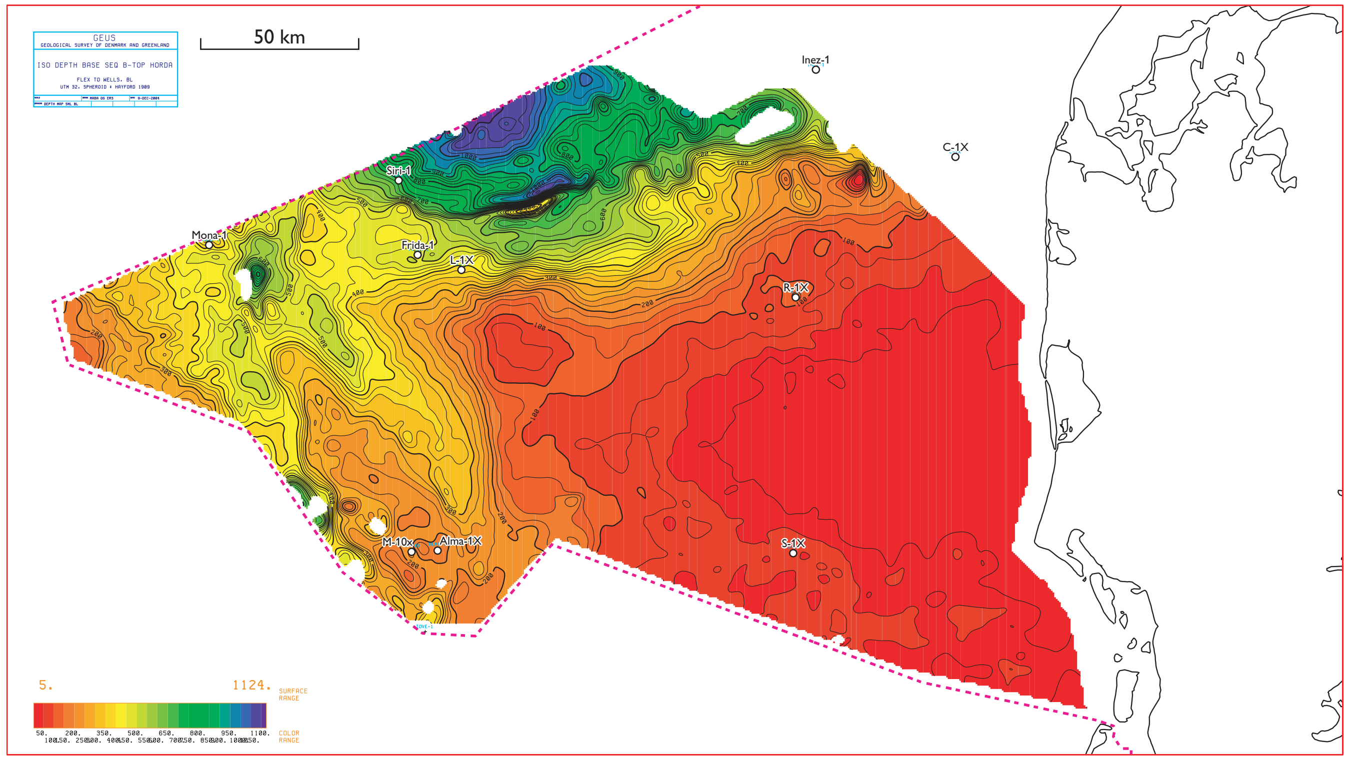

50 km
Inez-1
C-1X
Siri-1
Mona-1
Frida-1
L-1X
R-1X
M-10x
Alma-1X
S-1X
5.
1124.

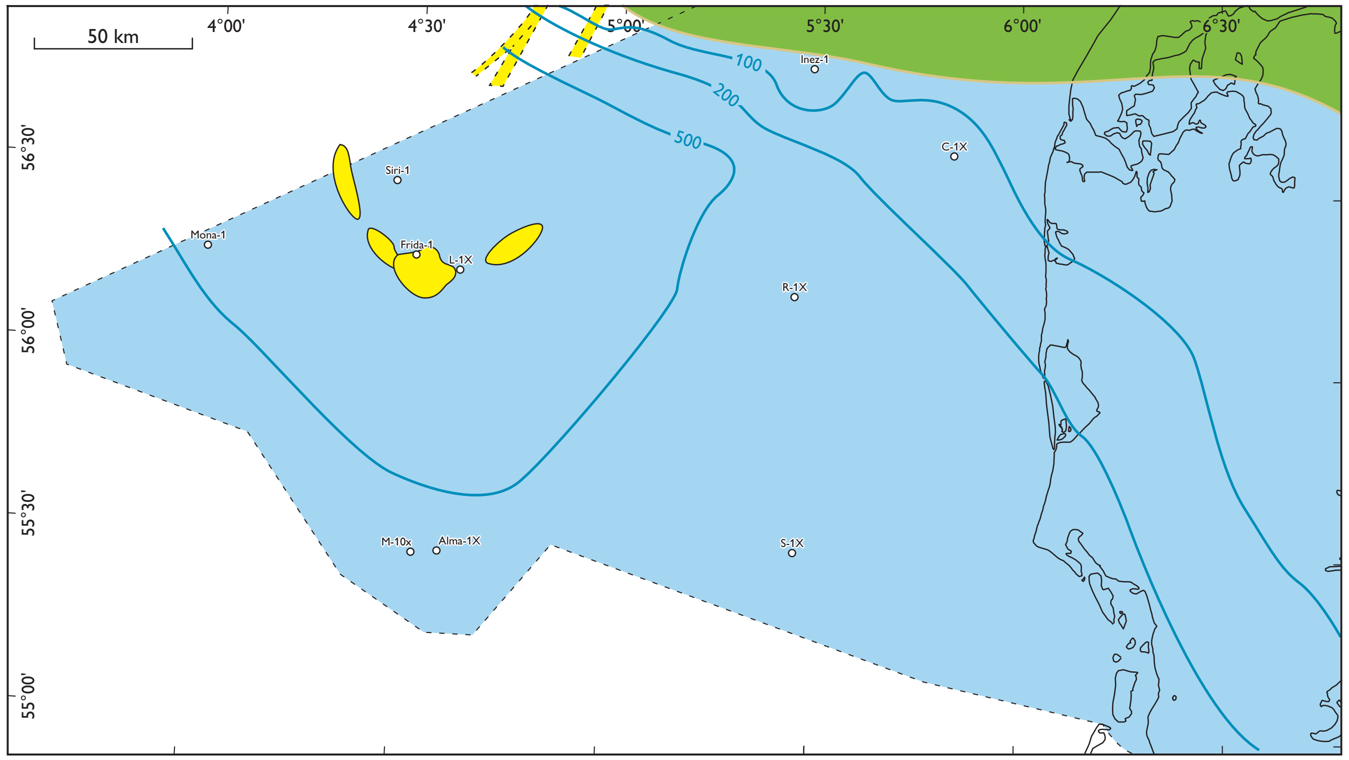

50 km
4°00'
4°30'
5°00'
5°30'
6°00'
6°30'
100
200
500
56°30'
56°00'
55°30'
55°00'
Inez-1
Siri-1
C-1X
Mona-1
Frida-1
L-1X
R-1X
M-10x
Alma-1X
S-1X

Sequence B

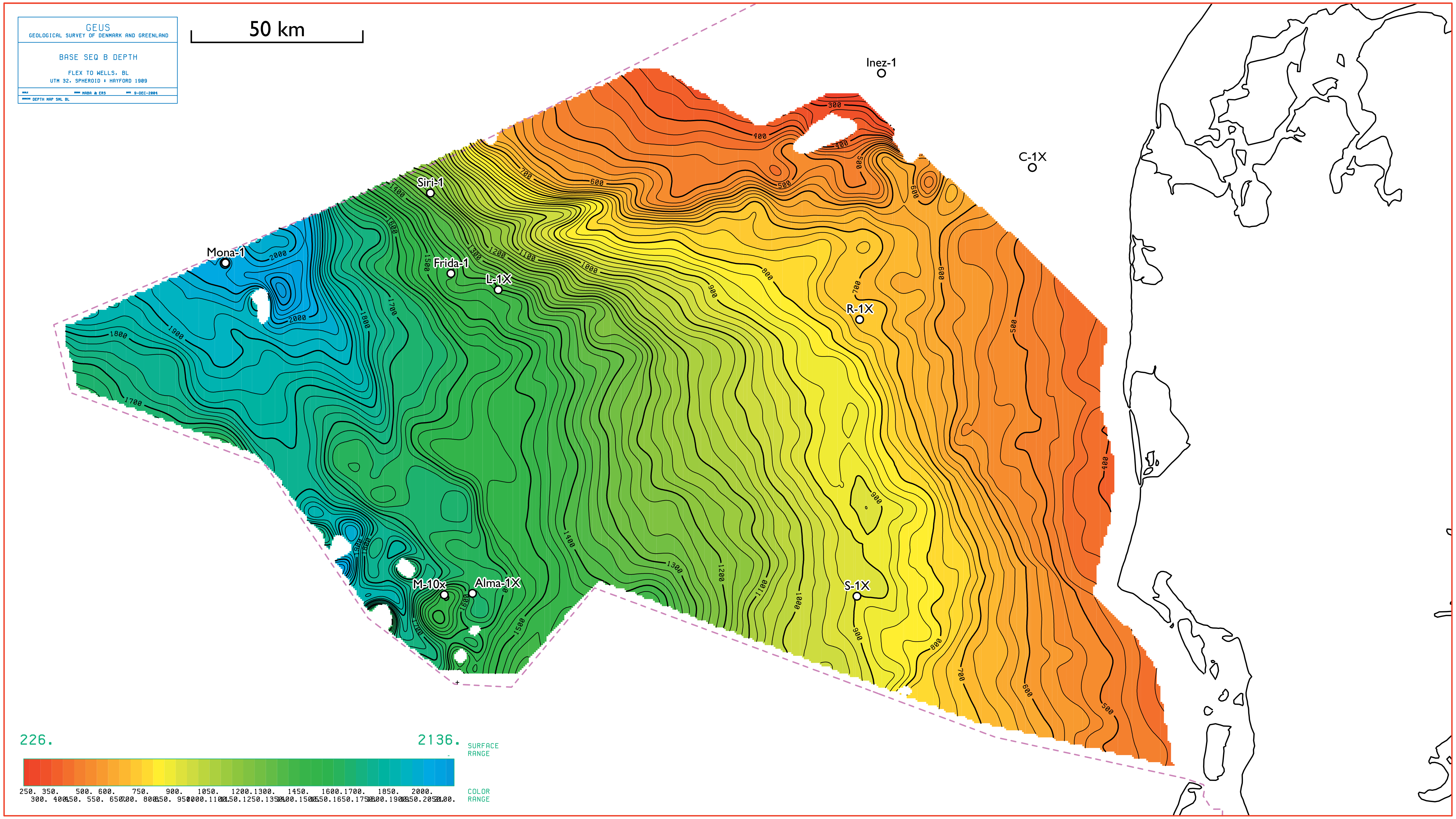

Fig. 11: Sequence B
The Base surface forms a west-south-westward-dipping monocline whose minimum depth is 226 m and maximum depth is 2136 m. Steepest dip of the surface is found south-west of the Inez-1 and west of the Frida-1 wells. Distinct variations in depth are found around diapiric structures in the extreme south-western part of the area. The thickness of the sequence varies from 0–449 m. The main depocentre was located around the Frida-1 and L-1 wells and south-west of the C-1 well. The reduced thickness in the northern part is a result of truncation of the sequence towards the north-east. The depositional environment was characterised by coastal plain and deltaic deposits in the north-eastern and eastern part of the area and by open marine conditions in the south-western part of the area. The water depth was up to 500 m in the western most part of the area.

Sequence B

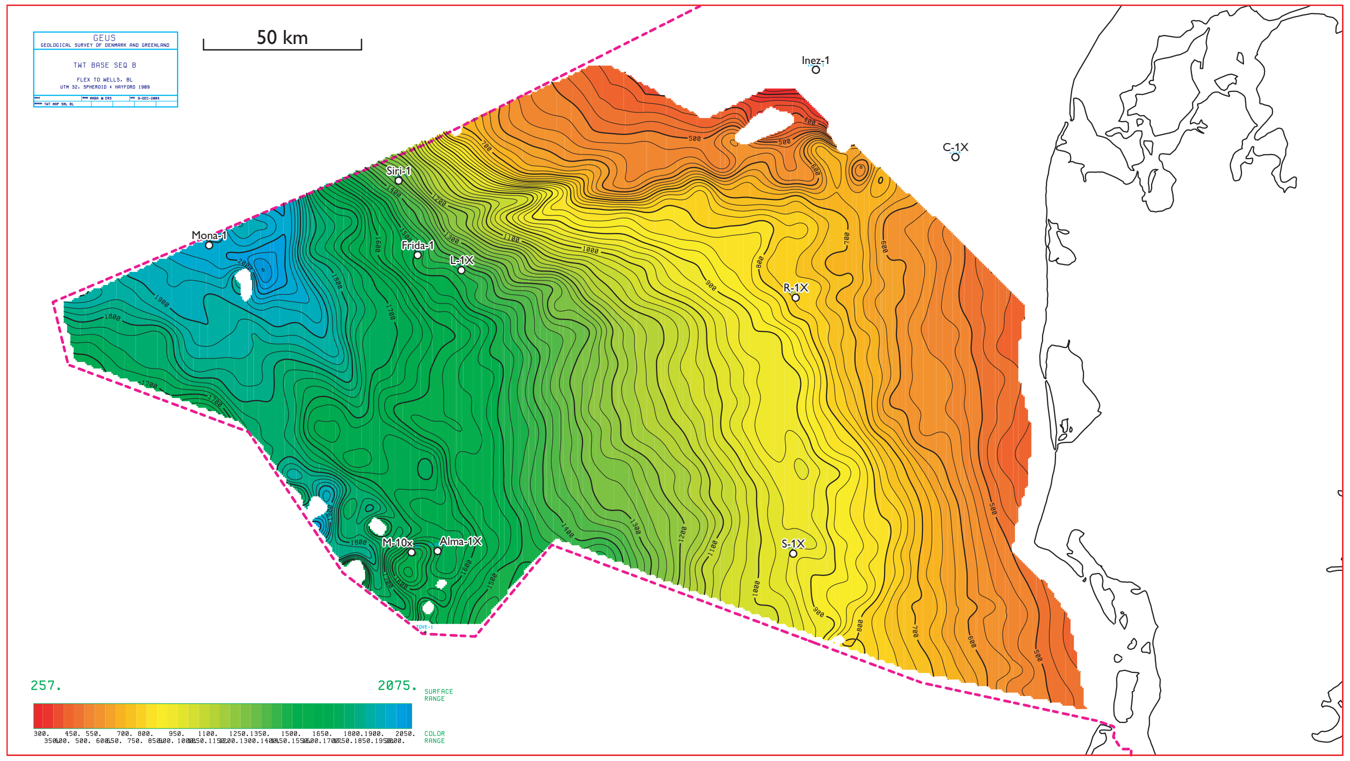
GEUS
TWT BASE SEQ B
50 km
Inez-1
C-1X
Siri-1
Mona-1
Frida-1
L-1X
R-1X
M-10x
Alma-1X
S-1X
257.
2075.

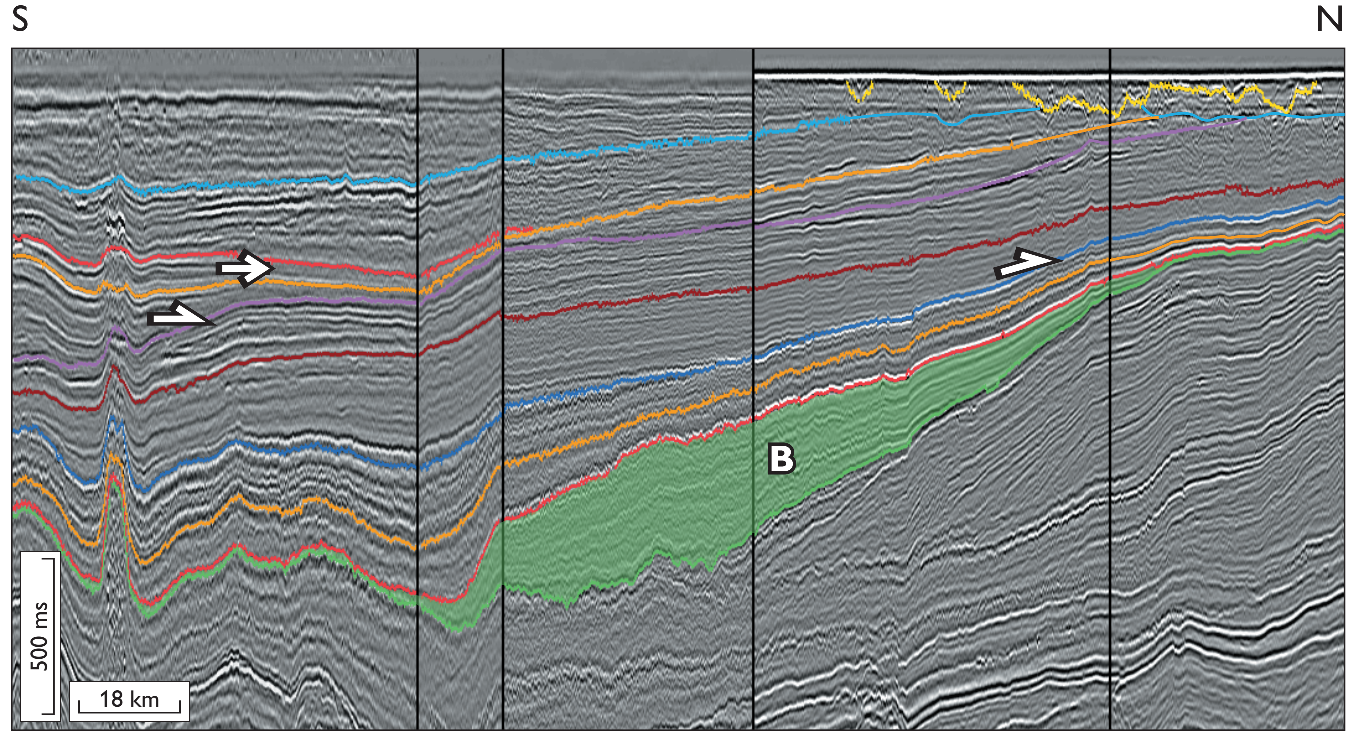
S
N
B
500 ms
18 km

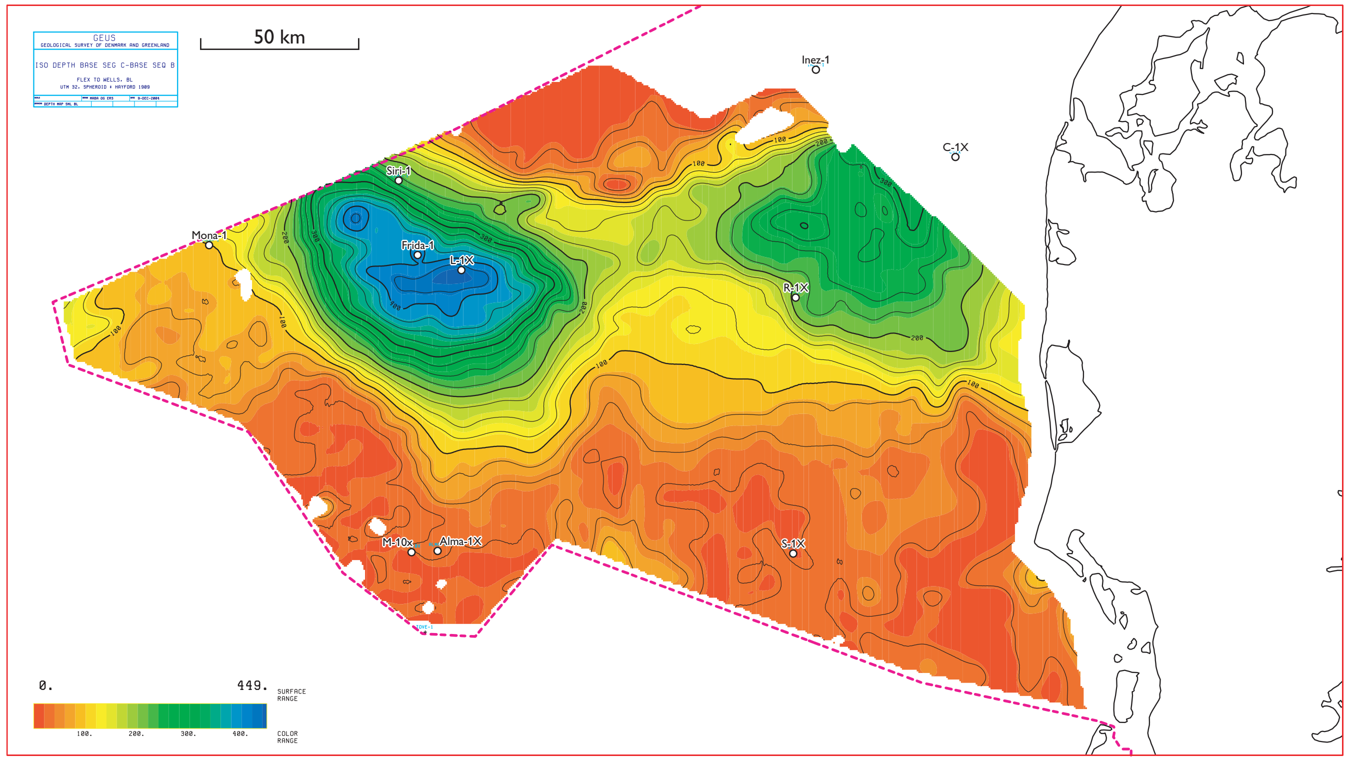
GEUS
ISO DEPTH BASE SEQ C-BASE SEQ B
50 km
Inez-1
C-1X
Siri-1
Mona-1
Frida-1
L-1X
R-1X
M-10x
Alma-1X
S-1X
0.
449.

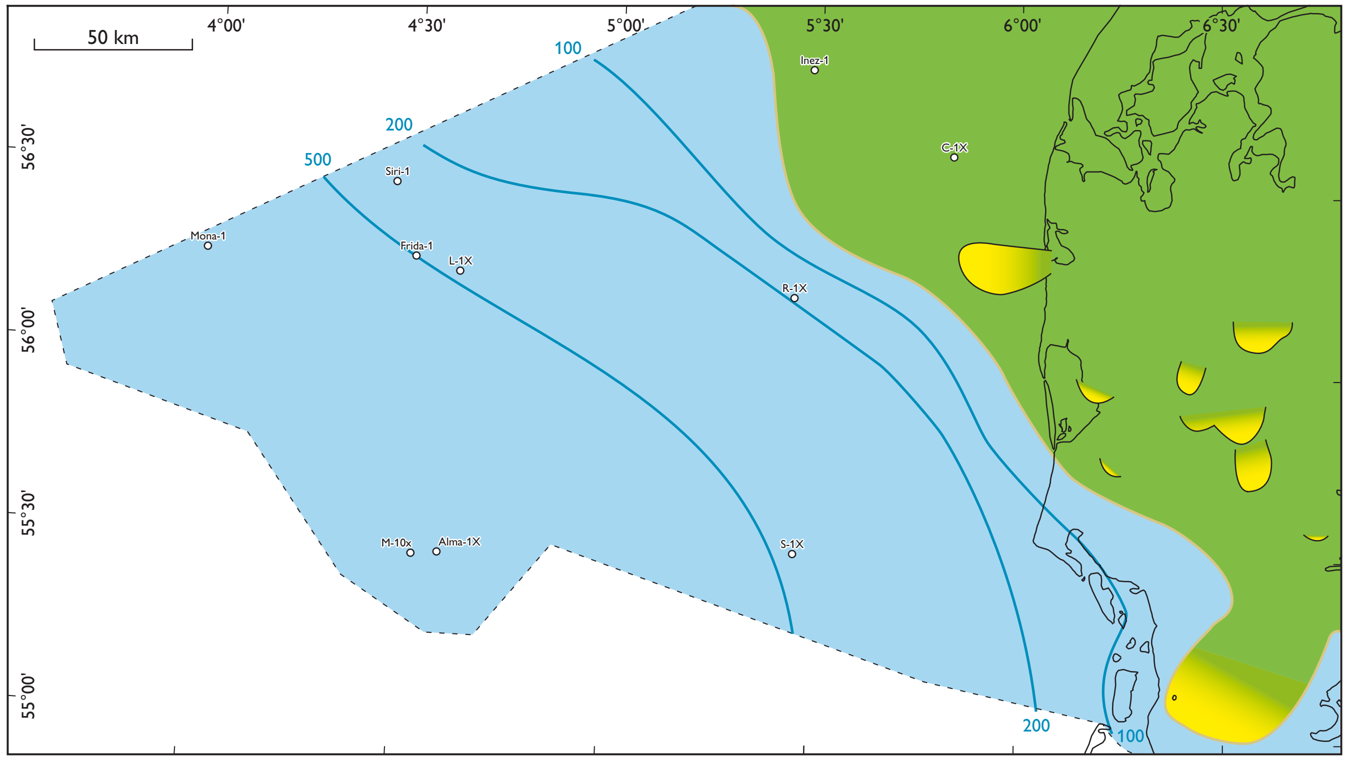
50 km
4°00'
4°30'
5°00'
5°30'
6°00'
6°30'
56°30'
56°00'
55°30'
55°00'
100
200
500
Inez-1
C-1X
Siri-1
Mona-1
Frida-1
L-1X
R-1X
M-10x
Alma-1X
S-1X
200
100

Sequence C

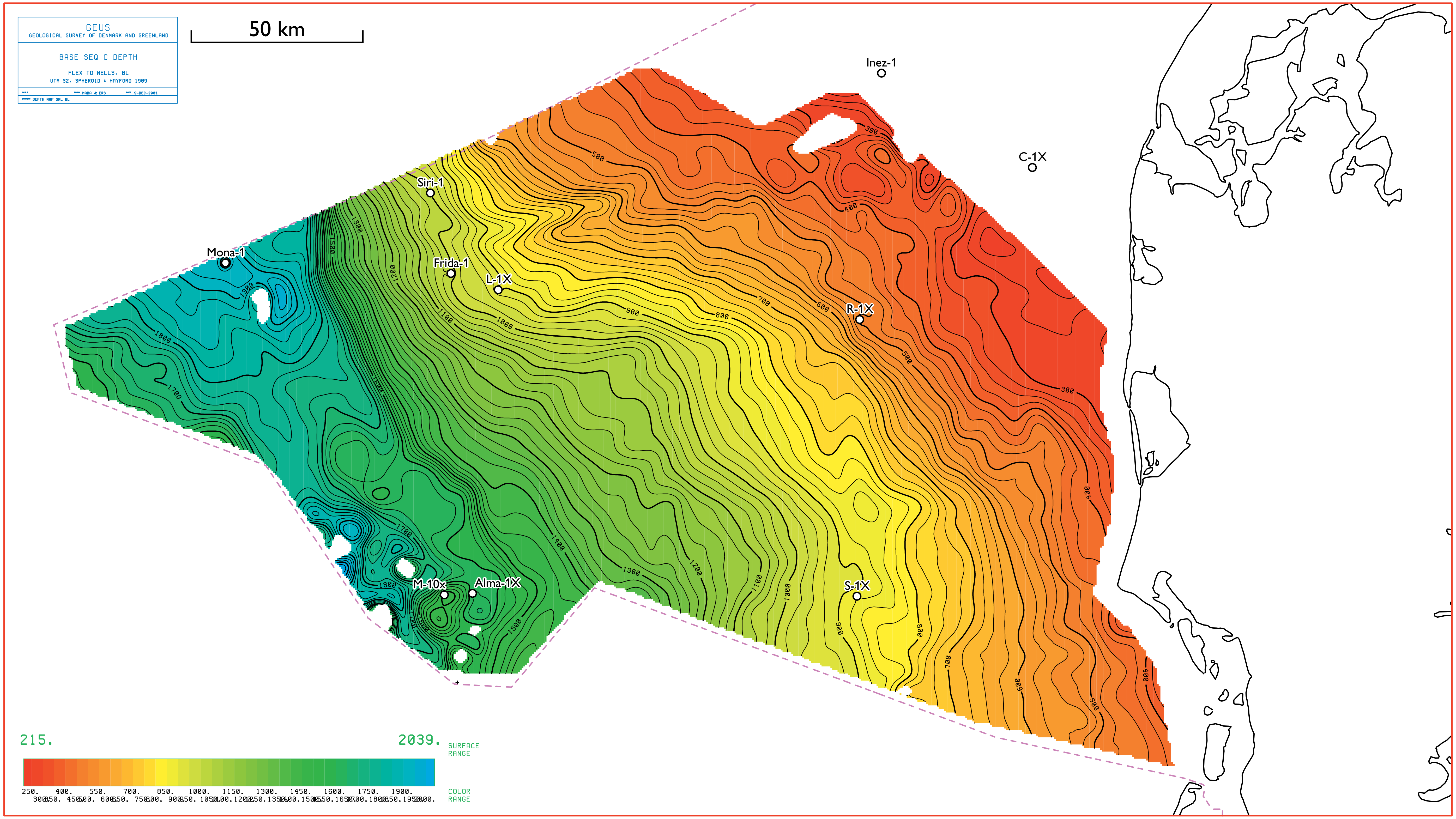

Fig. 12: Sequence C
The base surface forms a west-south-westward-dipping monocline whose minimum depth is 215 m and maximum depth is 2039 m. Steepest dip of the surface is found west of the Frida-1 well. Distinct variations in depth are found around diapiric structures in the extreme south-western part of the area.
The thickness of the sequence varies from 5–353 m. The main depocentre was elongated E–W- in the central part of the area between Alma-1 and R-1. The reduced thickness to the north is a result of truncation of the sequence towards the north-east. The depositional environment was characterised by coastal plain and deltas in the north-eastern part of the area and by open marine conditions in the south-western part of the area. Water depths were up to 500 m.

Sequence C

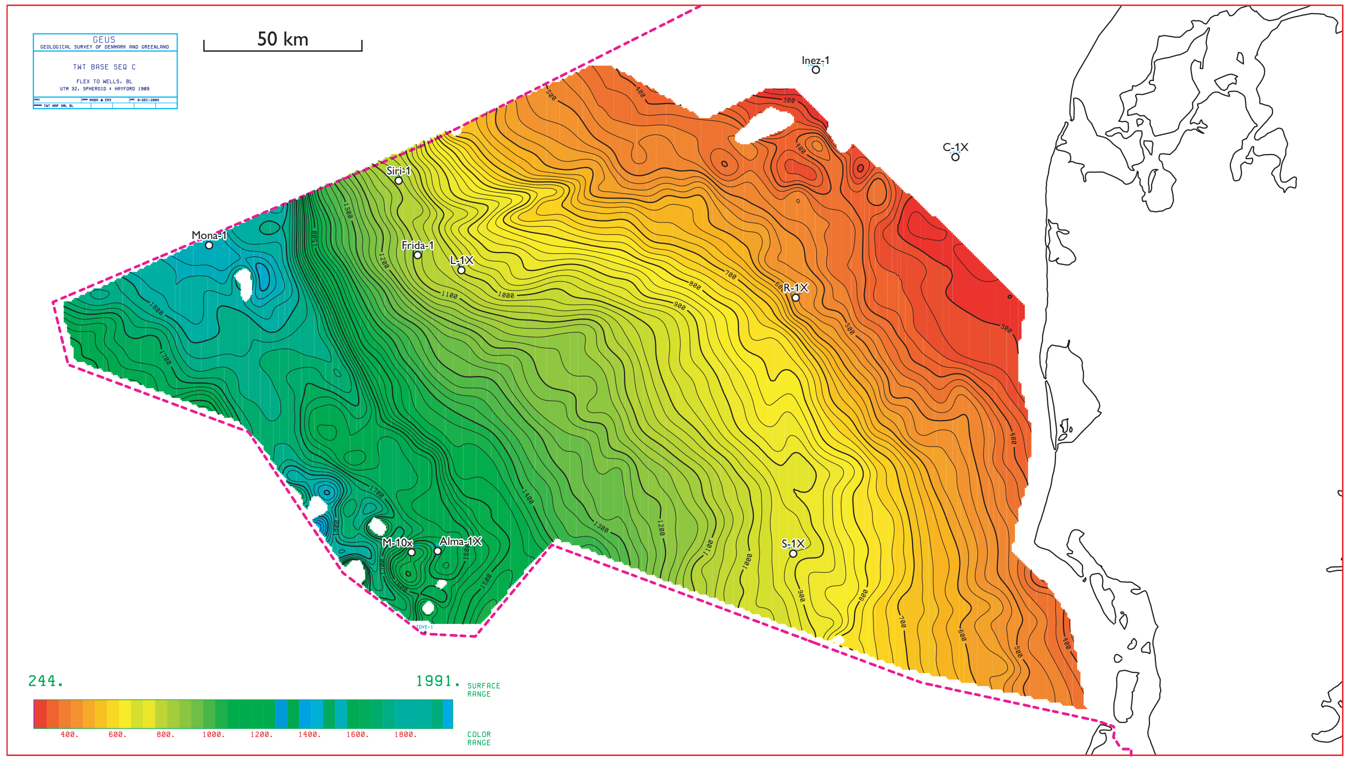

50 km
Inez-1
C-1X
Siri-1
Mona-1
Frida-1
L-1X
R-1X
S-1X
M-10x
Alma-1X
244.
1991.

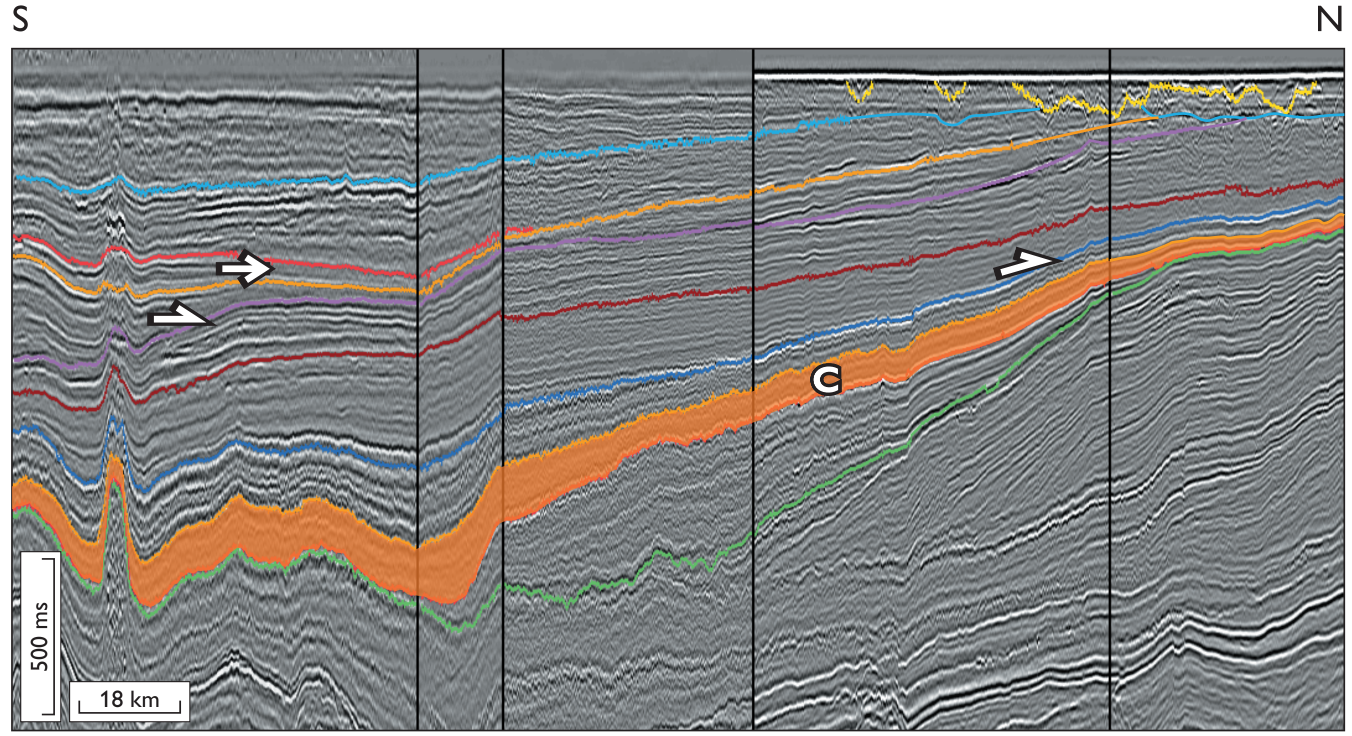

S
N
C
500 ms
18 km

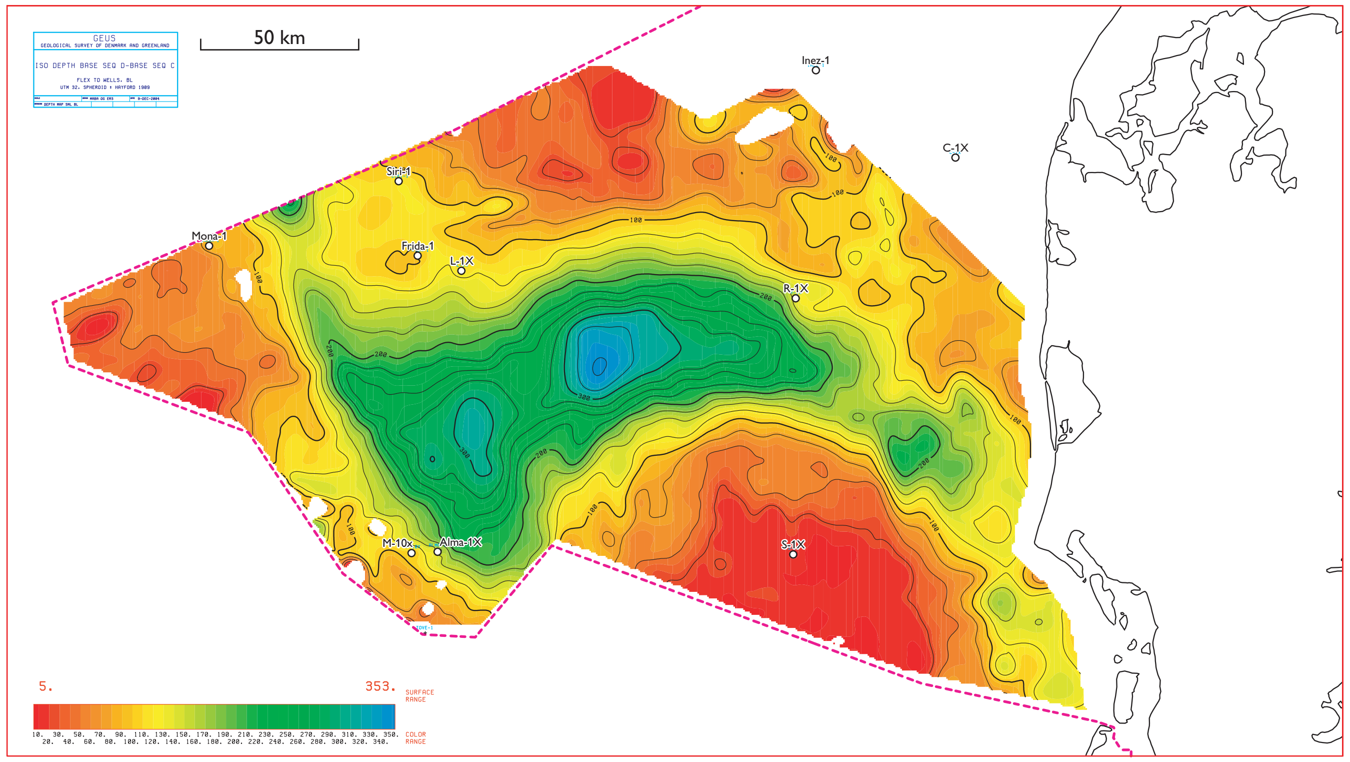

50 km
Inez-1
C-1X
Siri-1
Mona-1
Frida-1
L-1X
R-1X
S-1X
M-10x
Alma-1X
5.
353.

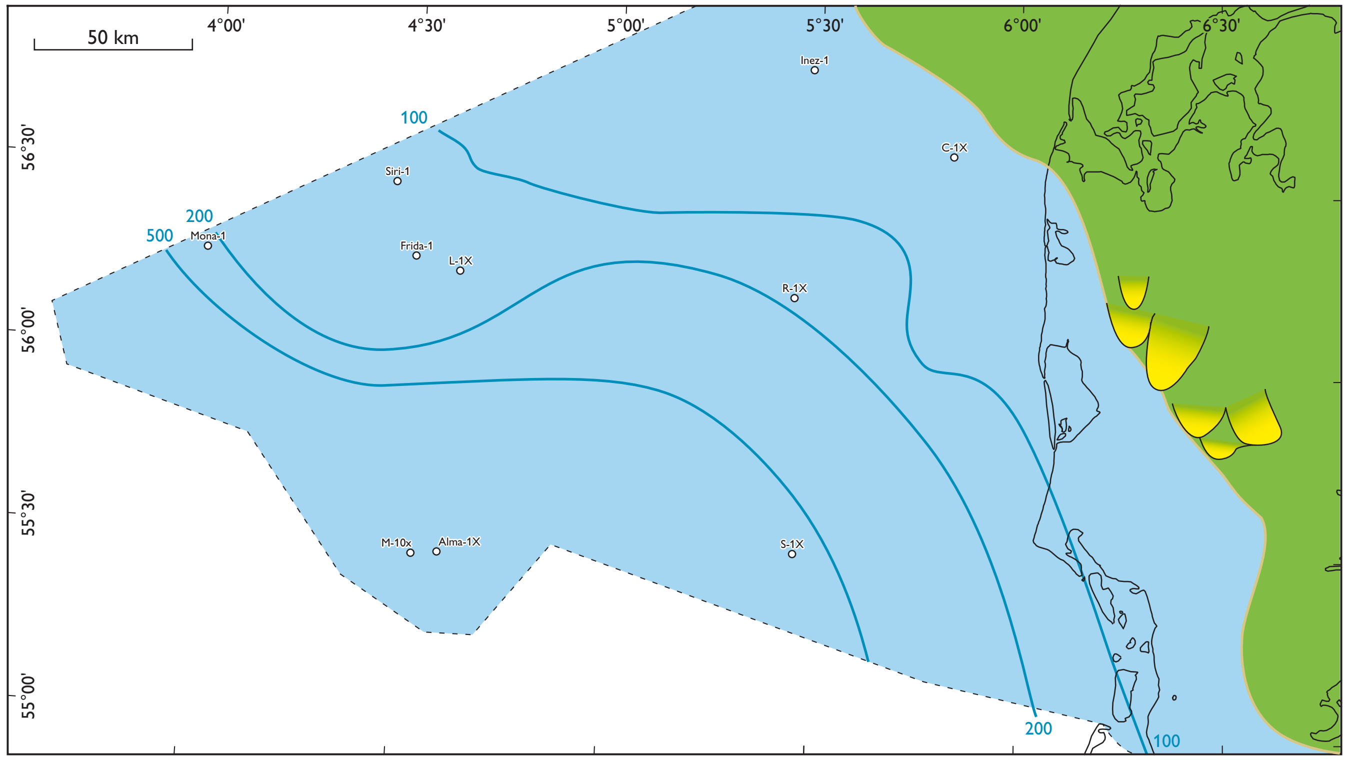

50 km
4°00'
4°30'
5°00'
5°30'
6°00'
6°30'
56°30'
56°00'
55°30'
55°00'
100
200
500
Inez-1
C-1X
Siri-1
Mona-1
Frida-1
L-1X
R-1X
M-10x
Alma-1X
S-1X
200
100

Sequence D

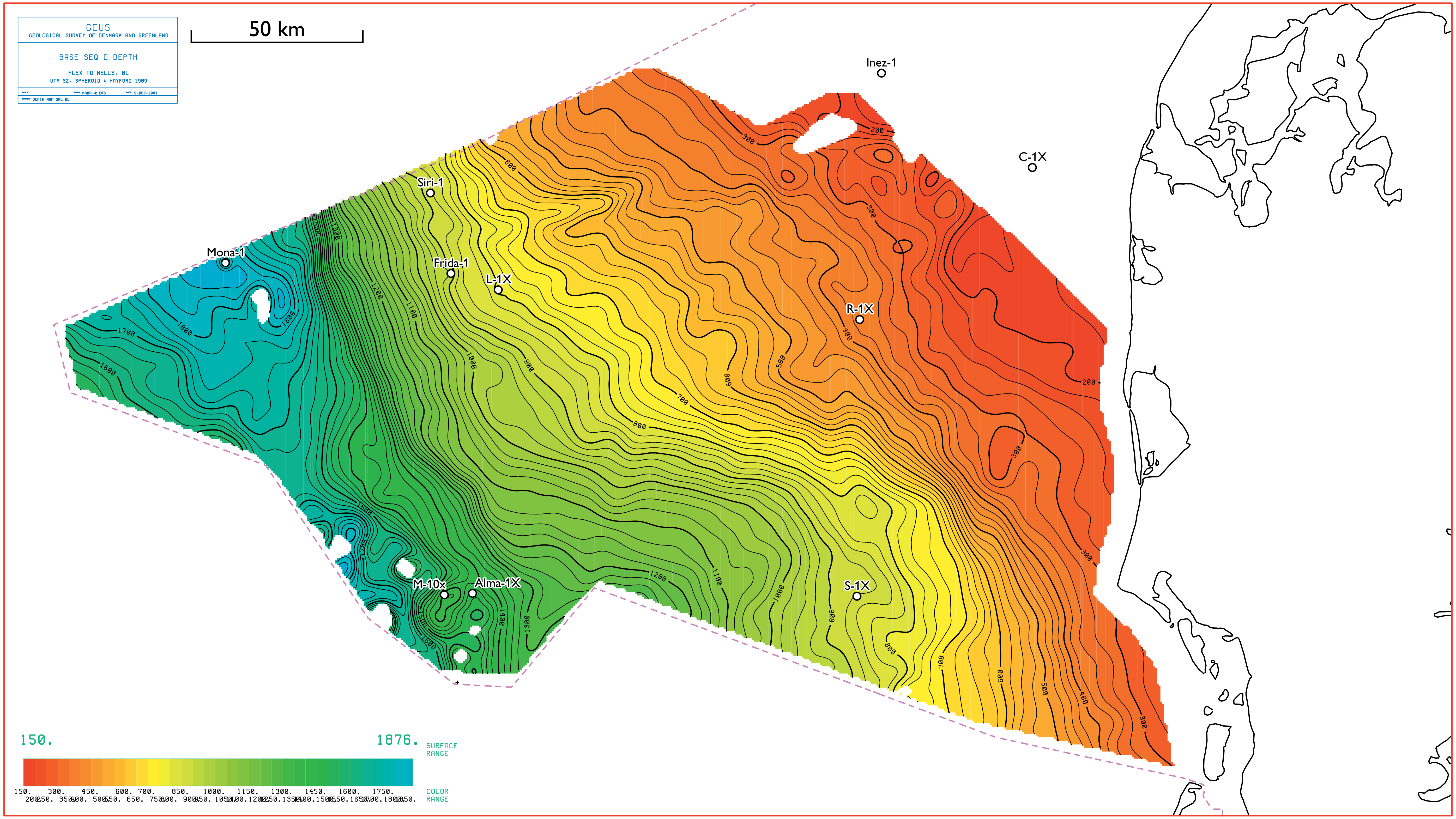

Fig. 13: Sequence D
The base surface forms a west-south-westward-dipping monocline whose minimum depth is 150 m and maximum depth is 1876 m. Steepest dip of the surface is found west of the Frida-1 well. Distinct variations in depth are found around diapiric structures in the extreme south-western part of the area.

The thickness of the sequence varies from 5–397 m. The main depocentre was located in the southern part of the study area. The reduced thickness to the north is a result of truncation of the sequence towards the north-east. The depositional environment was characterised by coastal plain and deltas in the north-eastern part of the area and by open marine conditions in the south-western part. Water depth were up to 500 m in the extreme south-western part of the area.

Sequence D

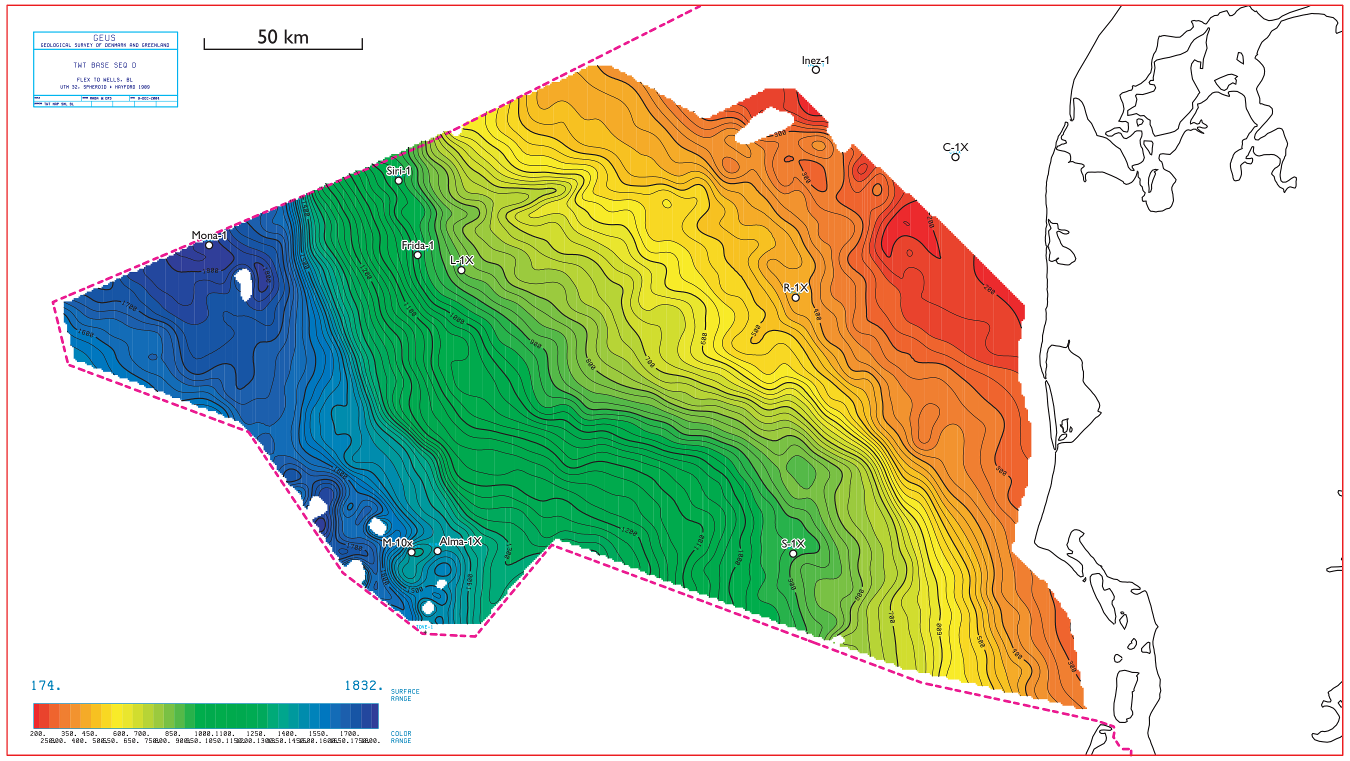
50 km
Inez-1
C-1X
Siri-1
Mona-1
Frida-1
L-1X
R-1X
M-10x
Alma-1X
S-1X
174.
1832.

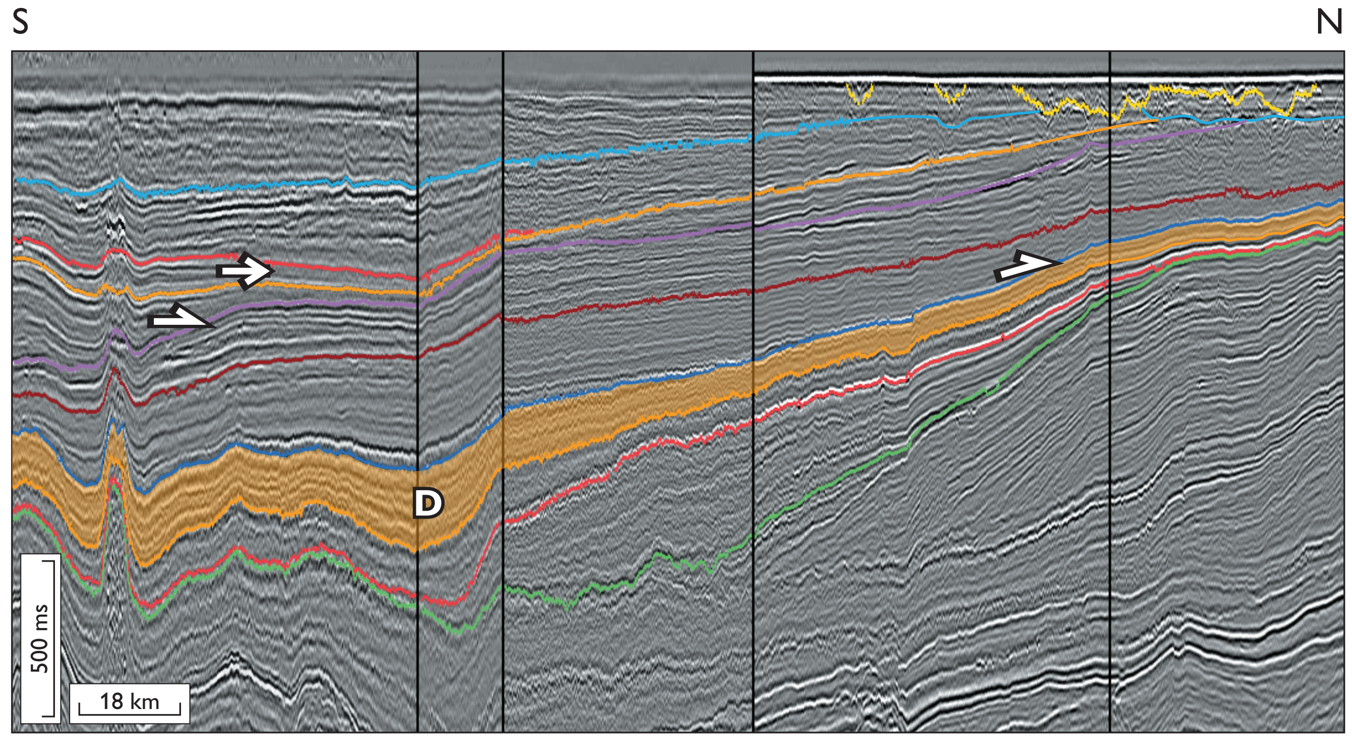
S
N
D
500 ms
18 km

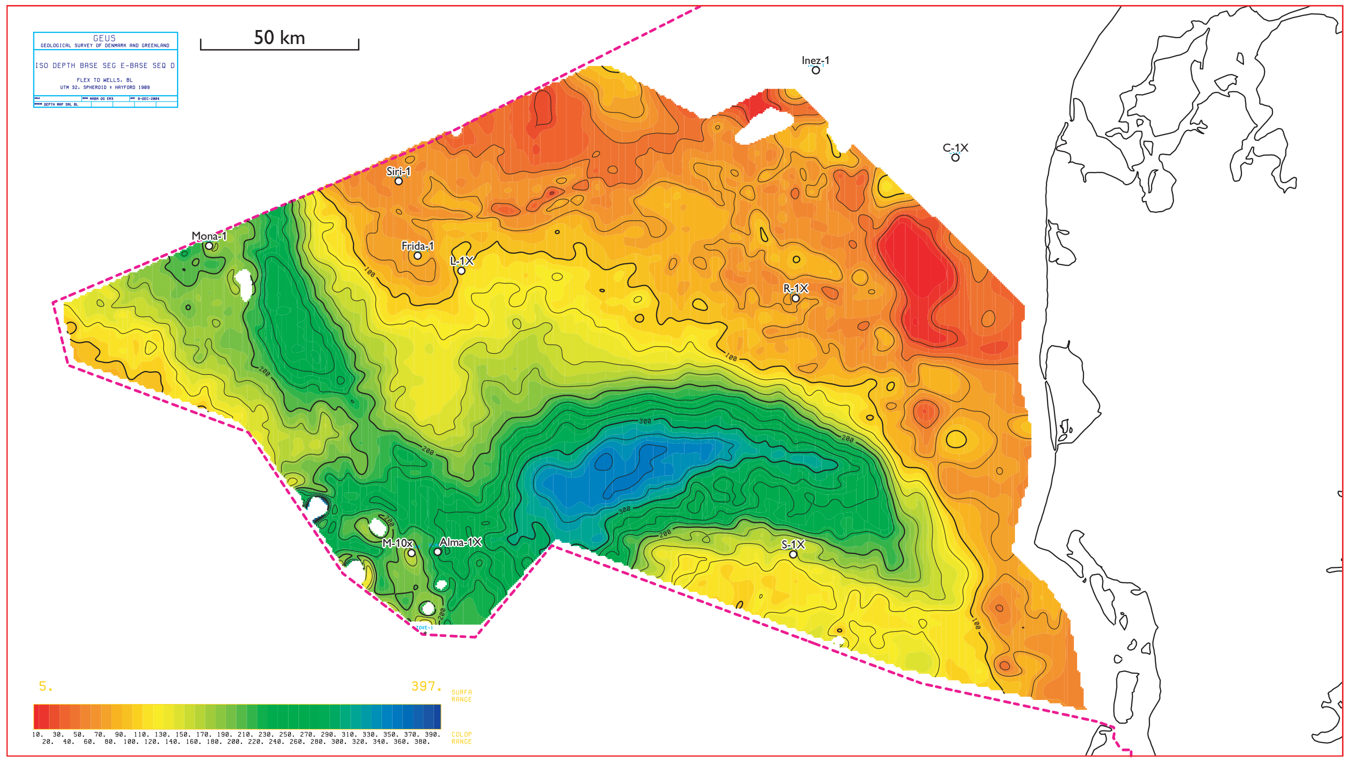
50 km
Inez-1
C-1X
Siri-1
Mona-1
Frida-1
L-1X
R-1X
M-10x
Alma-1X
S-1X
5.
397.

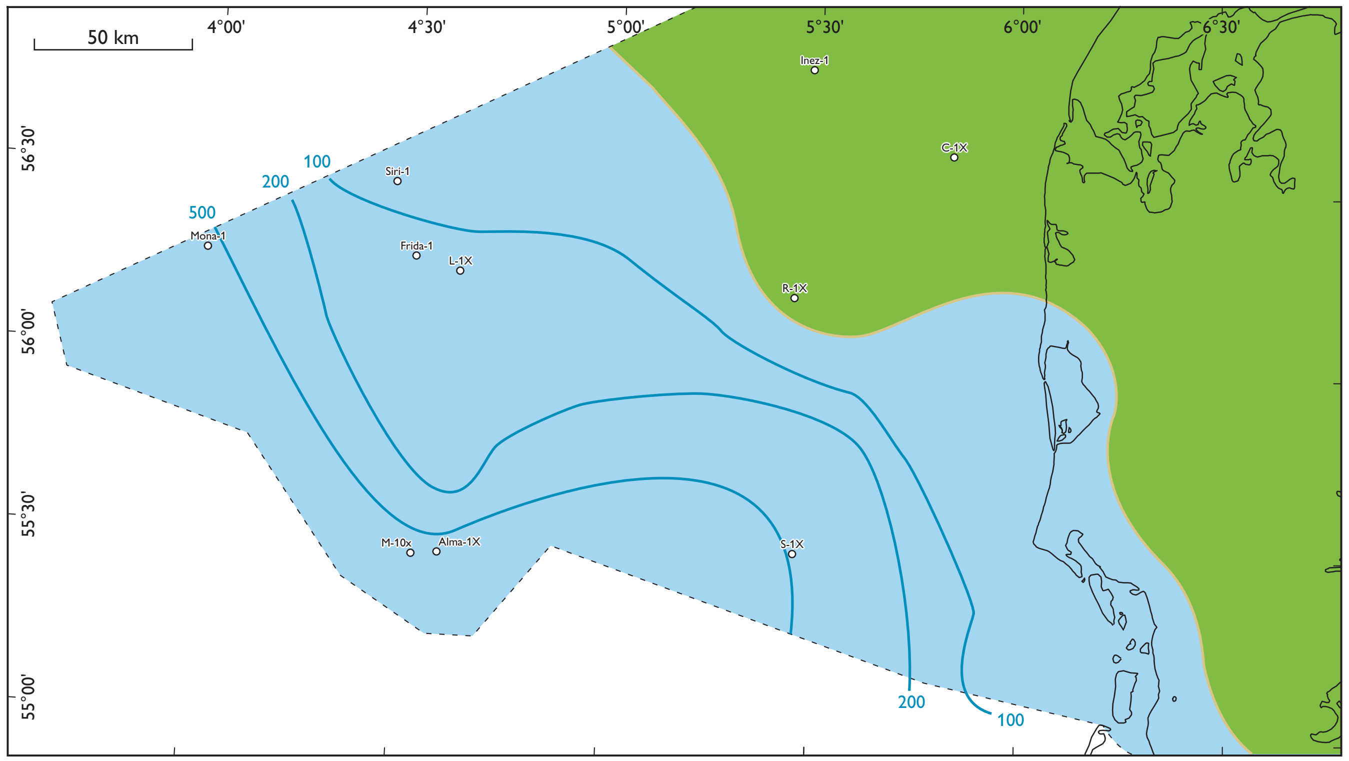
50 km
4°00'
4°30'
5°00'
5°30'
6°00'
6°30'
56°30'
56°00'
55°30'
55°00'
500
200
100
200
100
Inez-1
C-1X
Siri-1
Mona-1
Frida-1
L-1X
R-1X
M-10x
Alma-1X
S-1X

Sequence E

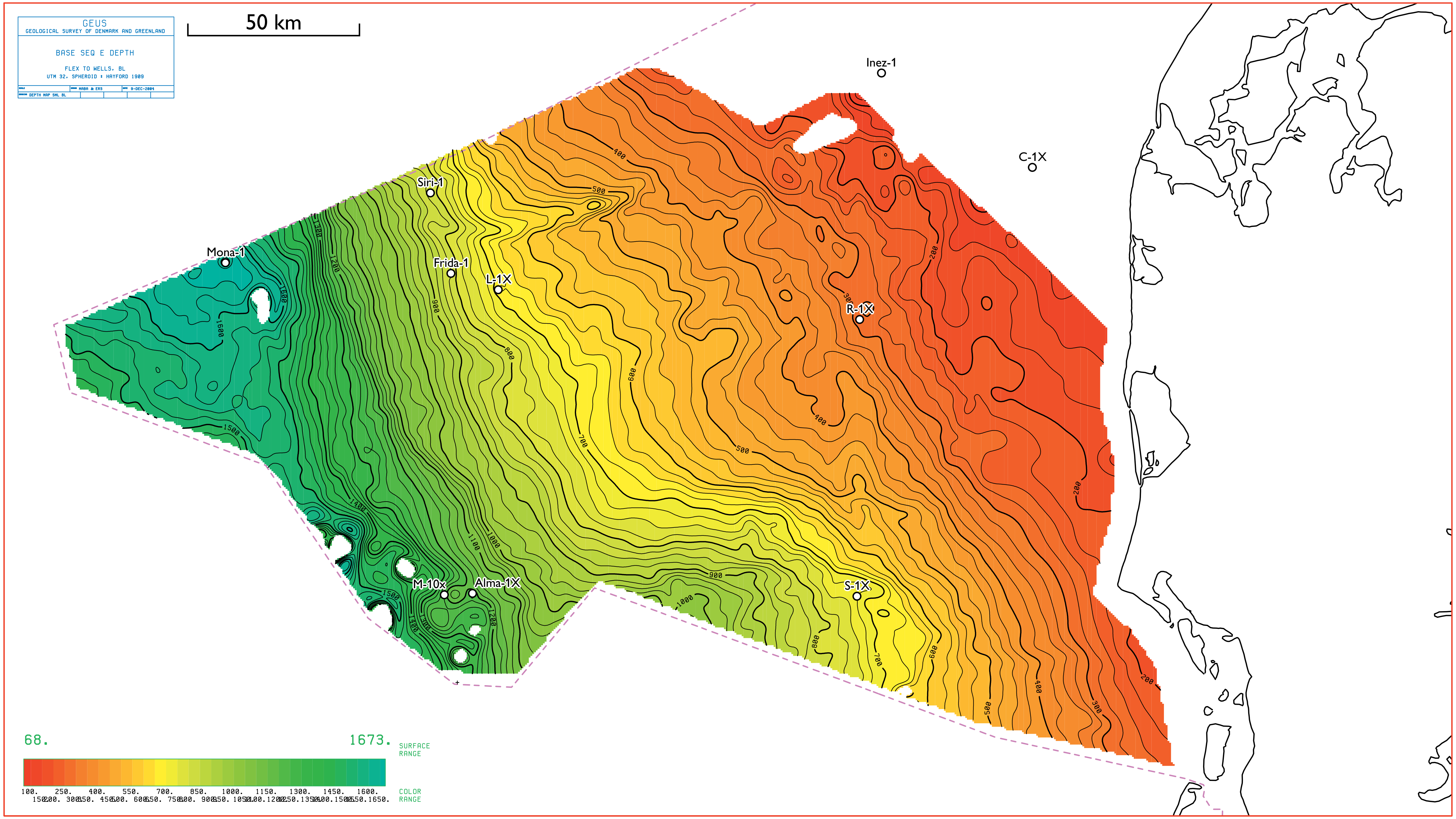

Fig. 14: Sequence E

The base surface forms a west-south-westward-dipping monocline whose minimum depth is 68 m and maximum depth is 1673 m. Steepest dip of the surface is found west of the Frida-1 well. Distinct variations in depth are found around diapiric structures in the extreme south-western part of the area.

The thickness of the sequence varies from 34–600 m. The main depocentre was located west of the Frida-1 well and south of the S-1 well. The reduced thickness to the north is a result of truncation of the sequence "towards the north-east. The depositional environment was characterised by open marine conditions in the whole area. The water depth was up to 500 m in the extreme western part of the area.

Sequence E

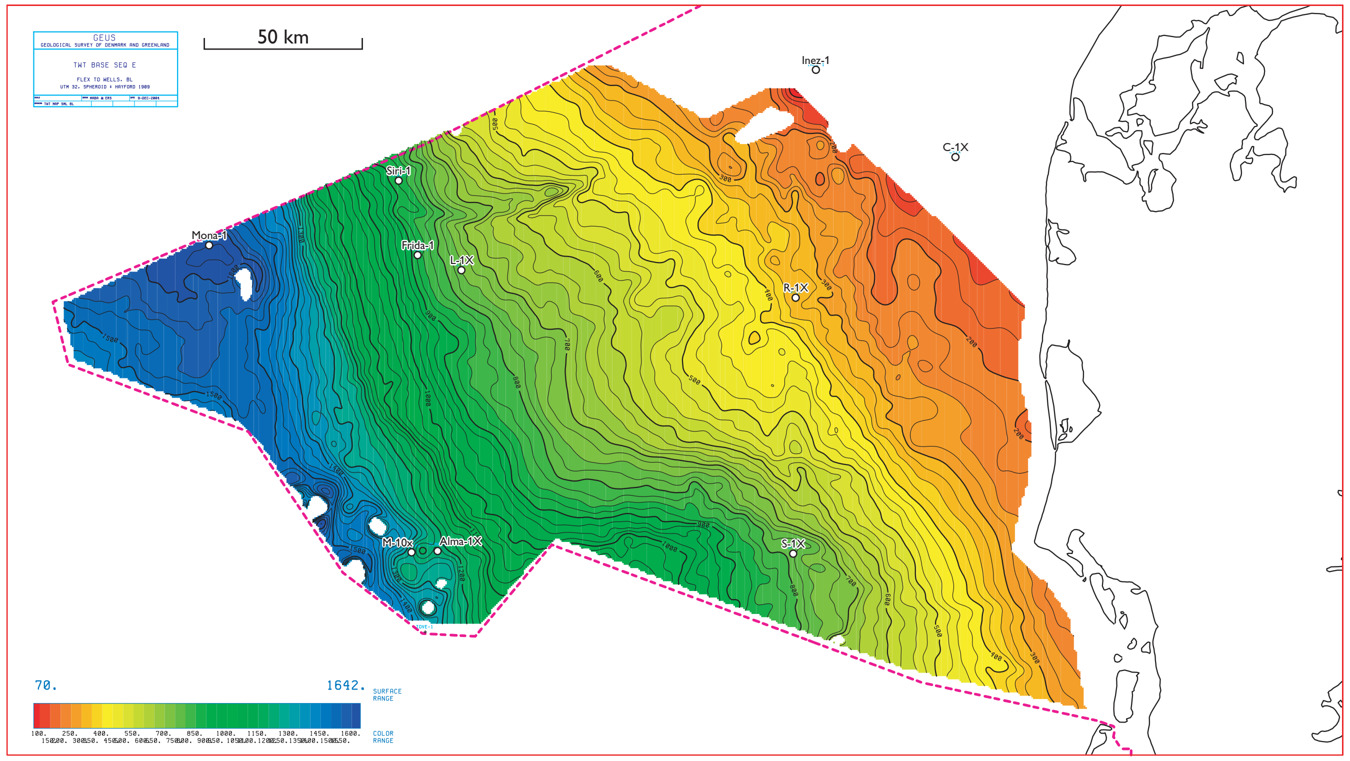
50 km
Inez-1
C-1X
Siri-1
Mona-1
Frida-1
L-1X
R-1X
M-10x
Alma-1X
S-1X
70.
1642.

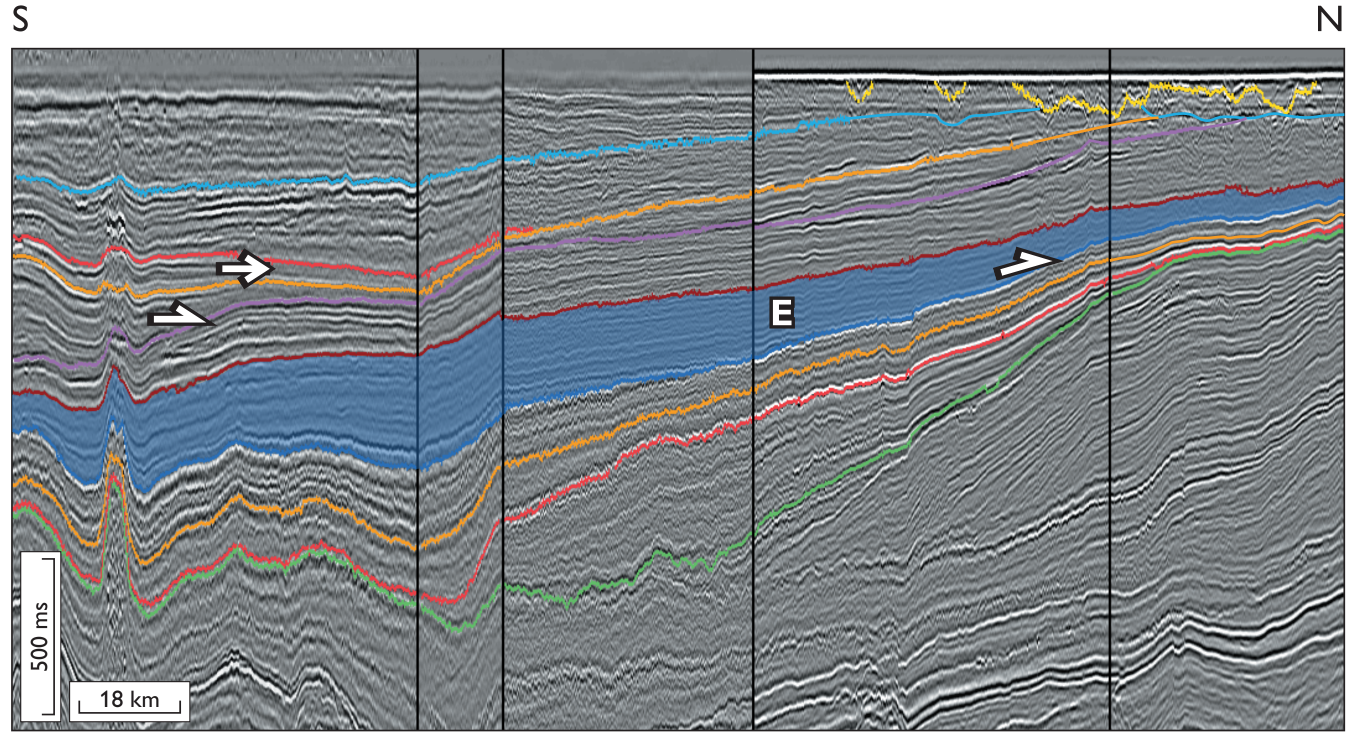
S
N
E
500 ms
18 km

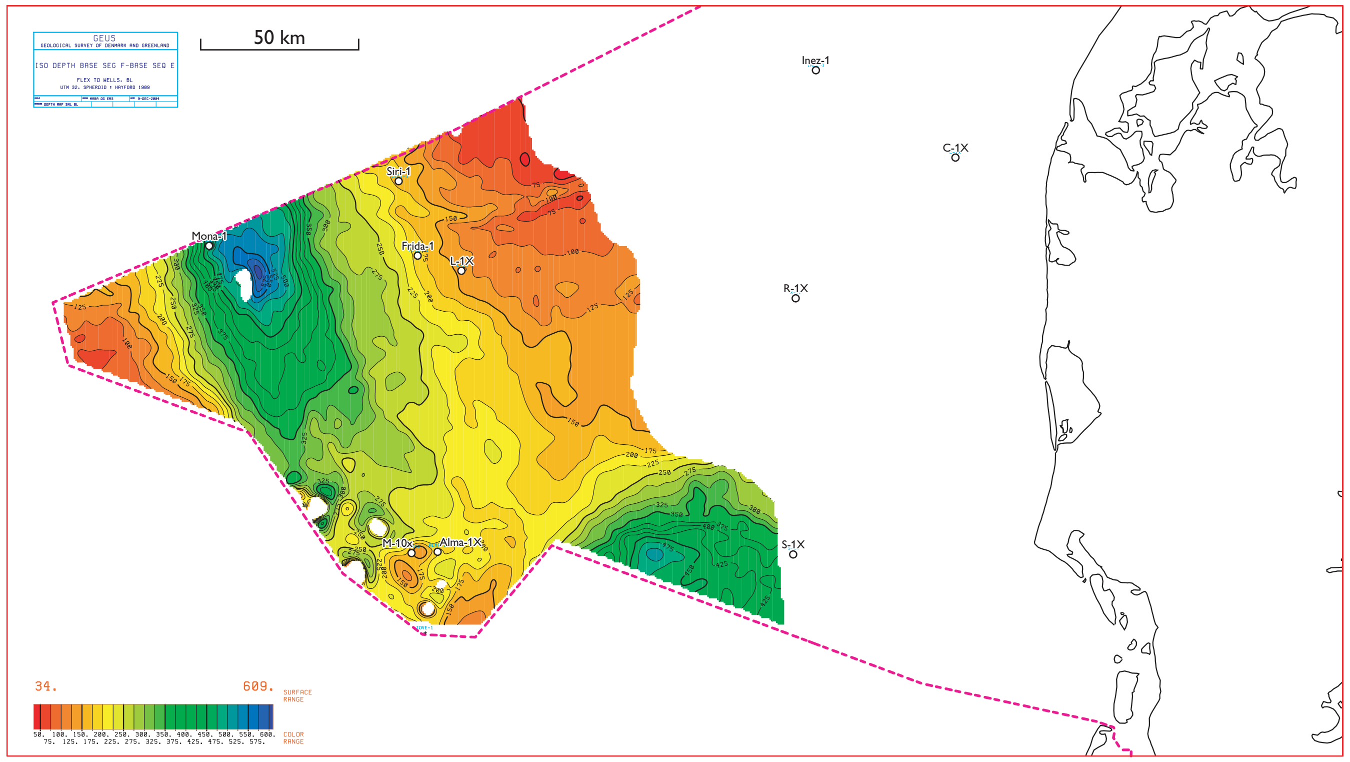
50 km
Inez-1
C-1X
Siri-1
Mona-1
Frida-1
L-1X
R-1X
M-10x
Alma-1X
S-1X
34.
609.

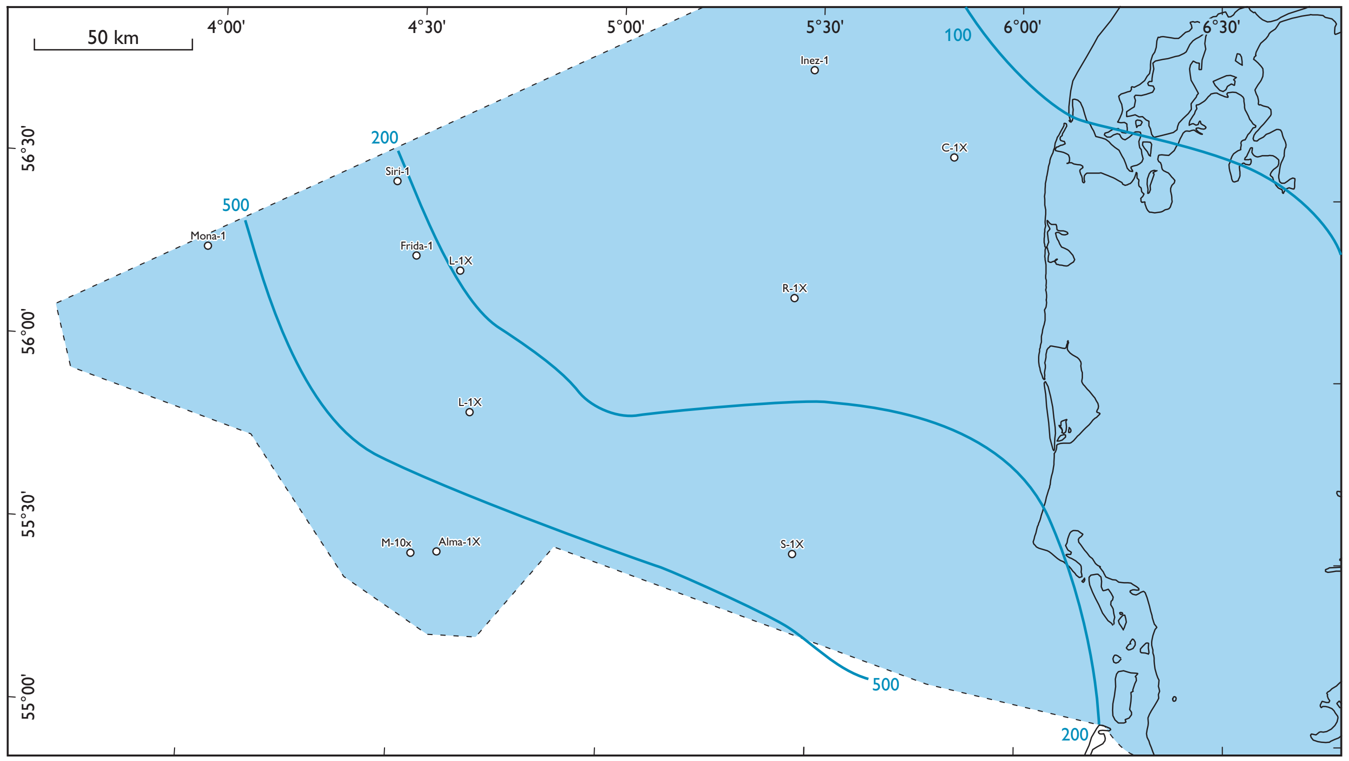
50 km
4°00'
4°30'
5°00'
5°30'
6°00'
6°30'
56°30'
56°00'
55°30'
55°00'
100
200
500
Inez-1
C-1X
Siri-1
Mona-1
Frida-1
L-1X
R-1X
M-10x
Alma-1X
S-1X

Sequence F

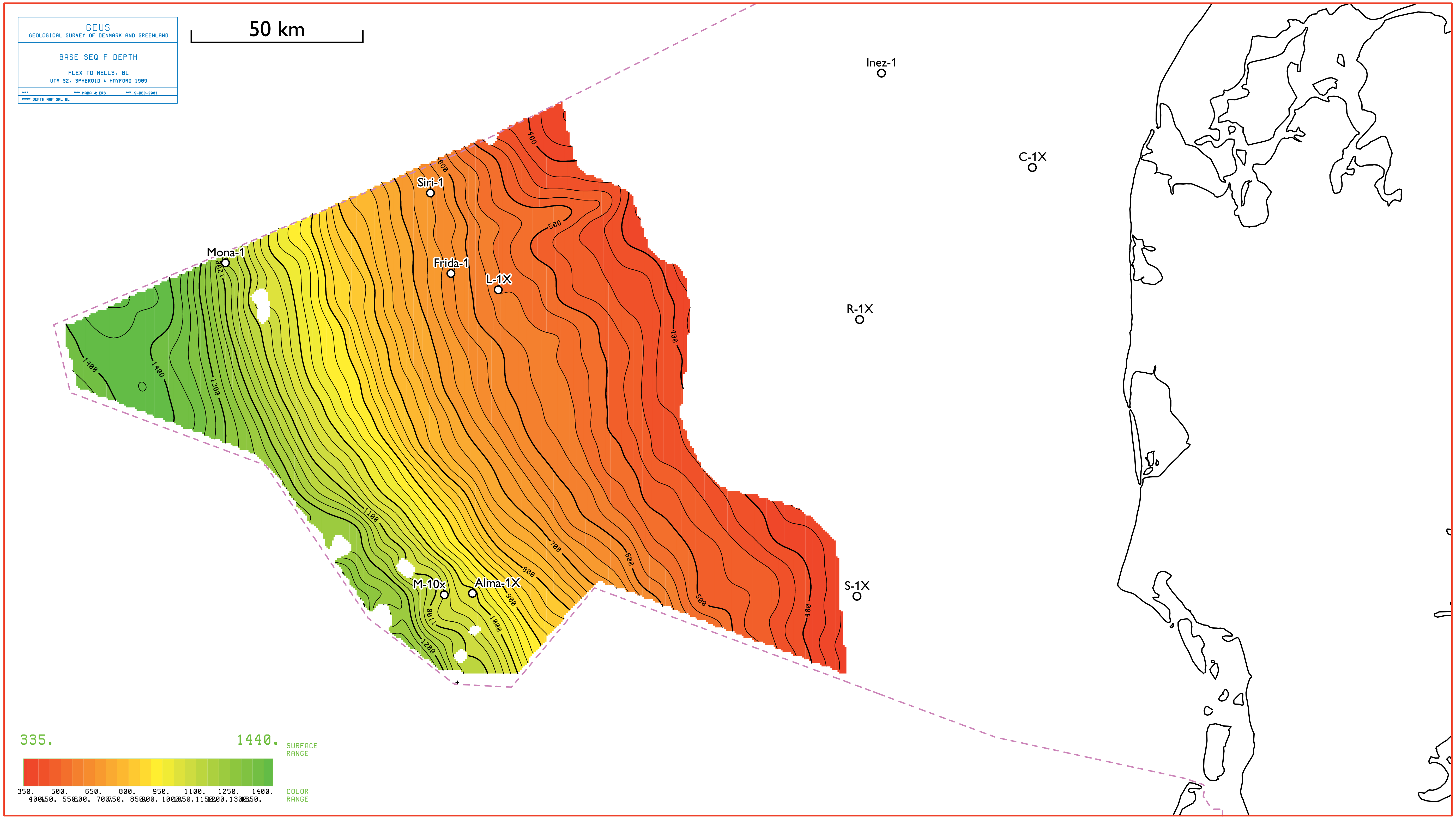

Fig. 15: Sequence F
The base surface forms a west-south-westward dipping monocline whose minimum depth is 335 m and maximum depth is 1440 m. The thickness of the sequence varies from 5–330 m. The main depocentre was located west of the Mona-1 well and east of the Alma-1 well. The reduced thickness to the north is a result of truncation of the sequence towards the north-east. The depositional environment was characterised by coastal plain and deltas in most of the area. Open marine conditions exsisted in the extreme south-western part of the area. The water depth was over 300 m in the western part.

Sequence F

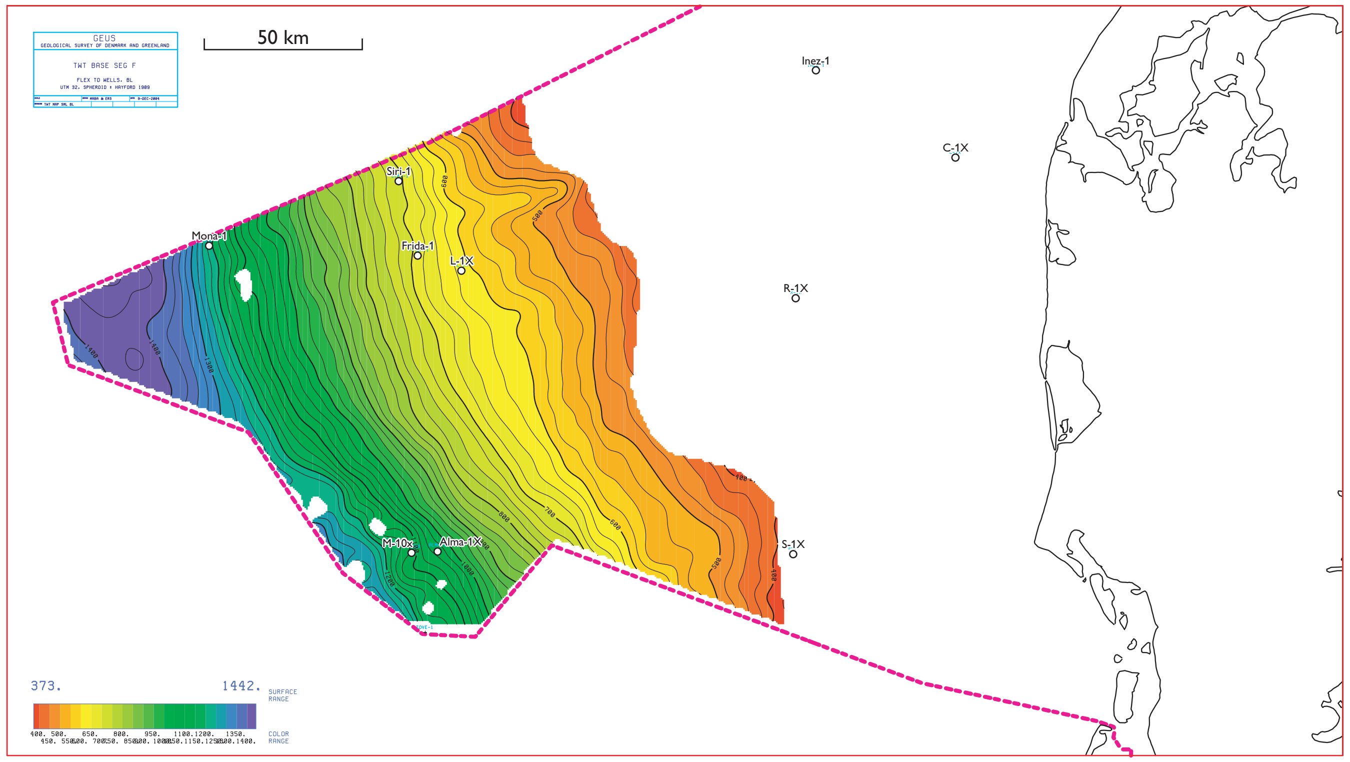
50 km
Inez-1
C-1X
Siri-1
Mona-1
Frida-1
L-1X
R-1X
S-1X
M-10x
Alma-1X
373.
1442.

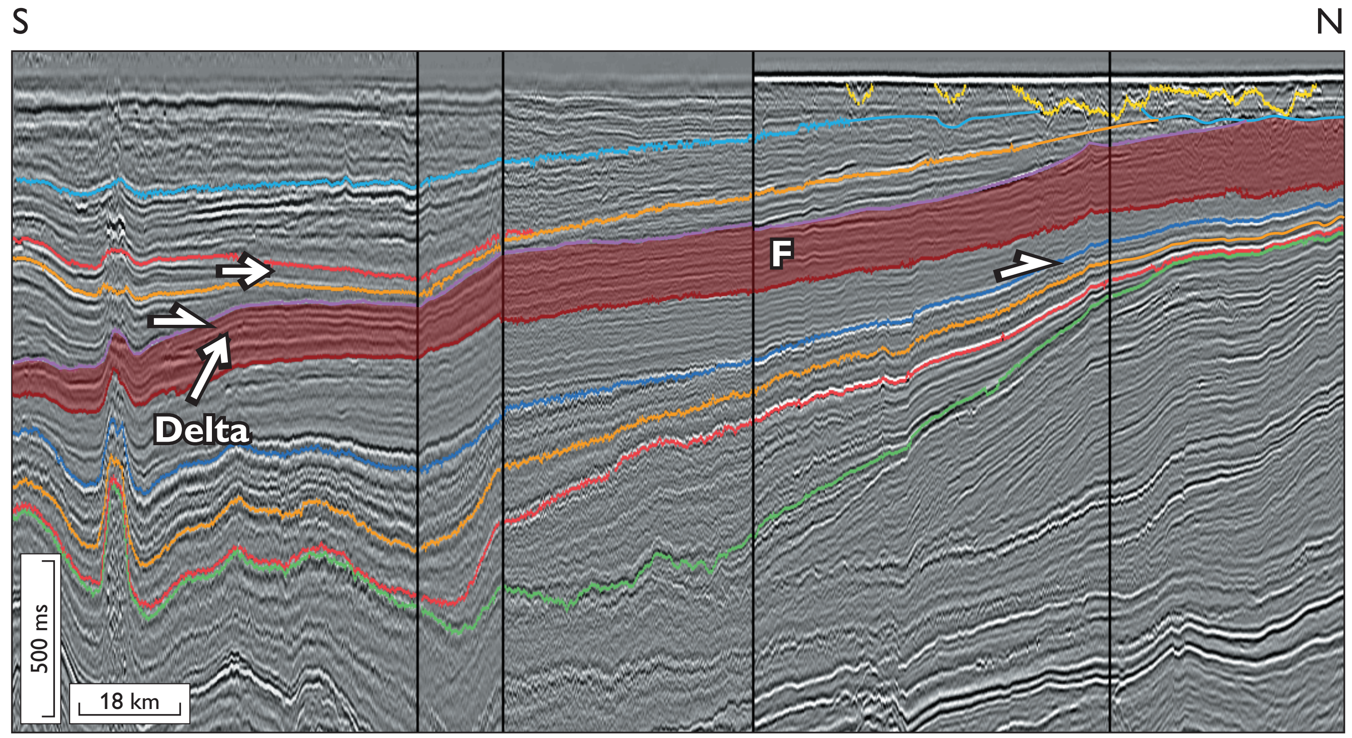
S
N
F
Delta
500 ms
18 km

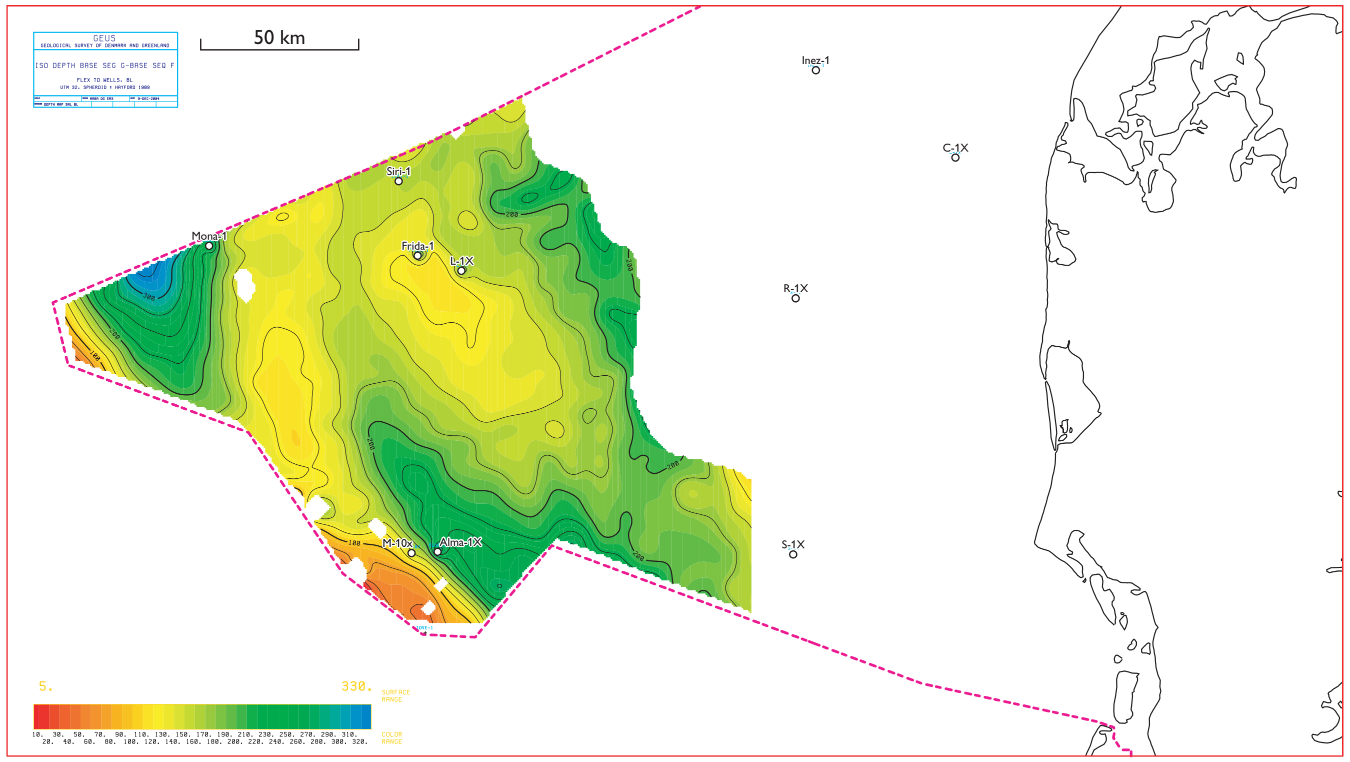
50 km
Inez-1
C-1X
Siri-1
Mona-1
Frida-1
L-1X
R-1X
S-1X
M-10x
Alma-1X
5.
330.

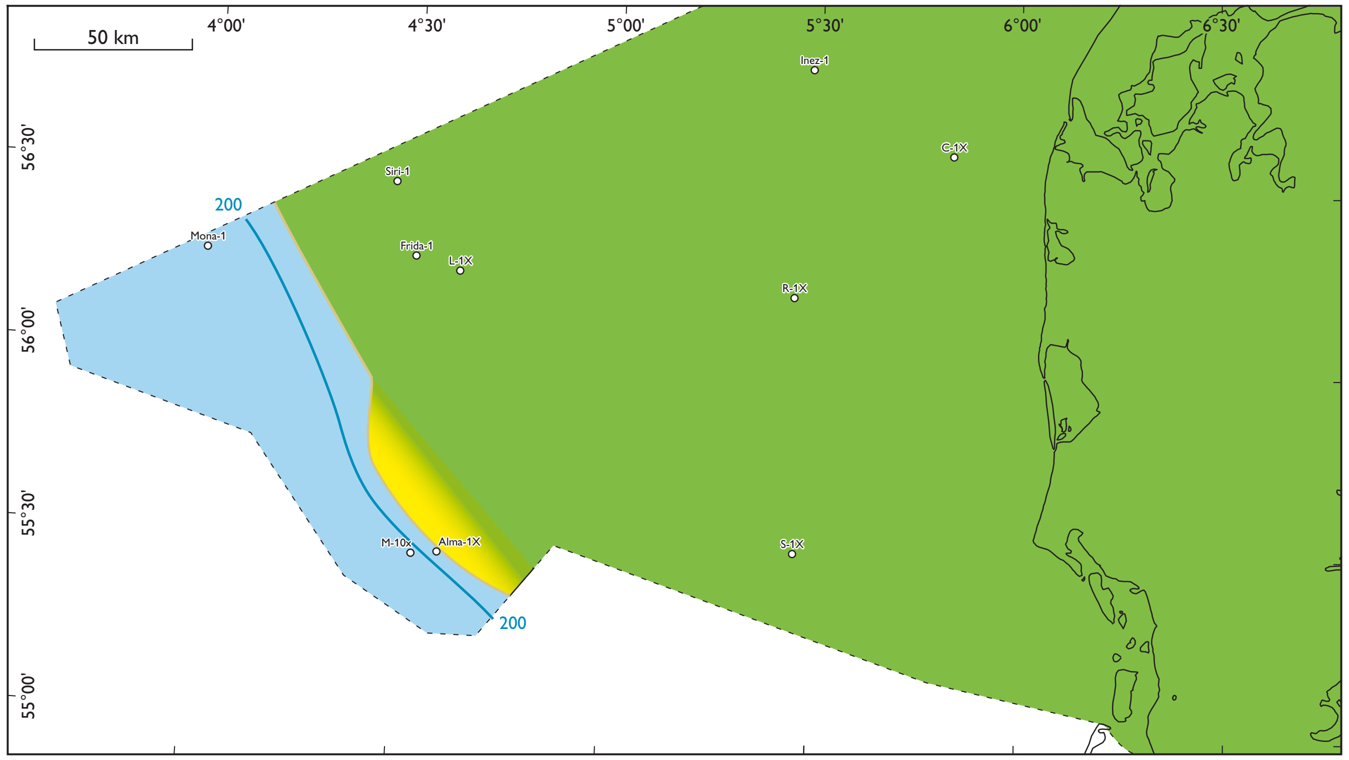
50 km
4°00'
4°30'
5°00'
5°30'
6°00'
6°30'
56°30'
56°00'
55°30'
55°00'
200
Inez-1
C-1X
Siri-1
Mona-1
Frida-1
L-1X
R-1X
S-1X
M-10x
Alma-1X
200

Sequence G

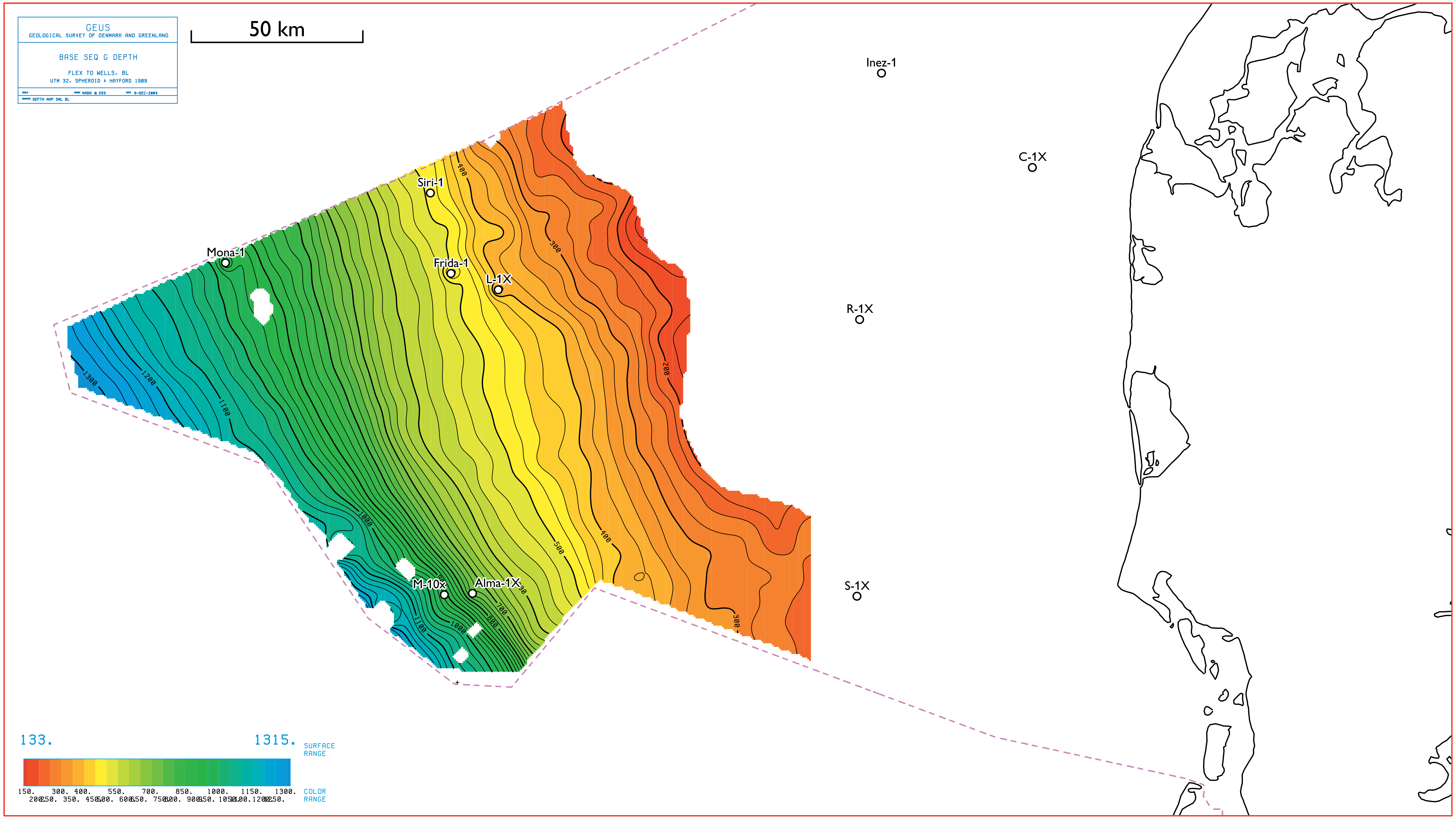

Fig. 16: Sequence G
The base surface forms a west-south-westward dipping monocline whose minimum depth is 133 m and maximum depth is 1315 m. The thickness of the sequence varies from 62–448 m. The main depocentre was located around the Tove-1 well in the southern part of the area. The reduced thickness to the north is a result of truncation of the sequence towards the north-east. The depositional environment was probably "characterised by coastal plain in the north-eastern part of the area and by open marine conditions in the south-western part of the area. The water depth was up to 500 m.

Sequence G

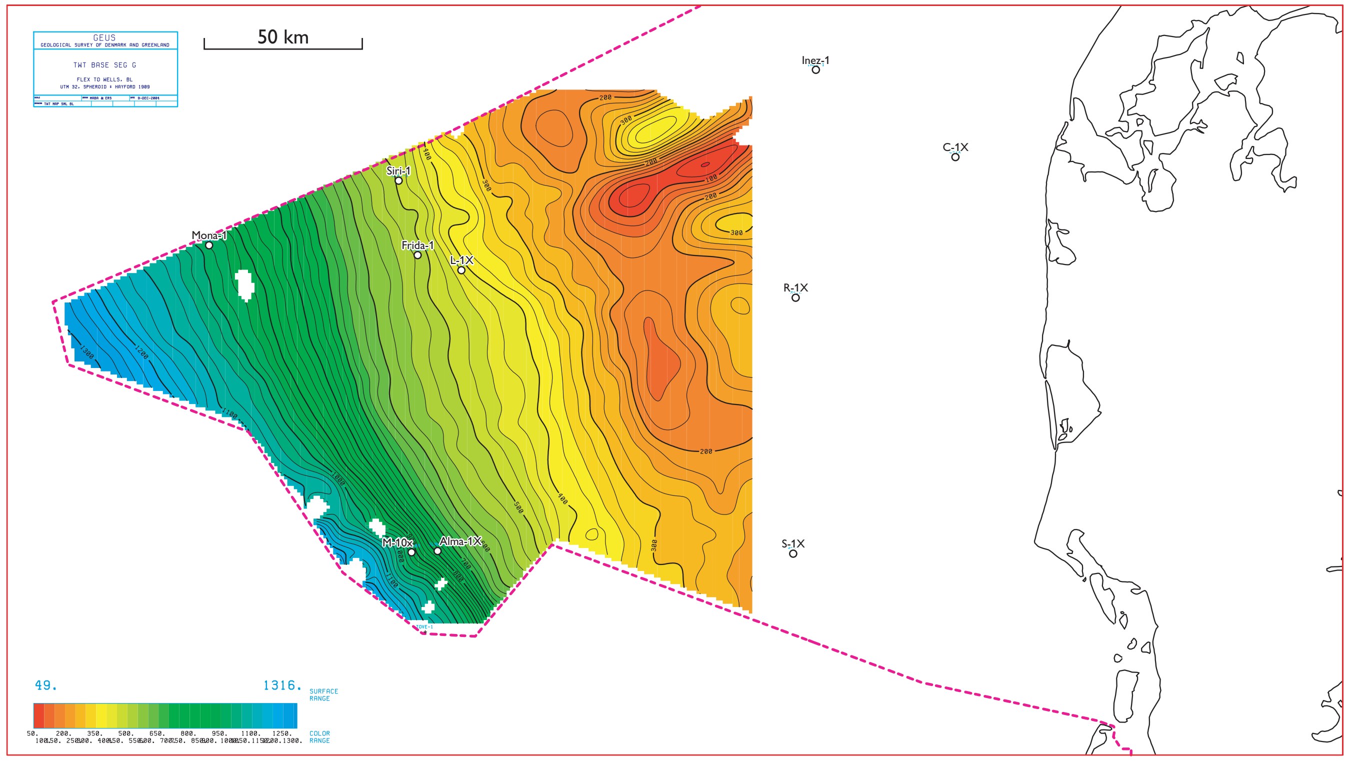

50 km
Inez-1
C-1X
Siri-1
Mona-1
Frida-1
L-1X
R-1X
M-10x
Alma-1X
S-1X
49.
1316.

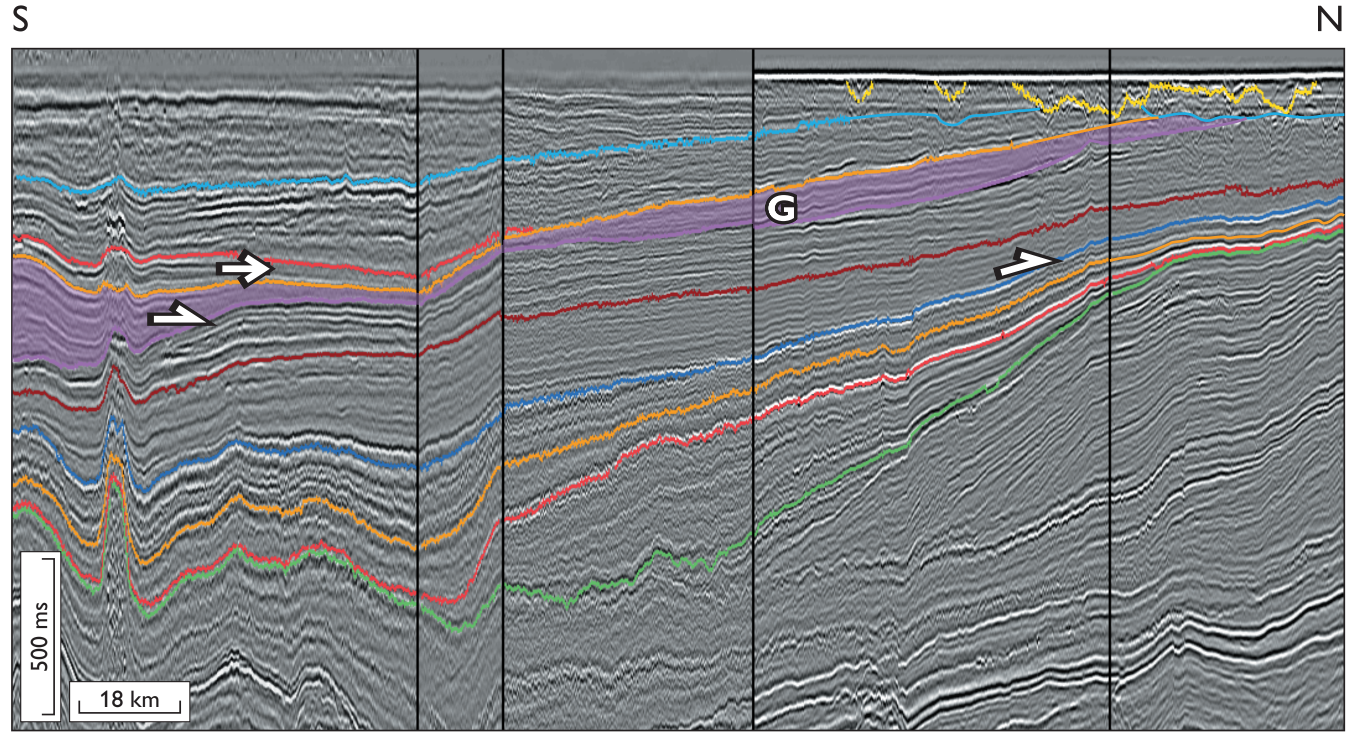

S
N
G
500 ms
18 km

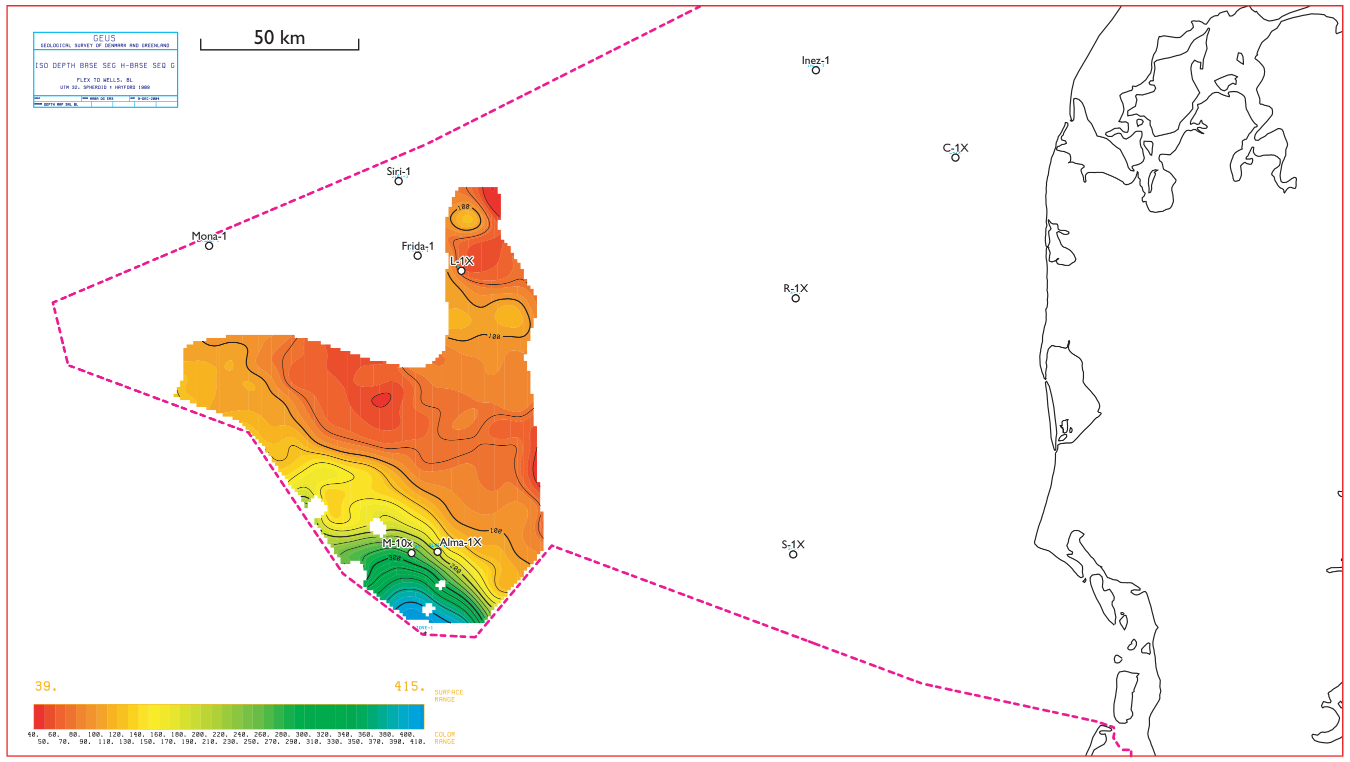

50 km
Inez-1
C-1X
Siri-1
Mona-1
Frida-1
L-1X
R-1X
M-10x
Alma-1X
S-1X
39.
415.

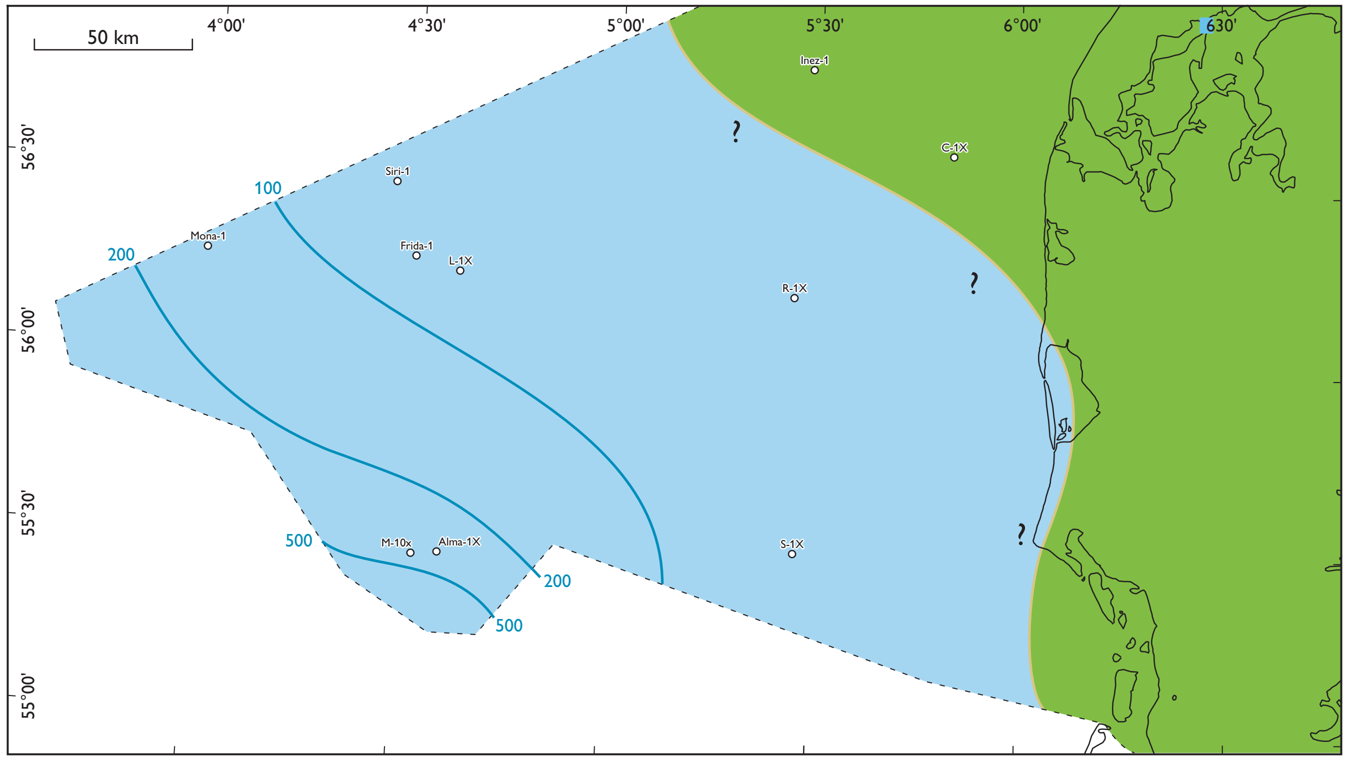

50 km
4°00'
4°30'
5°00'
5°30'
6°00'
6°30'
56°30'
56°00'
55°30'
55°00'
Inez-1
C-1X
Siri-1
Mona-1
Frida-1
L-1X
R-1X
M-10x
Alma-1X
S-1X
100
200
500
200
500
?
?
?

Sequence H

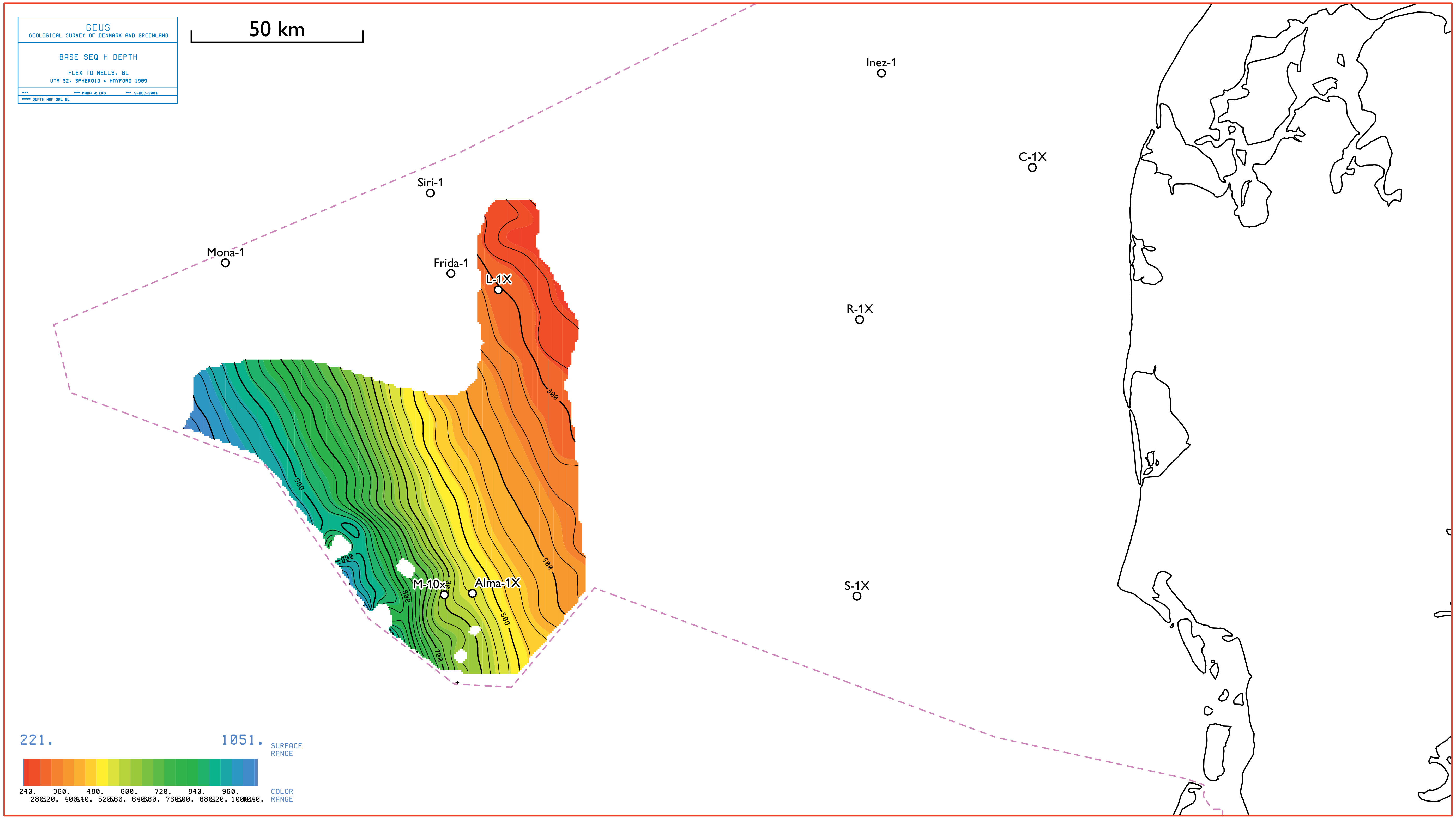

Fig. 17: Sequence H

The base surface forms a west-south-westward dipping monocline whose minimum depth is 221 m and maximum depth is 1051 m. The thickness of the sequence varies from 7–226 m. The main depocentre was located west of the M-10X well. The sequence pinches out towards the north and east. The depositional environment was characterised by coastal plain in the north-eastern part of the area and by open marine "conditions in the south-western part of the area. The water depth was up to 500 m in the extreme south-western part of the area.

Sequence H

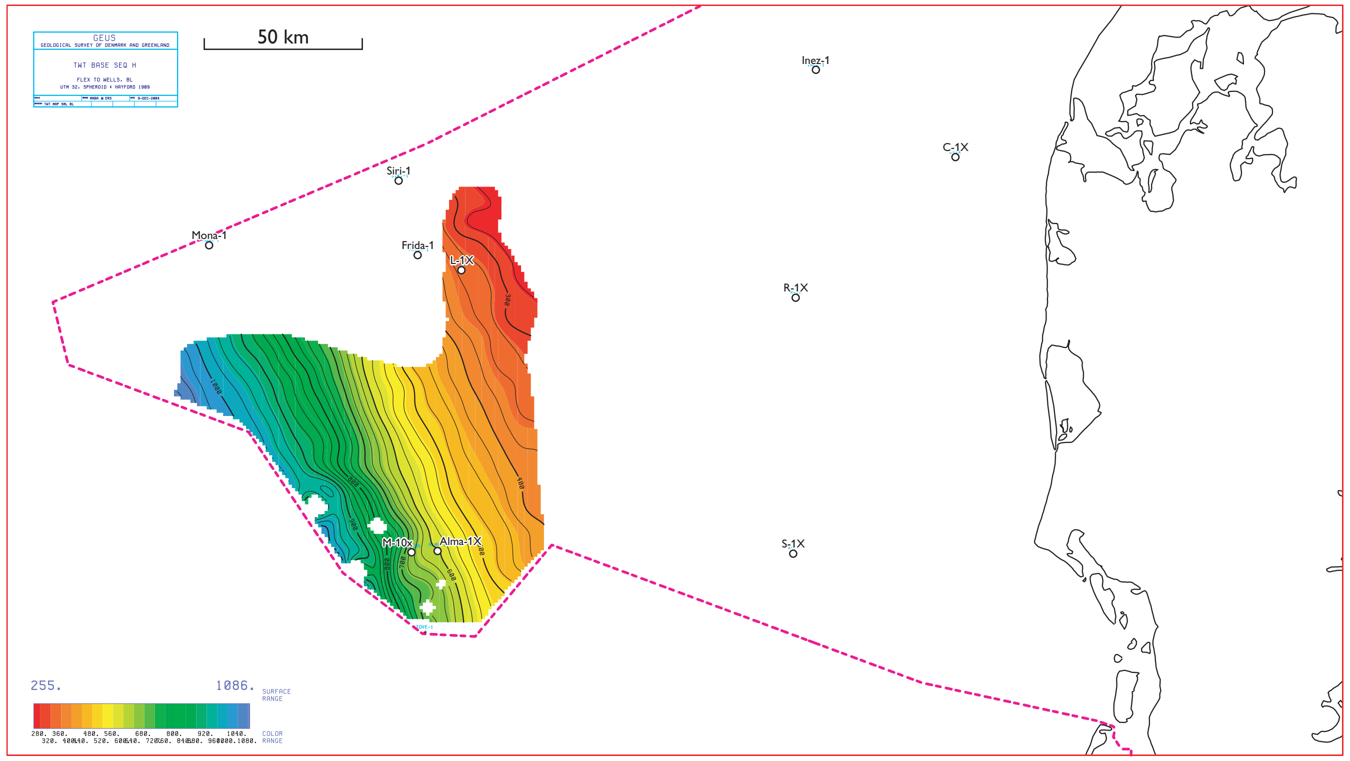
50 km
Inez-1
C-1X
Siri-1
Mona-1
Frida-1
L-1X
R-1X
S-1X
M-10x
Alma-1X
255.
1086.

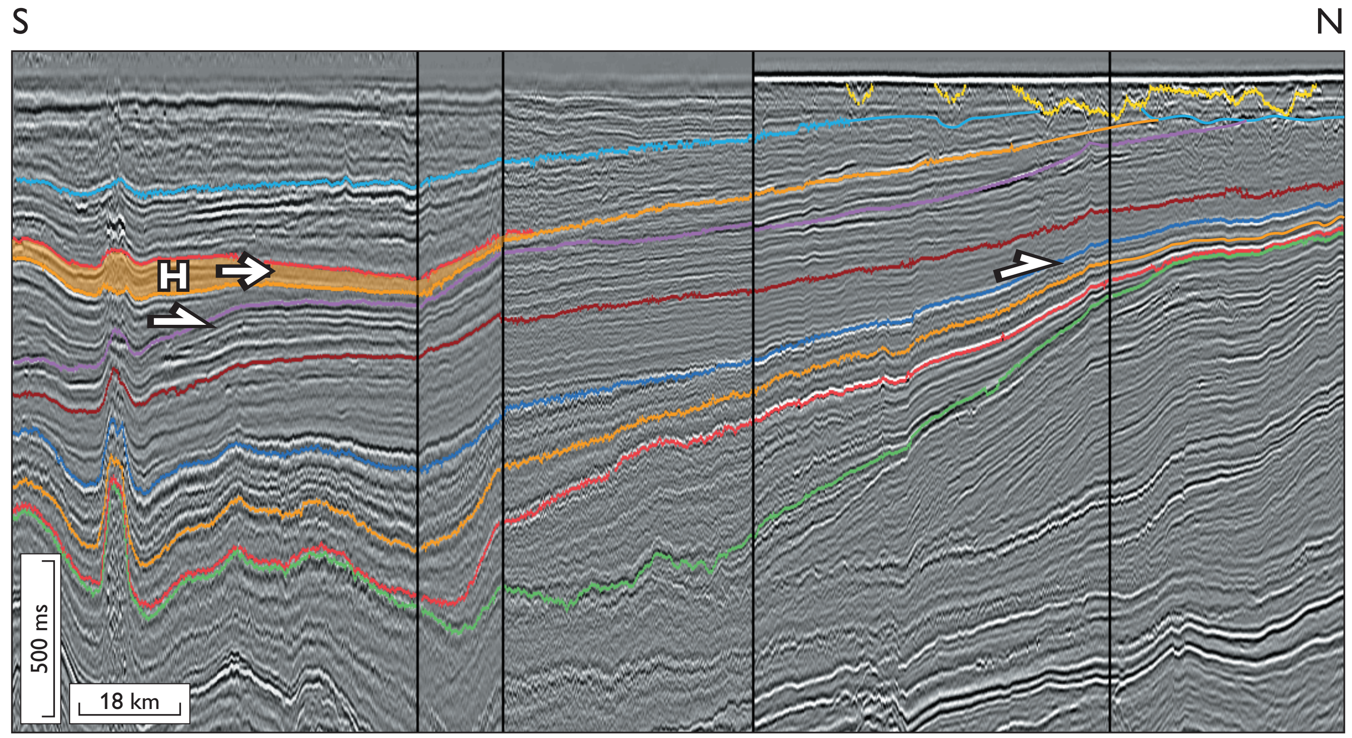
S
N
H
500 ms
18 km

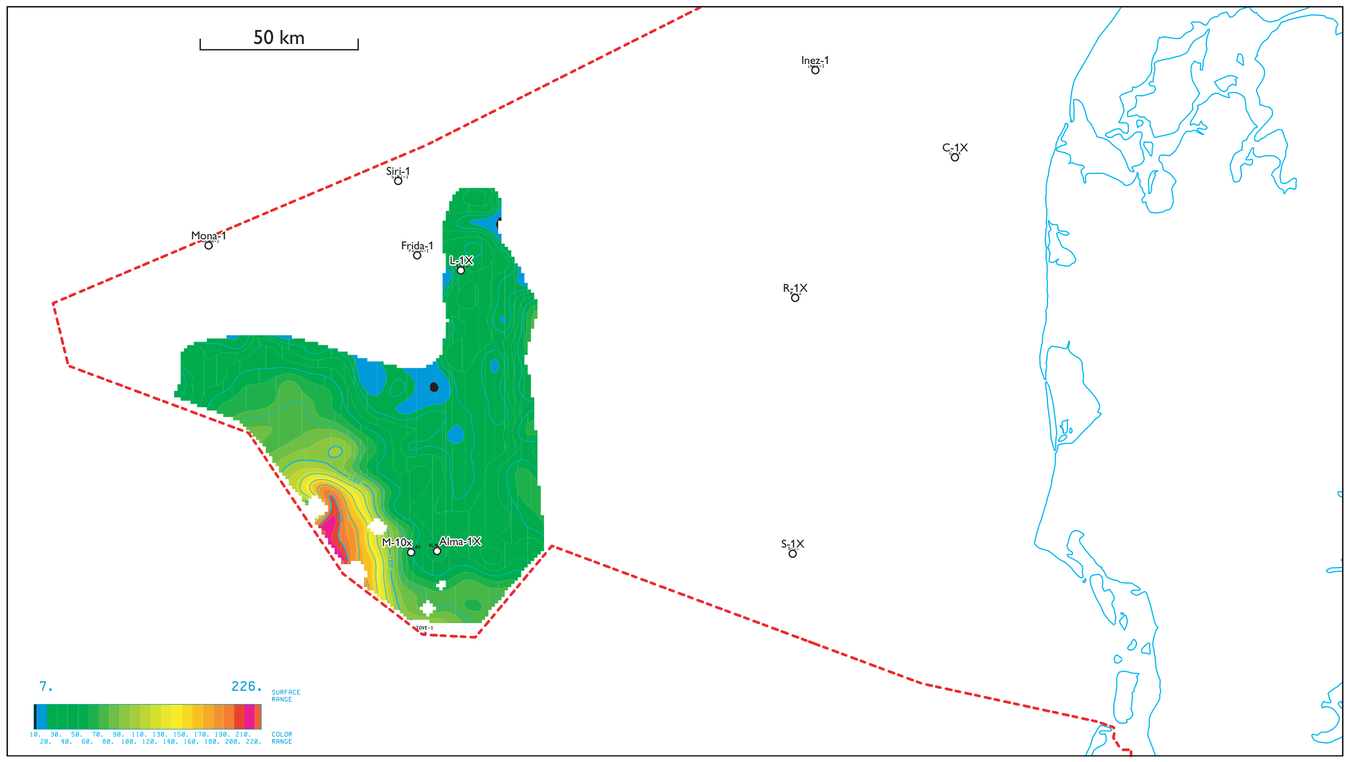
50 km
Inez-1
C-1X
Siri-1
Mona-1
Frida-1
L-1X
R-1X
S-1X
M-10x
Alma-1X
7.
226.

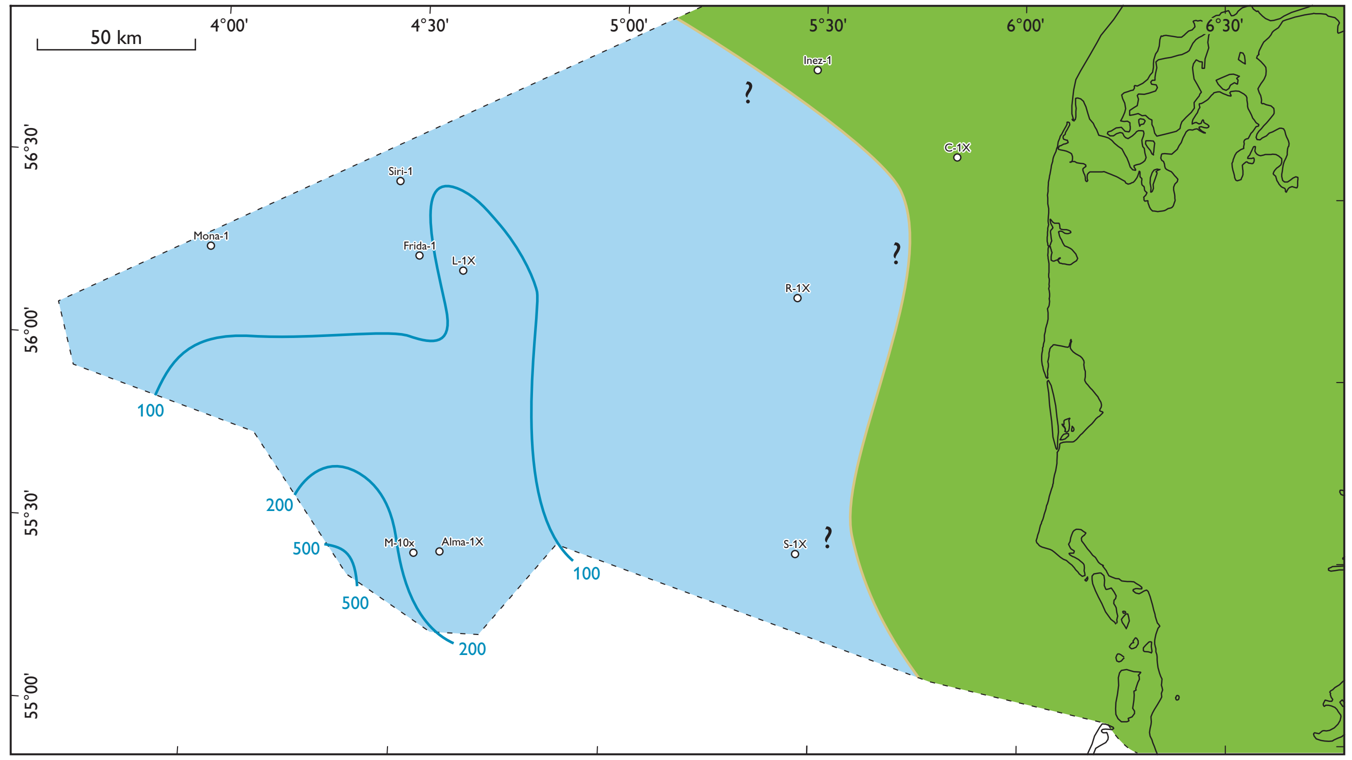
50 km
4°00'
4°30'
5°00'
5°30'
6°00'
6°30'
56°30'
56°00'
55°30'
55°00'
Inez-1
C-1X
Siri-1
Mona-1
Frida-1
L-1X
R-1X
S-1X
M-10x
Alma-1X
?
100
200
500

Sequence I

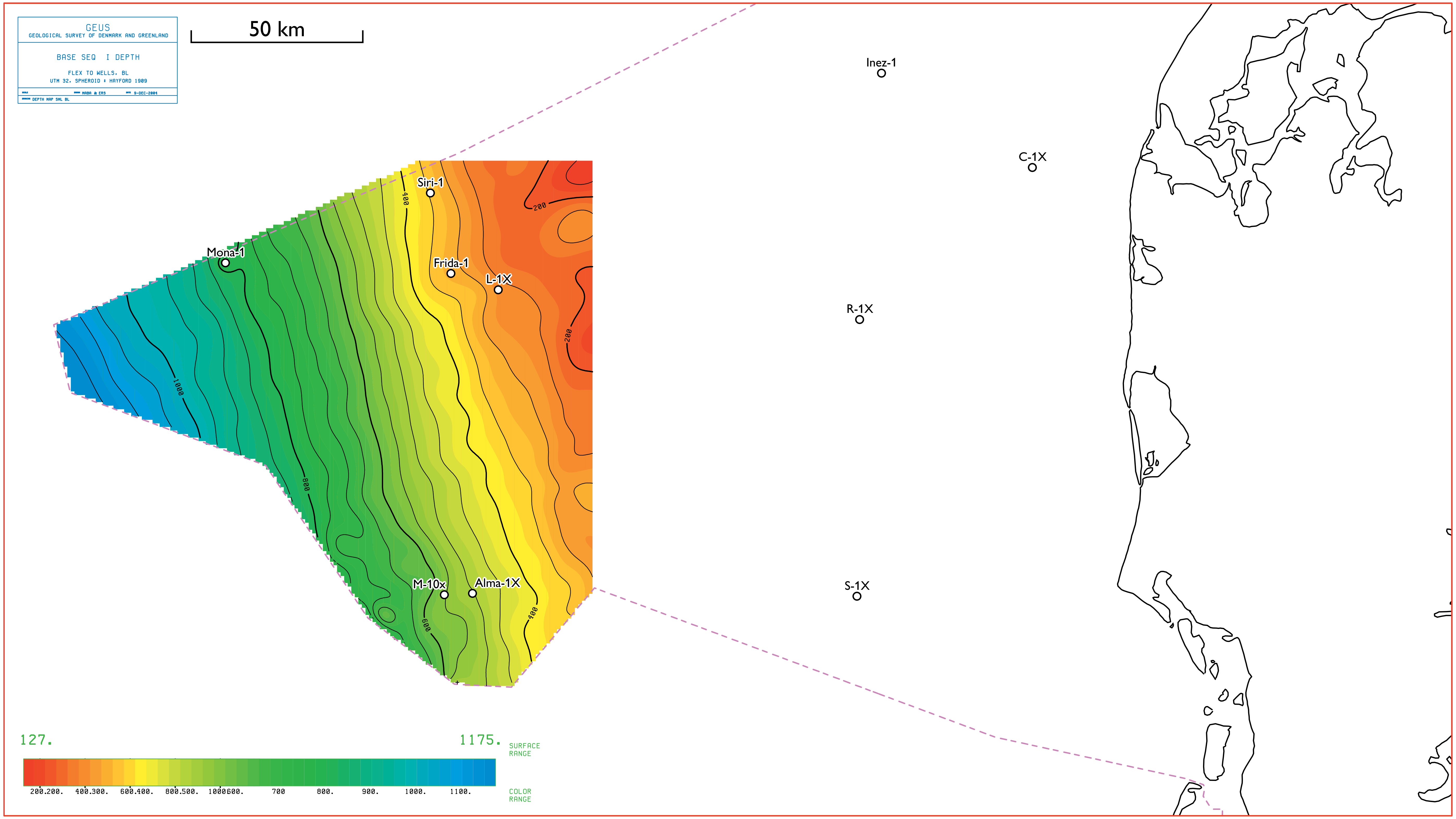

Fig. 18: Sequence I

The base surface forms a west-south-westward dipping monocline whose minimum depth is 127 m and maximum depth is 1168 m. The thickness of the sequence varies from 19–430 m. The main depocentre was located west of the Mona-1 well. The reduced thickness to the north is a result of truncation of the sequence towards the north-east. The depositional environment was characterised by coastal plain and deltas in most of the area and by open marine conditions in the extreme western part of the area. The water depth was more than 400 m.

Sequence I

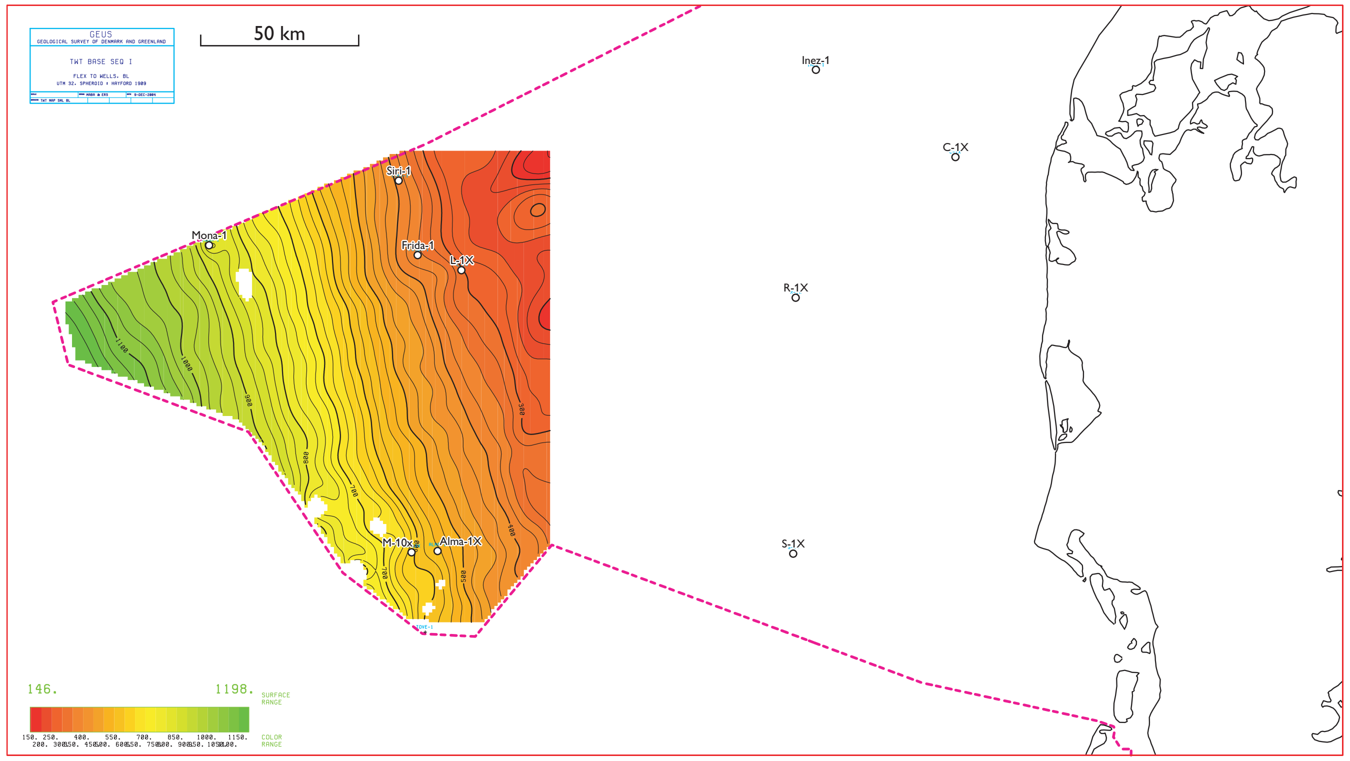

50 km
Inez-1
C-1X
Siri-1
Mona-1
Frida-1
L-1X
R-1X
S-1X
M-10x
Alma-1X
146.
1198.

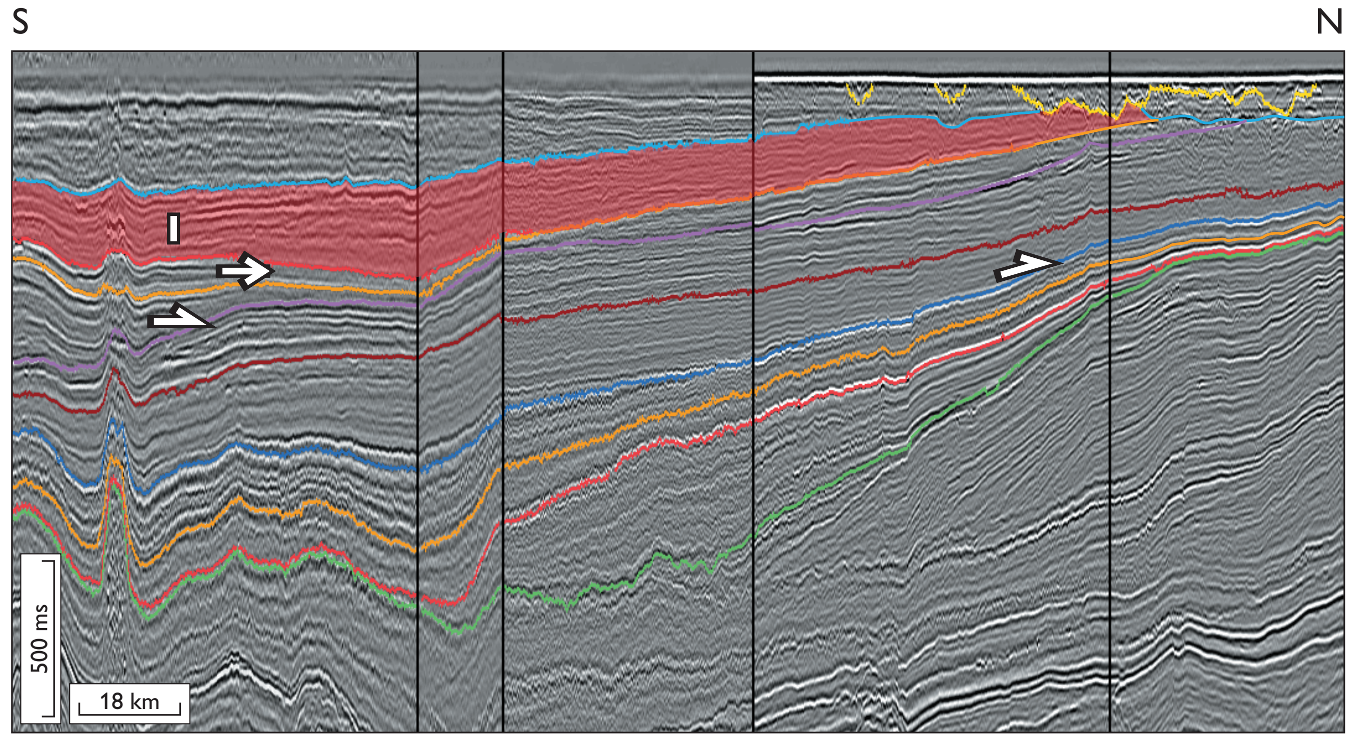

S
N
I
500 ms
18 km

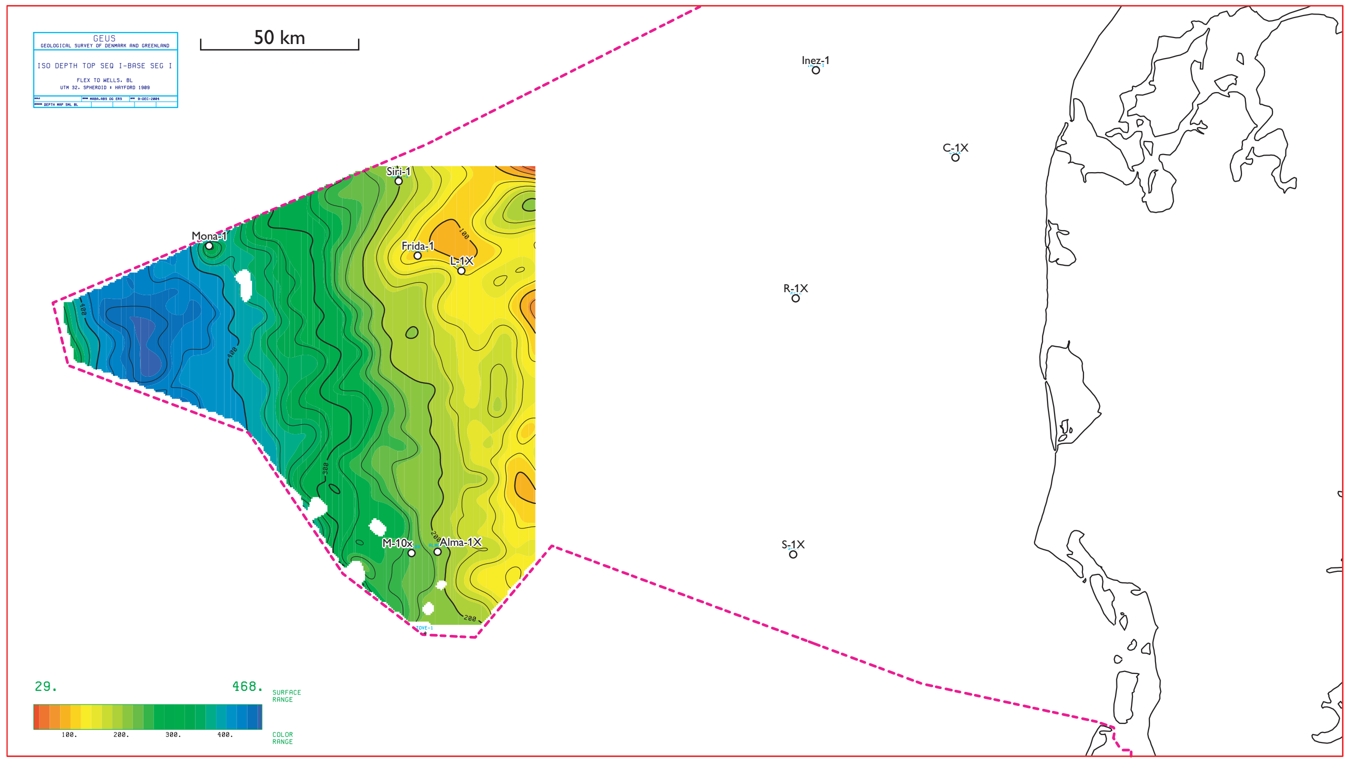

50 km
Inez-1
C-1X
Siri-1
Mona-1
Frida-1
L-1X
R-1X
S-1X
M-10x
Alma-1X
29.
468.

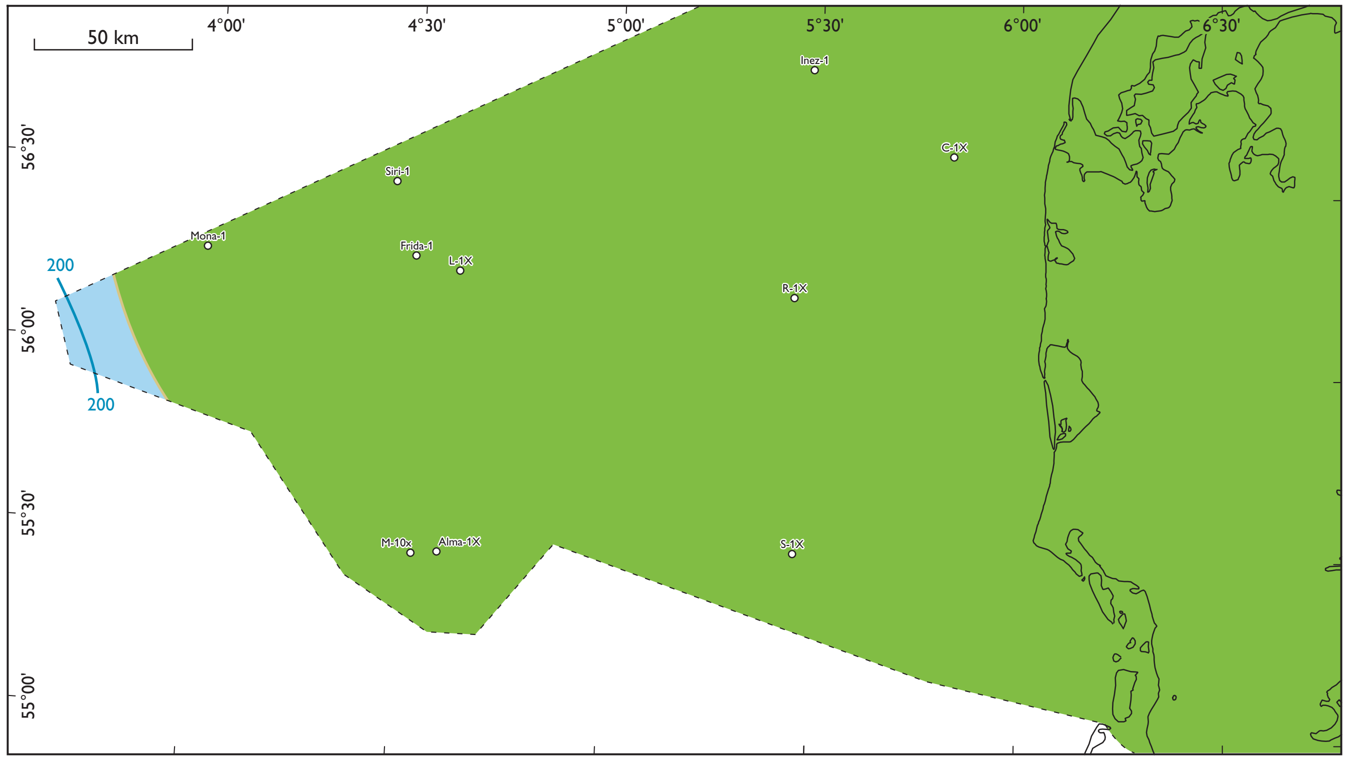

50 km
4°00'
4°30'
5°00'
5°30'
6°00'
6°30'
56°30'
56°00'
55°30'
55°00'
200
200
Inez-1
C-1X
Siri-1
Mona-1
Frida-1
L-1X
R-1X
M-10x
Alma-1X
S-1X

Base Pleistocene

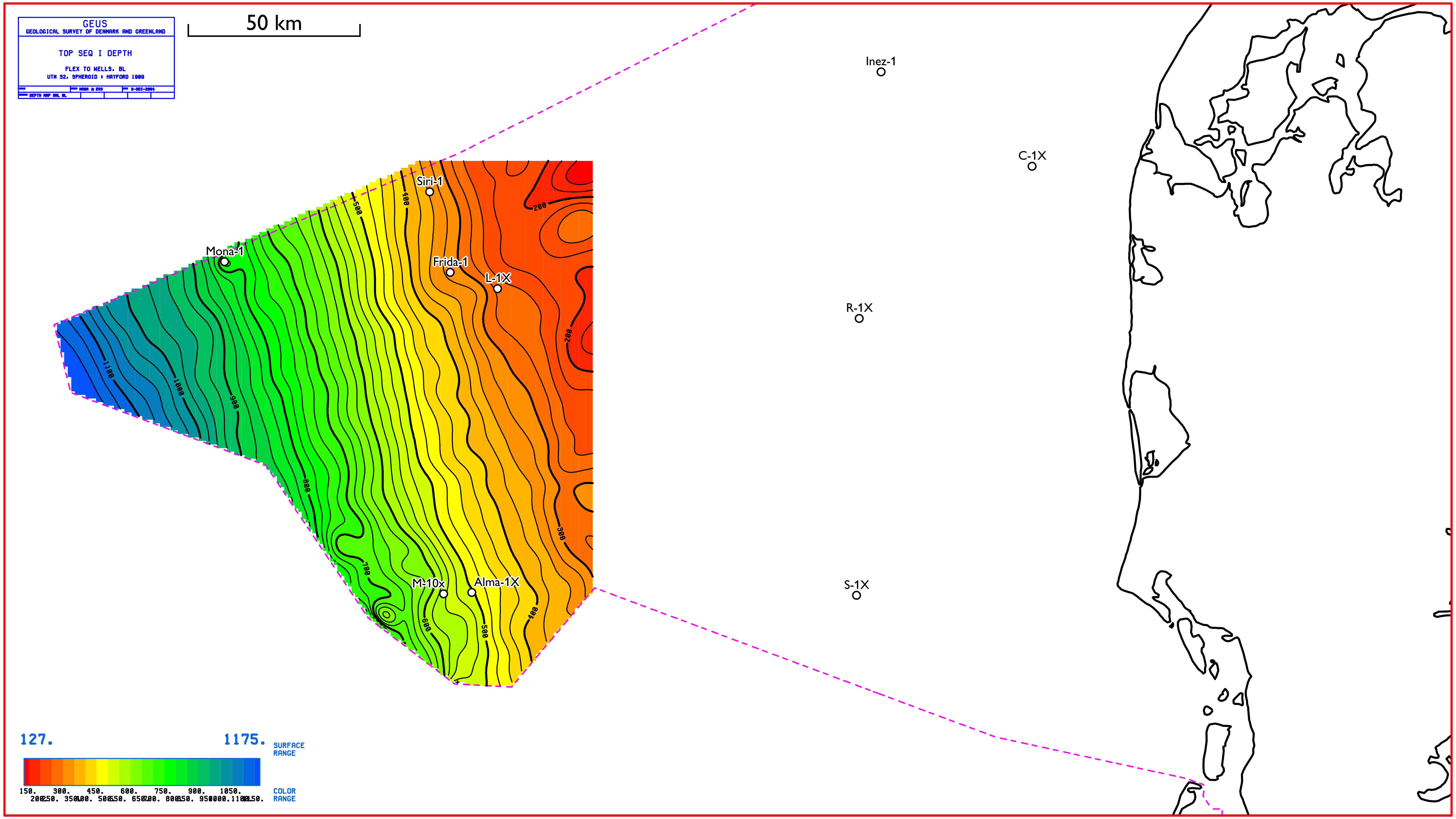

Fig. 19: Base Pleistocene
The surface forms a west-south-westward dipping monocline whose minimum depth is 70 m and maximum depth is 866 m.

Base Pleistocene